ISSN: 2331-1959 Volume 7, Number 2, April 2019

Scientific Research Publishing

Archaeological Discovery

ISSN: 2331-1959
9 772331 195007 02

www.scirp.org/journal/ad

Journal Editorial Board

ISSN Print: 2331-1959 ISSN Online: 2331-1967

http://www.scirp.org/journal/ad

Archaeological Discovery, 2019, 7, 31-154
http://www.scirp.org/journal/ad
ISSN Online: 2331-1967
ISSN Print: 2331-1959

Table of Contents

Volume 7 Number 2 April 2019

Archaeological Discovery (AD)
Journal Information

SUBSCRIPTIONS

The *Archaeological Discovery* (Online at Scientific Research Publishing, www.SciRP.org) is published quarterly by Scientific Research Publishing, Inc., USA.

Subscription rates:
Print: $39 per issue.
To subscribe, please contact Journals Subscriptions Department, E-mail: sub@scirp.org

SERVICES

Advertisements
Advertisement Sales Department, E-mail: service@scirp.org

Reprints (minimum quantity 100 copies)
Reprints Co-ordinator, Scientific Research Publishing, Inc., USA.
E-mail: sub@scirp.org

COPYRIGHT

PRODUCTION INFORMATION

For manuscripts that have been accepted for publication, please contact:
E-mail: ad@scirp.org

Archaeological Discovery, 2019, 7, 31-53
http://www.scirp.org/journal/ad
ISSN Online: 2331-1967
ISSN Print: 2331-1959

World's First Known Written Word at Göbekli Tepe on T-Shaped Pillar 18 Means God

Manu Seyfzadeh, Robert Schoch

Institute for the Study of the Origins of Civilization, College of General Studies, Boston University, Boston, MA, USA
Email: manu@cheopspyramid.com, schoch@bu.edu

How to cite this paper: Seyfzadeh, M., & Schoch, R. (2019). World's First Known Written Word at Göbekli Tepe on T-Shaped Pillar 18 Means God. *Archaeological Discovery, 7,* 31-53.
https://doi.org/10.4236/ad.2019.72003

Received: January 10, 2019
Accepted: January 29, 2019
Published: February 1, 2019

Abstract

Göbekli Tepe is a prehistoric, man-made megalithic hill site in today's south-east Turkey which is riddled with walled circular and rectangular enclosures lined by and surrounding T-shaped monolithic pillars proposed to represent supernatural humanoid beings. We examined if H-shaped carvings in relief on some of these pillars might have a symbolic meaning rather than merely depicting an object of practical use. On Pillar 18 in Enclosure D, for example, one such "H" is bracketed by two semi-circles. An almost identical symbol appears as a logogram in the now extinct hieroglyphic language of the Bronze Age Luwians of Anatolia and there it meant the word for "god". Further supporting a linguistic connection between Luwian hieroglyphs and images at Göbekli Tepe are to date untranslated Luwian symbols resembling the T-shape iconography of Göbekli Tepe and an H-like symbol which was the Luwian word for "gate". We conclude that the T-shaped pillars at Göbekli Tepe were in fact built and symbolically marked to represent a god, possibly a bull-associated being, which guarded the entry to the human and animal afterlife. We propose that this theme may have been inspired by real celestial images of the then prevailing night sky, ritually reenacted and celebrated for centuries by hunter-gatherer pilgrims to this hill and then spread by their descendants across Anatolia still influencing language in the region spoken and written thousands of years later.

Keywords

Göbekli Tepe, Luwian, Hieroglyphic, Anatolia, T-Shaped Pillar, Pillar 18, Enclosure D, God

1. Introduction

Origin of Writing. The invention of writing is commonly attributed to Sumer

and Egypt and the earliest evidence of either language dates to the late fourth millennium B.C.E. (Damerow, 2006). The first alphabet was created from Egyptian hieroglyphs by Canaanite miners in Sinai approximately one thousand years later at the beginning of the second millennium B.C.E. (Goldwasser, 2016). While the *terminus ante quem* of the origin of writing in the world can thus be traced to the Chalcolithic Age of Egypt and Mesopotamia, prehistoric civilizations may have expressed thought as recorded symbols long before, but evidence of such early writing may have been lost due to the decay of the medium, due to cultural invasion and replacement, or may yet be discovered. For example, traces of a pictographic script used in predynastic Buto and the region of the Nile Delta at large survived as hieroglyphic symbols in the mixed phonetic and ideogrammic script of dynastic Egypt while the rest of the language was apparently phased out by the time of Horus Den during the First Dynasty (Helck, 1987, Chapter 11, page 138).

The oldest recording system to date appears to have been clay tokens used to account for food stores which were discovered at Tell Mureybet by the western Euphrates in that site's layer III whose beginnings date to circa 9300-8600 B.C.E. (Senner, 1991: pp. 29-30). From this discovery and others, a widely-held model of cultural evolution by 20th century archeologists implies that written language was invented after the development of agriculture based on the domestication of plants and livestock, and thus, like urban living, social stratification, and religion, represents an expression and outgrowth of materialistic culture, the ultimate driving force of cultural change in this model. The two main successive phases of this change from prehistoric hunter-gatherers to ancient historic dynastic city-state or nation dwellers were originally defined as the Neolithic and Urban Revolutions by V. Gordon Childe (Smith, 2009).

Jacques Cauvin (2000), however, who led France's CNRS-sponsored excavations at Tell Mureybet in the mid-1970s, proposed the antithesis to this model by Childe: That symbolic thought and a belief system did not only predate domestication of food sources and the sedentary life-style of permanent settlements, but that it was instrumental in fostering them. In other words, the Neolithic revolution, according to Cauvin, was first and foremost a prehistoric revolution of the world-view of the people alive in that epoch at the end of the ice age in the 10th millennium B.C.E. It was this new world-view which shaped the insight to cope with a changing environment by employing a new life-style based on farming and settling in larger communities. Thus, ideologic or spiritual belief, first, enabled inventive thinking, second. Prehistoric people needed a reason to congregate. Once that happened, innovation and implementation became more likely when many people, previously physically separated, exchanged ideas, worked together, and shared the toil of living. In modern economics, this phenomenon is called agglomeration. Recorded symbolic language, like world-view and spirituality, could thus also be considered an expression of such new awareness, besides sculpture, architecture, and murals, made long before food was

grown and stored and needed to be accounted for. Symbolic, "religious" thinking and expanded awareness may even have been a requisite (Hodder, 2011: p. 112).

Given that the origin of the Indo-European branch of languages can be traced both to Anatolia and to a timeframe which overlaps with the aceramic Neolithic era (Bouckaert et al., 2012), megalithic monuments from this place and time may hold clues as to the need to capture spoken language with symbols and preserve them in stone for later generations (Schoch, 2012: p. 41). This need may have arisen with a desire for permanence beyond death and a sentiment for ancestry evident in the practice of skull removal of the buried dead, artistic modifications to human skulls (as found on human skull fragments at Göbekli Tepe; Gresky et al., 2017), and circulating them throughout the community as is evident from the archeological record at Çatalhöyük (Hodder, 2011: pp. 114-116). In this paper, we will present primordial evidence of pre-agricultural symbolic language related to the religious beliefs of an early Neolithic society of so-called "hunter-gatherers"[1] in southeast Anatolia at Göbekli Tepe. Our investigation, however, begins with an examination of hieroglyphic Luwian, a language in use across most of Bronze Age Anatolia thousands of years after prehistoric people built Göbekli Tepe.

Luwian Hieroglyphic Script. The Luwian hieroglyphic script, while discovered in the early 19th century, was fully deciphered only in the 1970s and shown to be a close dialect of cuneiform Luwian and a sister language of cuneiform Hittite, the official script of the ruling class of Bronze Age Anatolia during the Empire Period (circa 1200-1000 B.C.E), which it both preceded and survived by centuries (Goedegebuure, 2016, 2107). Thus, Luwian is one of the oldest, if not the oldest, known Indo-European languages and a likely descendant of the hypothetical Proto-Indo-European (PIE) common ancestor of all members of this language family. Current archeological evidence in the form of seals, reliefs, steles, lead strips, and wood panels, across almost one-hundred Anatolian sites, including some within 30 km of Göbekli Tepe, dates the emergence of the hieroglyphic script used to write in Luwian to the late 15th century B.C.E., i.e. a time coinciding with Egypt's 18th Dynasty of the New Kingdom, when Anatolia and Egypt interacted both in trade, diplomacy, and war. The Luwians, for example, may have been the "Sea People" with whom Ramses III fought, the Trojans with whom the Myceneans fought during Homer's Trojan War, and the confederate power which brought down the Hittites, all events occurring during the Late Bronze Age when several civilizations collapsed and recorded history entered a so-called Dark Age (Zangger, 2016).

Waal (2013) proposed an even earlier time of development of hieroglyphic

[1]It should be noted that "hunter-gatherers" may be a misnomer, because the builders of Göbekli Tepe were probably not equivalent to modern "hunter-gatherers" as discussed in the general anthropological literature; if anything, the Göbekli Tepe people may have been closer to so-called "complex hunter-gatherers" such as the Northwest Coast cultures of North America (see, for instance, Ames, 1994).

Luwian, around 2000 B.C.E. Developed exclusively for the Luwian language, which together with Hittite, Lycian, Lydian, Palaic, and Carian comprises the Anatolian branch of the Indo-European major language phylum, its origins can be traced to both spoken Hittite and Luwian (**Figure 1**). Some Luwian symbols encode full words in the form of logograms but most encode phonographic sounds. In the latter case, the phonetic values still relate to the pictographic idea of the symbols through acrophony, i.e. the sounds of the script's phonographic symbols are defined by the beginning of the sound of the words whose ideas they depict. For example, the Luwian word for walk "tia" produces the phonetic syllable "ti" encoded by a foot symbol. The Luwian word for ox "uwa" produces the phonetic sound "u" encoded by an ox head symbol. The Luwian word for donkey "tarkasna" produces the phonetic syllabic sound "ta". Some Luwian hieroglyphic symbols obtained their phonetic value not from the Luwian spoken language but from Hittite words. It is this bilingual origin of the script which suggests that the region of its invention was in eastern Anatolia where both languages were spoken (**Figure 1**; Goedegebuure, 2016).

The development of the script over time also suggests that it started with pictographs and that phonograms were gradually added later. This development contrasts with Egypt's proto-dynastic writing system which incorporated phonograms in its earliest known records discovered in tomb UJ (Baines, 2004). We therefore asked if the Luwian script, at its inception, may have incorporated surviving themes and especially symbols (i.e. iconic pictographs) of the long-gone

Figure 1. Map of ancient Anatolia showing the locations of Luwian (Luwic) writing discovered from the Empire Period (circa 1480-1200 B.C.E.). Megalithic sites with T-shaped Pillars west and east of the Euphrates River are indicated in black letters. GT: Göbekli Tepe; NC: Navali Çori; U: Urfa; HT: Hamzan Tepe; K: Karahan; ST: Sefer Tepe; TT: Tašli Tepe; K: Kilisik. Four language zones are marked. Palaic, Hattic, Hittite, and Luwic (Luwian). The overlap between Hittite and Luwic occurred in the zone approximated by the green circle. Map courtesy of Tayfun Bilgin, https://www.hittitemonuments.com, (v. 1.61), modified.

people who had lived nearby in southeast Anatolia and had built one of the oldest known megalithic complexes in the world from which the Neolithic Revolution expanded across the fertile crescent and eventually further into the continents of Europe, Asia, and possibly parts of Africa and elsewhere.

Göbekli Tepe. Göbekli Tepe Layer III is a Neolithic Pre-Pottery, megalithic phase at a prominent and widely visible location in the upper Euphrates Valley zone, which makes up the northern extent of the fertile crescent marking the transition between ancient Mesopotamia's plains to the southeast and Anatolia's mountainous highlands to the northwest. The complex was built on a limestone ridge over a period of about 800 or more years in the 10th and 9th millennia, further extended with ancillary structures in Layer II for a period of 1800 years during the 9th and 8th millennia, and then completely buried and abandoned by circa 7000 B.C.E. (Schmidt, 2000, 2011, 2012). Originally discovered as a possible site of interest in 1963 by the Universities of Istanbul and Chicago led by Halet Çambel and Robert Braidwood, respectively, it was found to be a very ancient megalithic site in 1994 during initial excavations undertaken by the German Archeological Institute's late Klaus Schmidt (Schmidt, 2000, 2011). Schmidt's excavations over the years into this man-made hill unearthed several stone circles surrounding, and lined with, T-shaped pillars (**Figure 2**) onto which animal figures and, as he had already witnessed at Navali Çori, humanoid features like arms and hands were carved in relief (**Figure 3(a)**), for example on Pillar 18 at the center of Enclosure D in the hill's southeast quadrant (**Figure 3(b)** & **Figure 3(c)**).

Pillar 18 rests on a pedestal with bird reliefs on its façade (**Figure 3(c)**). Besides a foxlike animal on its "torso" (**Figure 3(b)**), it features a finely carved belt with several "H"-shaped symbols (**Figure 3(g)** & **Figure 3(h)**) and a buckle from which an animal hide loincloth hangs (**Figure 3(c)**). At the top front of the pillar is a set of three symbols composed (from top to bottom) of another "H"-shaped symbol and an umbilicated disc hovering within the concavity of a

Figure 2. Göbekli Tepe's Layer III site plan looking west from the east with north to the right in this image. Four enclosures are shown, and their conventional designations A, B, C, and D are indicated above. All eight central pillars and some of the peripheral pillars are marked including all those discussed in this paper. Pillar 33 in Enclosure D is nestled between Pillars 32 and 38 and is not fully visible in this image. Composite image courtesy of Robert Schoch and Catherine Ulissey.

Figure 3. Central and peripheral pillars, limestone plate, and porthole, Göbekli Tepe, Turkey. (a) Pillar 31 and (b-d; g-h) Pillar 18, from Enclosure D; (e-f) carved limestone plate found by Pillar 31 showing severed heads (marked in red by D.A.I.); (i) Pillar 28 from Enclosure C; (j) Pillar 43 from Enclosure D; (k-l, red arrow in (l) by D.A.I.) Porthole stone close-up and *in situ* from above, Enclosure B; (m-n) Pillar 33 from Enclosure D. Images courtesy of Robert Schoch and Catherine Ulissey (b-d, g-i, m-n), Berthold Steinhilber (j) and the German Archeological Institute (D.A.I., a, e-f; D.A.I.'s N. Becker, k-l) with permission.

crescent (Figure 3(d)). Of note, the "head" of the pillar is unmarked, though there are other pillars whose topmost parts are ornately carved with animal and geometric motifs. No facial features have been found on any pillar unearthed to date. The significance of the T-shape and its association with humans remain a mystery, but most agree that supernatural beings were meant to be displayed in stone.

Within the back-fill debris surrounding Pillar 31, the other megalith in the center of Enclosure D next to Pillar 18, a limestone plate with reliefs showing severed heads (Figure 3(e) & Figure 3(f); marked with red circles) next to a vulture and also two life-size human limestone heads were discovered demonstrating that the humanoid T-shape of the pillar heads was deliberately chosen to contrast with the realism of the human heads. Seemingly complementing the severed heads by Pillar 31 (see Gresky et al., 2017: p. 5, their Fig. 4a, for a photograph of a decapitated human statue from Göbekli Tepe), a small headless torso is depicted in relief at the bottom of Pillar 43's west-facing side (at the bottom of

the pillar, again next to a vulture; **Figure 3(j)**). Pillar 43 was integrated within the enclosure wall immediately behind Pillar 31 (see **Figure 2**) to the northwest (the enclosure wall is most likely of a later period—that is secondary—relative to the pillars; see Schoch, 2017: p. 458). The headless torso on Pillar 43 appears small next to the much larger animals also shown (**Figure 3(j)**), for example a vulture immediately next to it. These motifs of vultures and headless human torsos reappear two-thousand years later on murals of a temple-like structure at Çatalhöyük hundreds of kilometers to the west demonstrating their cultural importance (Sandars, 1979).

While the purpose of the entire complex at Göbekli Tepe, still largely unexcavated, continues to be debated, the anthropomorphic yet "alien" character of the over-sized T-pillars suggests that they depict supernatural beings or gods and that the site therefore had a spiritual congregational function though other, possibly more secular, purposes cannot yet be ruled out given, for instance, evidence of feasting and other activities at the site (see, e.g., Banning, 2011). T-shaped pillars have also been discovered at nearby sites east and west of the Euphrates, i.e. Navali Çori, Urfa, Hamzan Tepe, Karahan, Sefer Tepe, Tašli Tepe, and Kilisik, with Göbekli Tepe assuming the central focus of this cultural zone (**Figure 1**).

Symbolism and Meaning. The meaning of the animal depictions and other relief markings on the T-pillars, as well as the pillars themselves and the circles they form, remain a mystery to date and while several theories have been proposed, such as relating them to Orion's belt stars (Schoch, 2012: pp. 54-55), to stars in the north (Deneb; Collins, 2014: pp. 80-82), Sirius (Magli, 2013, 2016), or foreign symbols (e.g. Putney, 2014), unequivocal proof remains elusive. The fact that dwellings at Çatalhöyük were found to contain adult burials always on the north side of the living space (Hodder, 2012: p. 305) sometimes marked by aurochs skulls and often by vulture paintings with headless corpses (Hodder, 2012: p. 306), lends support to the hypothesis that the approximate north-south orientation of most of Göbekli Tepe's T-pillar circles may be integral to the ideas which inspired their construction. The central T-pillars themselves may represent a god or gods "looking" out to the sky at a bull (for instance, Taurus) or associated with a bull (for instance, Orion, who is in the same general portion of the sky as Taurus; see Schoch, 2012: p. 55). Virtually all the other animals depicted on the pillars and associated stone carvings, i.e. snakes, lizards, spiders, scorpions, foxes, boars, lions, leopards, and various birds including a vulture, cranes, and an eagle were indigenous to the regional fauna of Holocene southeast Anatolia (Schmidt, 2011, 2012).

Klaus Schmidt interpreted Göbekli Tepe as a ritual center to which hunter-gatherers from surrounding settlements congregated to feast and commemorate or even bury some of their significant dead but did not rule out a shamanic purpose (Schmidt, 2011, 2012). He read the pillar carvings as a form of storytelling while the high-relief animal sculptures had a symbolically protective function. He emphasized the significance of the symbolic dominance of the human

features of the megaliths over those of the fear-instilling animals and singled out Göbekli Tepe as unique in this respect among other contemporary Neolithic sites. To Schmidt, Göbekli Tepe's main theme was the conquest by man-like gods of the wilderness world and this spiritual theme unmistakably predated the pragmatically driven transition from hunting and gathering for food to growing and storing it as the changing environment after the Younger Dryas may have dictated.

Here, we present new evidence that one, especially peculiar, carving may represent a written symbol, as previously suspected (Ercan, 2015), which identifies one of the most prominent and central of the T-pillars as a deity and thus supports the idea that Göbekli Tepe was in fact a temple complex[2] dedicated to at least one god which formed perhaps a symbolic gateway to the afterlife as well as protecting the still living. We discuss the possible origins of this symbol, its significance within the ritual context of the entire site, which may have its origins in imagined celestial images.

2. Results

One often-appearing Luwian symbol is the word for "god", Laroche #360 "DEUS[3]" (**Figure 4**; Laroche, 1960). Many examples can be observed at the almost one-hundred sites from which written records were discovered. This symbol depicts an oval with two opposing semi-circles and two vertical parallel lines between them. For example, it is well shown on rock inscriptions in Develi by Fraktin (**Figure 5**) and from Arslan Tepe (**Figure 6**) and several instances of it can be seen on a storm god stele from Aleppo (**Figure 7**). At Hanyeri, a symbolic association can be observed between "DEUS" and "MONS", where both are used on the same line of text translated as "king of the mountain god" (**Figure 8**). Close inspection of "MONS" (**Figure 9**), reveals that the only difference to "DEUS" are the long converging lines in "MONS" separating its opposing semi-circles as opposed to the two parallel vertical lines separating them in "DEUS".

The "H"-shaped Luwian symbol is the logogram for PORTA ("gate"; Petra Goedegebuure, personal communication) and is seen in detail for example in an inscription from Arslan Tepe (**Figure 10**). There are "T"-shaped Luwian symbols, the meaning of which still eludes translation. One such symbol, Laroche #457 (2) (**Figure 11**) shows a "T" on a steep mount. An example can be seen *in situ* at Sivasa (**Figure 12**).

3. Discussion

Linguistic link between Luwian and Göbekli Tepe's Iconography. It appears that when the Luwian script was invented, it adopted some Anatolian icons predating its inception (between 2000 and 1400 B.C.E.) by thousands of years. Since

[2]Whether *solely* a "temple complex", as Göbekli Tepe is often referred to, or something more, such as the equivalent of a center of learning, ritual, teaching, and protecting traditions and knowledge, is a subject that is up for discussion based on further evidence.

[3]Luwian logograms are translated into Latin by convention.

360 « DIEU. »

Variantes :

1. Déterminatif divin.

Yazilikaya 43 : ^{d}*He-pa-tu* « Hebat »; 42 : ^{d}W CIEL « Tešub (du) ciel »; 35 : ^{d}LUNE « Lune-Kušuḫ »; 34 : ^{d}SOLEIL CIEL « Šimegi du ciel », etc.
Karatepe 13 : ^{d}W-*hu-ī-s* « Tarhunda » = phén. *Bʿl*.
Kargamis, A 11 a 6 : ^{d}W-*s* ^{d}*Ká* + *r-hu-há-s* ^{d}*Ku*-OISEAU-*pa-s-há* « Tarhunda, Karhuha et Kubaba ».
Hamath V 1 : ^{d}*Ba-há-la-ti-sà-pa-wa* TEMPLE + *mí-ī* « et le temple de Baʿalat ».
Karadağ 1 : ^{d}GRANDE MONTAGNE.

2. Id. « dieu, déesse »; compl. phon. *-na-*.

Hanyeri, gauche : (1) ROI (de la) MONTAGNE-DIVINE ^{d}*Sarruma*.
Karatepe 54 = 54′ et suiv. : ^{d}W-*hu-ta*$_4$-*ti*$_4$ DIEU-*na-a* + *ta/i-há* « grâce à Baʿal et aux dieux » = phén. *b-ʿbr bʿl w-ʾlm*; cf. ibid. 329-330.
—— 288 et suiv. : FORT. *ha* + *r-na-ša-sá* DIEU-*ná-i* « les dieux de la forteresse » = phén. *ʾln qrt;* 289′ : DIEU-*sa*$_4$!-*i*.
—— inédit : CIEL ^{d}W-*hu-ī-ś* CIEL ^{d}SOLEIL-*ī-ś* ^{d}*A-ā-ś* TOUT-*mi-i-há* DIEU-*ná-i* « Baʿal des cieux, Soleil du ciel, Aa et tous les dieux » = phén. *w-kl dr bn ʾlm*.

Figure 4. Laroche #360 Luwian hieroglyph denoting "god". From Laroche (1960: p. 187).

Figure 5. Luwian rock inscription, Gümüşören (Fraktin) village of Develi, circa 1300-1200 B.C.E. The "god" symbol Laroche #360 is shown at the top next to the head of the figure on the left. Image courtesy of Tayfun Bilgin, https://www.hittitemonuments.com, (v. 1.61).

Figure 6. Luwian rock inscription from Arslan Tepe at the Anatolian Civilizations Museum in Ankara, Turkey; circa 900 B.C.E. The "god" symbol Laroche #360 is shown at the top next to the head of the storm god (Tešup) figure on the left. Immediately below is the logogram for "lightning", Laroche #199. Image courtesy of Tayfun Bilgin, https://www.hittitemonuments.com, (v. 1.61).

Figure 7. Storm God Relief and Stele from Aleppo, Istanbul Archeology Museum. Marked with red circles are instances of Laroche #360 on the stele and its transcription. Images courtesy of Tayfun Bilgin, https://www.hittitemonuments.com, (v. 1.61), modified.

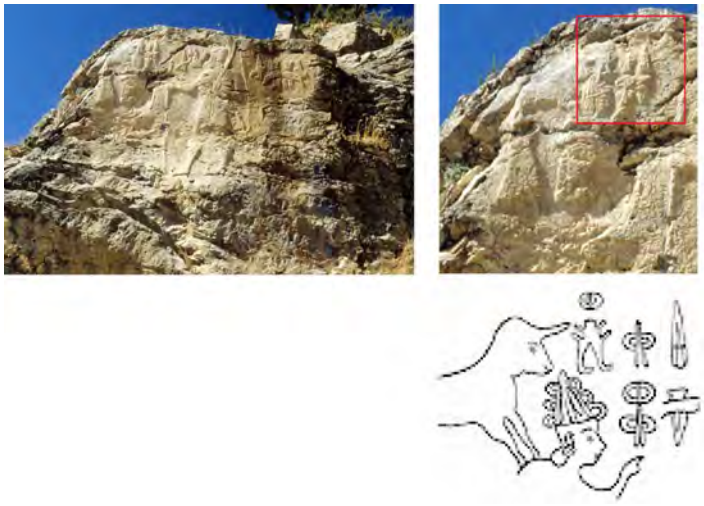

Figure 8. Luwian rock inscription at Hanyeri, circa 1300-1200 B.C.E. The three-part relief is shown on the left and the magnified left part on the top right. Below is the transcription. The top row of symbols reads from right to left: "King of the Mountain god, Sharruma" (REX MONS DEUS.*SARMA*) and the second row reads "Sword, the divine mountain" (ENSIS DEUS.MONS). Images and graphic courtesy of Tayfun Bilgin, https://www.hittitemonuments.com, (v. 1.61), modified.

207  1. « MONTAGNE. » 2. wa_4.

Ligature de DIEU (n° **360**) et d'une montagne.

Variantes : 

I. — Id. et déterminatif pour « montagne »; lect. phon. inconnue.

1. « montagne (divine) ».

Hanyeri, gauche : (1) ROI (de la) MONTAGNE ^{d}*Sarruma* (2) **53** ^{d}MONTAGNE : désignent l'animal et l'être anthropomorphe.

Figure 9. Laroche #207 Luwian hieroglyph denoting "Mountain". From Laroche (1960: p. 112).

Figure 10. Luwian rock inscription from Arslan Tepe at the Anatolian Civilizations Museum in Ankara, Turkey; circa 1100-1000 B.C.E. The "H"-shaped symbol is shown marked in red. Image courtesy of Tayfun Bilgin, https://www.hittitemonuments.com, (v. 1.61), modified.

239 (1) (2) (3)

(1) Emirgazi 1.4 = 2.1 = 3.2 : **239**-*mi*; ibid. 1.5 = 2.2 = 3.3 : **239**-*mi-pi*.
(2) Karahöyük-Elbistan 11 : **239**-*ī*.
(3) Maraş, 8.5 : **239**-*ī*.

Selon Hrozný, IHH (1937) 412 et suiv. : « porte ».

261

Sorte de bâtiment ?

1. Id. verbal; compl. phon. -*taru*-, sens incertain : « bâtir ? ».
   Kargamis, A 11 a 4 : ^{d}W-*ti* TEMPLE-*tà* [BÂTIR$_2$]-*tà-ru-há* « j'ai bâti (?) un temple au dieu de l'orage »; de même A 2.4.
   —— A 13 d 7; 25 a 1 : BÂTIR$_2$-*tà-ru-tú*, 3^{e} sg. imp.
2. Id., verbal, compl. phon. -*tapa*, sens inconnu.
   Kargamis, A 2.5 : REL-*s ī-'-ā* TEMPLE-*há-tà* '+*tá* BÂTIR$_2$-*ta$_4$-pa-a* « celui qui . . . ra ce temple ».

« Bâtir » chez Meriggi, Glossar (1934) 27, 99. — Rayer le « vestibule » de Hrozný, IHH (1935) 161, 206 n. 11, 221.

263 (1) (2)

1. New York, Metr. Mus. 1 : **263**-*sa$_5$-a*, nom propre.
2. Karahöyük-Elbistan 10 : compl. ou lect. phon. -*tá-na-sa$_5$*.

457 (1) *li$_4$*. (2)

(1) Karatepe 31 : JOUR *há-li$_4$-i* = JOUR *há-li-ā-ī*, n° **358.**
(2) Suvasa D 1 : contexte obscur.

Selon Bossert, Oriens 1 (1948) 192, (1) = (2) = **458.**

Figure 11. Laroche #239, 261, 263, and 457. #457 (1) has the phonetic value of "li". #239 translates into "Gate" and #263 and #457 (2) are unknown (Petra Goedegebuure, personal communication). #261 is uncertain. From Laroche (1960: pp. 129, 137, 237); modified.

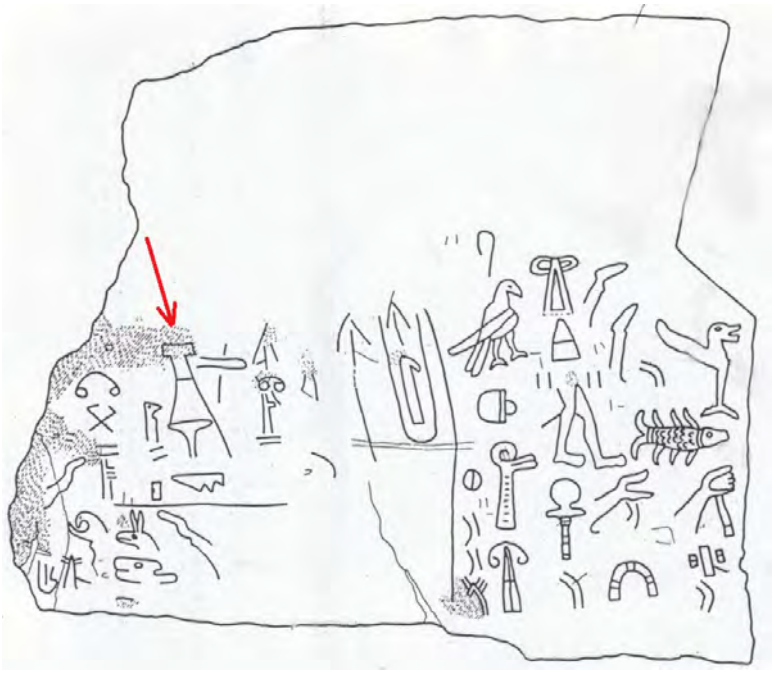

Figure 12. Transcribed Luwian rock inscription from a rock still *in situ* at Sivasa/Suvasa/Gökçetoprak. Laroche #457 (2) is marked with the red arrow. Graphic courtesy of Tayfun Bilgin, https://www.hittitemonuments.com, (v. 1.61), modified.

Luwian contains, by our survey, at least four symbols directly related to iconography found at Göbekli Tepe, we think random chance is unlikely. However, even if Luwian adopted symbolic themes from its distant ancestors, we have to consider the more trivial scenario that people who lived in southeast Anatolia during the Bronze Age may have discovered decorated T-shaped pillars, ascribed importance to the symbolism of the pillars and some of the reliefs found on them, and consequently attached a meaning to these icons unrelated to that intended by the builders of Göbekli Tepe, which itself may be a trivial depiction of the details of a hunter's belt. The main reasons why we think this is unlikely are that: 1) the "H" symbols occur both as part of the belt bracketed by semi-circles on Pillar 18 of Enclosure D, as a part of an apparently purely symbolic element on the front of Pillar 18 along with a disk inside a crescent, alone on the front of Pillar 28 in Enclosure C bracketed by two semi-circles (**Figure 3(i)**), and as a focal point for the direction of where animals are heading as shown on Pillars 43 and 33 in Enclosure D (**Figure 3(j)**, **Figure 3(m)** & **Figure 3(n)**), and 2) that this idea of a focal point is consistent with the concept of a gate, the meaning given to the "H"-shaped symbol in Luwian. Therefore, it is possible that the original meaning behind Göbekli Tepe's iconography was verbally preserved in Anatolia's prehistoric and ancient legends and myths until a written script was made incorporating those prehistoric symbols along with their archetypal meaning.

The Luwian "god" symbol is not perfectly identical though close to the "H"-shaped symbol inside two semi-circles as seen on the belt of Pillar 18 (**Figure 3(g)**) and the chest of Pillar 28 (**Figure 3(i)**). The main difference is that

the cross bar is missing, and the two vertical bars are closer together. Nevertheless, we think this Luwian iconography still preserves the concept of a passage, originally depicted blocked, then open in the Luwian symbol. The common position of Laroche #360 in Luwian texts is at the top of a column of symbols within a row of text suggesting that the god so named was in the sky. One way to interpret the idea of a gate inside a circle in the sky is a passage through a vortex such as the celestial north pole of the night sky around which the circumpolar stars slowly wander each night and whose focal point gradually shifts due to the combined effects of axial and apsidial precession.

Our analysis does not reveal if the Luwian T-shaped symbols, Laroche #261, 263, and 457 (2) (**Figure 11**) are words or sounds. However, the fact that an aurochs' cranium is depicted on the front of Pillar 31 in Enclosure D (**Figure 3(a)**), on top of the porthole of Enclosure B (**Figure 3(k)** & **Figure 3(l)**), and on later Anatolian pottery decorations where the T-shape is evidently part of a bull head (**Figure 13** and **Figure 14**) suggests that they represent the prehistoric word for "bull" or a syllable sound related to that word.

Spiritual Theme. Taken together, this evidence suggests that the T-shaped pillars at Göbekli Tepe were likely meant to represent a god in the form of a bull-like being. But what was its power or function within the context of circles? The answer to this question may come from the lay-out of the dwellings found at Çatalhöyük. There, the adult dead were commonly buried on the northeast side of the homes and sometimes marked with bucrania (**Figure 15**). This suggests the god in question was a guardian of the dead. In the same context, the vulture with the headless torso marked the north side of the dwelling. At Göbekli Tepe the general orientation of most circles unearthed so far is approximately south to north (**Figure 16**). The animals are shown to seemingly migrate towards the

Figure 13. Terracotta vase from southwest Turkey at Haçilar, late 6th millennium B.C.E. National Museum of Oriental Art, Rome, Italy. Photo courtesy of MM-Own work, CC BY-SA 3.0, https://commons.wikimedia.org/w/index.php?curid=29823064.

Figure 14. Decorated pottery from southwest Turkey at Haçilar, late 6th millennium B.C.E. Ankara Anatolian Civilizations Museum, Ankara, Turkey. Image courtesy of Dick Osseman, with permission: http://www.pbase.com/dosseman/profile.

Figure 15. Northeast platform burial site in building 77 of the Pre-Pottery Neolithic B settlement in south Turkey at Çatalhöyük, 8th to 7th millennium B.C.E. Image courtesy of Verity Cridland-Çatalhöyük, CC BY 2.0, https://commons.wikimedia.org/w/index.php?curid=7429553.

Figure 16. Aerial view of Enclosures A-D from the south looking north. Image courtesy of the German Archaeological Institute's (D.A.I.) E. Kücük, with permission.

bull-like god represented, we argue, by the gate symbol "H", and on the north side of Enclosure D, a vulture is shown next to a headless torso (i.e. the limestone plate found by Pillar 31, **Figure 3(e)** & **Figure 3(f)**, and Pillar 43 immediately northwest, **Figure 3(j)**) in analogous fashion as to what is seen on north-wall murals inside dwellings at Çatalhöyük (**Figure 17**). Therefore, the view of the world suggested by this iconography could be interpreted as revolving around the inevitability of the death of all creatures, animals and humans, symbolized by the vulture and the headless torso, and that this passage from life to death involves an encounter with a god who stands at the gate of a passage (Collins, 2015) between life and death[4]. The discovery of limestone heads by Pillar 31, decorated fragments of human skulls at Göbekli Tepe, and plastered skulls at Çatalhöyük suggests that this word-view also made room for the notion of coming back to life (also suggested by Collins, 2014) and that this resurrected life spiritually resided inside of the head of the dead.

Astronomical Imagery. This idea of an H-shaped gateway to the afterlife and the head as the seat of the life force may originate from what was visible in the night sky of the time. During the 10th Millennium B.C.E., the north pole was occupied by the H-shaped constellation Hercules near the bright star Vega in the constellation Lyra next to Cygnus (**Figure 18**). We think this iconography of a rotating, never-setting "H" in the night sky next to a bright point source of light, therefore, may have been interpreted as a headless being with its detached head next to a vulture-like figure nearby and its eternal life related to the fact that it, unlike most other stars, was visible every night. An alternative interpretation of either Vega or the star Deneb (in Cygnus) suggests that it may have inspired the "H"-symbol (Sweatman & Tsikritsis, 2017: p. 239) though Collins has suggested that Deneb was instead represented by the "Soul Holes" found in two of the enclosures (see Figure 9 and Figure 10 in Collins, 2015). The celestial torso from which the head (i.e. Vega in our interpretation) was severed may also have been inspired by the constellation Orion, also possibly imagined as a headless humanoid figure (Schoch, 2012: p. 55).

The snake-like constellation Draco (**Figure 18**) may explain the iconography of the many snakes on the T-shaped pillars and on the back of a limestone head found at Nevalı Çori and their seeming migration depicted on some pillars towards the "H" symbol (e.g. **Figure 3(m)**) is neatly explained by Draco's and Boötes' (possibly imagined as a scorpion) proximity to Hercules. The vulture "flying" and "chasing" after the "torso" of Hercules during the hours of the night could have been seen in Cygnus (represented on Pillar 43; Collins, 2017) and we agree that this is more likely than another interpretation which suggests it was meant to represent Sagittarius (Sweatman & Tsikritsis, 2017: p. 237), as the

[4]Andrew Collins has interpreted the meaning of a bone plaque found at Göbekli Tepe to show a path taken by a person in between two T-shaped pillars and towards the "soul hole", opening through limestone slabs placed at the north ends of Enclosures C and D (Collins, 2015). A similar passage-like iconography is shown in Laroche #207 (**Figure 9**), a ligature of "god" and "path" which was the Luwian word for "mountain".

Figure 17. Recreation of a typical wall mural on the north wall of a dwelling at Çatalhöyük showing a vulture and headless human torsos reminiscent of a T-shape with arms and legs. Çatalhöyük site museum, Turkey. Image (2013) courtesy of Robert Schoch and Catherine Ulissey.

Figure 18. View of the northern star zone from the perspective of Göbekli Tepe in 9600 B.C.E. (Julian year-9599) recreated using Stellarium (version 0.14.3). In the center is the constellation Hercules. The brightest star in the northern star zone Vega is highlighted. The circumpolar region was then populated by the constellations Hercules, Draco, Cygnus, Aquilla, Lyra, and Boötes.

former view is better anchored in our own reconstruction of prehistoric Anatolia's imagined afterlife and better supported by the evidence from Çatalhöyük as Collins (2017) has also noted. This astronomical interpretation is also consistent with the general north-south orientations of enclosures A-D, but the exact positions of Hercules and Vega and the circumpolar constellations in remote times need to be confirmed using astronomical software which can recreate remote

periods of time (e.g. the Carte du Ciel star mapping project; see Conclusion in De Lorenzis & Orofino, 2015).

Another confounding variable may be introduced by tectonic plate movement. Göbekli Tepe is located northwest of the East Anatolian Fault on the Anatolian plate and rotates counterclockwise due to northward push from the Arabian Plate on its eastern end (Cavalié & Jónsson, 2013, see **Figure 1** of citation). This means that the perspective from Anatolian monuments on the ground very slowly rotates west of north relative to the stars in the night sky. The extent to which this may affect alignments to certain stars measured today should be confirmed to be negligible, but it cannot be ignored *a priori*.

The bull-like T-shaped god statues of Göbekli Tepe are not facing toward the north and the circumpolar region, but are rather turned toward the south. It is possible that the southeastern night sky with the constellation Taurus and Orion's belt asterism, previously suggested by one of us (Schoch, 2012: p. 55), may have been associated with the T-shaped anthropomorphic pillars, and with the cranium of an aurochs. Indeed, the god in question (represented by the central pillars of Enclosure D) was facing toward the region of the sky containing Orion—with its strong belt stars, perhaps represented by the belts on the pillars—and Taurus, the bull or aurochs, on the vernal equinox during Göbekli Tepe times (Schoch, 2012).

It is also possible that prehistoric sky watchers associated either the bull, or the T-shape, or both with the southern hemispheric cross-shaped constellation Crux, which was visible in Anatolia during the 10th Millennium B.C.E. Likewise, the nearby constellation Centaur's inverted "U"-shape may have inspired the same symbol on the belt buckle of Pillar 18, the circular shape of Enclosures A-D, and the "U"-shaped stone entrance to Enclosure C to its south. The Milky Way, on which Crux can be seen, forms a starry path to the circumpolar region and this may have been symbolized as the path to the afterlife in the north. T-shaped megalithic pillars on the southern side of the island of Menorca called Taulas surrounded by horseshoe-shaped enclosures built by the Talayotic (Talaiotic) Civilization (circa 1300-800 B.C.E.) were also likely oriented to the low altitude constellations Crux and Centaur (Hoskins et al., 1990) and the sites were abandoned at the same time when Crux disappeared in the northern hemisphere due to Earth-axial precession hinting at a causal connection[5]. The Taulas are a compelling example of an ancient monumental recreation of starry images imagined in the night sky (**Figure 19**).

Animal Imagery. We may ask if it is necessary to invoke an association with celestial images in order to explain the ancient worship of animal-like gods or gods associated with certain animals. From the perspective of ancient people, the wild aurochs must have been an imposing and ferocious animal (**Figure 20**)

[5]Klaus Schmidt did not believe that the Bronze Age Menorcan Taulas had any relationship to the similarly T-shaped pillars at Göbekli Tepe because they were made from two stone elements instead of one monolith (Schmidt, 2012, Q & A session). However, it is not clear if Schmidt had considered that both, despite different manufacture, may have been inspired by the same imagined celestial image or by objects in the sky at all.

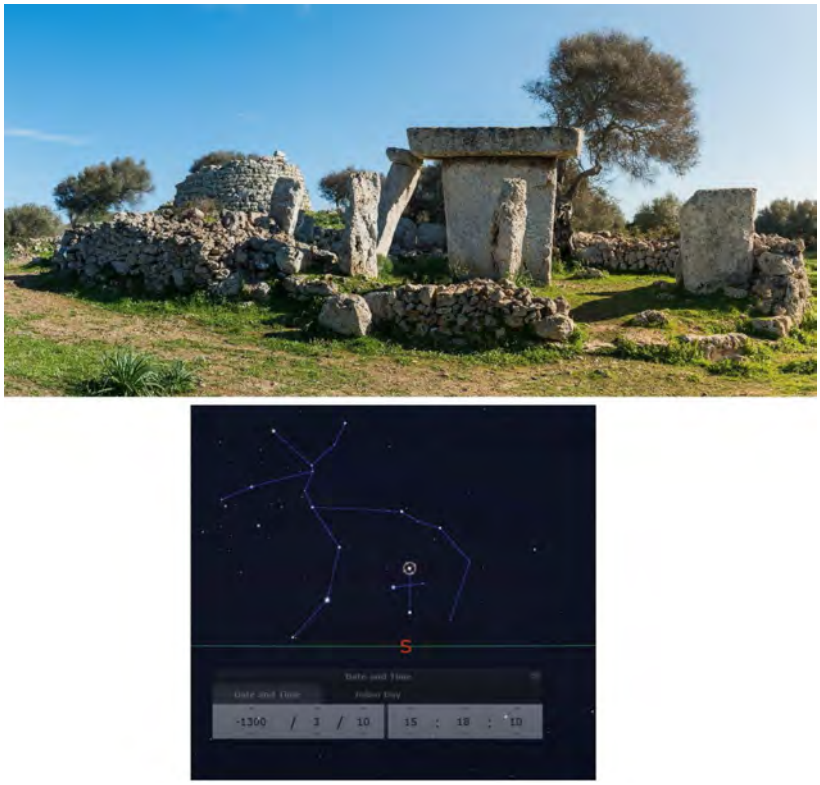

Figure 19. Above, a Taula on Menorca, Spain. Below, a screenshot view of the southern star zone in 1301 B.C.E. (Julian year-1300) from the perspective of Menorca recreated using Stellarium (version 0.14.3). In the center is the Constellation Crux (gamma Crux is highlighted), the southern cross. The constellation Centaur featuring the bright stars Alpha and Beta Centauri forms a horseshoe-like enclosure around Crux and this starry image may have concretely inspired the Taulas. Image (modified) courtesy of Shutter stock, Standard License #672366646 (January 2, 2019).

Figure 20. Wall mural at Çatalhöyük showing an aurochs hunt, discovered by James Mellaart (1961). Çatalhöyük site museum, Turkey. Image (2013) courtesy of Omar Hoftun, CC BY-SA 3.0, https://commons.wikimedia.org/wiki/File:Mural_from_%C3%87atalh%C3%B6y%C3%BCk_excavated_by_James_Mellaart_showing_neolithic_hunters_attacking_an_aurochs_(Bos_primigenius)..jpg.

perfectly suited to symbolize power and this association continued into the Bronze Age when the Anatolian storm god Tešup is seen with a bull (**Figure 6** and **Figure 8**). The vulture could have been uniquely associated with death as this bird could have commonly been witnessed consuming the carcasses of dead animals and humans, unlike other meat-eating animals which eat freshly killed prey. In ancient Egypt, as today, lions bask in the sun, baboons cheer at sunrise, falcons perform acrobatics in front of the glowing sun disk (Robert Bauval, personal communication), and scarab beetles emerge from the sands. Is it the behavior of these animals which turned them into Tefnut, Mehit, Horakhty, Babi, Horus, and Kheper, or was it their imagined likenesses in the starry night sky, that place no ancient human could ever reach, which made them god-like? We think one must consider both aspects of animals, how they behaved and how their likenesses might have been recognized in prominent groups of stars, to reconstruct what likely mattered in each case to ancient peoples' worship of animal-like gods. However, caution must be exercised when attempting to reconstruct what animal or human shapes different ancient cultures at different times imagined certain groups of stars to represent. The ancient Egyptians of the New Kingdom, for example, likely saw the hippopotamus goddess "reret", the scorpion goddess "serket", the falcon god "anu", and the ox thigh "mesekhtiu" in the circumpolar star group, while Claudius Ptolemaeus' *Almagest* (Alexandria, 2nd century C.E.) listed Draco, Ursa major and minor, and Boötes (Lull & Belmonte, 2009, Chapter 6, pp. 164-168).

Conclusions. In summary, we have drawn a semantic link between the dominant symbolism of Göbekli Tepe, T-pillars and H-symbols, and the words for god and gate in the Luwian script. Thus, the central pillars inside Göbekli Tepe's enclosures were meant to be gods, or one god, associated with bulls and the H-symbols on them were meant to explicitly mark them as such, i.e. beings, or one supreme spiritual being, presiding over the imagined path from life to death in the form of a symbolic gateway. This link confirms what others have long suspected: That Göbekli Tepe, at least in part, served as a temple site. The details of the rituals practiced there (as well as other activities) may not come to light, if ever, until the remaining circles are excavated; however, our analysis suggests that a passage rite involving decapitation of the deceased, and thus resurrection from the realm of the dead, may have been involved. The role of the god associated with a bull was that of the gatekeeper between the realms of the living and the dead and so it is possible, we might speculate, that resurrection in the form of decapitation required a price to be paid, possibly a sacrifice which was enacted inside of the circles. This may have been a spectacle watched by pilgrims to the site, and the incentive to make the long journey to Göbekli Tepe from the surrounding camps would have been the feasts held made from the animals sacrificed on these prehistoric altars.

From these early beginnings, the essential elements of this ritual would have eventually been "domesticated" at the later settlements of the region in a more

ritualized form of skull preservation and reverence as part of staying connected to ancestors. The roots of this ancestral worship however bear the marks of hunters and nomadic gatherers, not settled farmers. Only later, when edible plants were cultivated, a more relevant to farming, likewise astronomically inspired, shift of focus from the stars in the north and south to the Sun and Moon in the east and west may have occurred explaining the variant circle orientations of Enclosures A and F, the latter of which ^{14}Carbon-dates to the late 9th Millennium B.C.E. (De Lorenzis & Orofino, 2015: pp. 43-47). A similar more symbolic, and less actual, reenactment of a primeval, more physical, ritual would be the Mouth Opening Ceremony of Dynastic Egypt as the stylized version of the Statuette Making Ritual or the ritual killing and revival of an Egyptian king during the Heb-Sed festival as the stylized, i.e. more civilized, version of the actual killing of an ageing chieftain having to prove that he can still lead a hunt to procure food for his tribe or else be killed (Helck, 1987, Chapter 2, page 5).

The advent of the Neolithic Revolution in this model rested on a unifying concept of a superhuman, yet both human-like and bull-like spiritual being, a god, which brought otherwise scattered people into one location to build a monument for worship, perform rituals for the afterlife, and feast. Why this unifying spirituality arose during and after the end of the Younger Dryas in southeast Anatolia and was eventually buried together with the monumental creations expressing it remains unknown. It may have been epic ecological changes caused by a wide-spread catastrophe (Schoch, 2012: p. 99-103; Sweatman & Tsikritsis, 2017: p. 243), it may have been a charismatic shaman or tribal leader, and even distant origin cultural transfer has been proposed including from Australia (Fenton, 2017)[6]. Whatever inspired it—fear, charisma, or cultural transfer from elsewhere—the congregation it catalyzed made innovation[7], division of labor, and team work more likely, eventually (circa 8th millennium B.C.E. or earlier) setting the stage for the domestication of plants (Demiral, 2016: pp. 131-133) and animals by larger groups of people united by the same beliefs conveyed by its powerful spiritual symbolism. This, then, may have been the real catalyst in Cauvin's model of the origins of agriculture: The communal spirit of interacting in a large group captivated by iconic symbols recognized by many as opposed to hunting in the isolation of small bands composed only of a few closely-nit family members. It is this power of symbols which we think was the driving force behind the desire to record them in stone and the word for God fittingly would be the first such symbol recorded, making it the first word in recorded history.

[6]Bruce Fenton has suggested a close match between the H-symbols carved onto Pillars 18 and 28 at Göbekli Tepe and an Australian Aboriginal symbol for exchanging knowledge seen on some Churinga stones.

[7]For example, stone cutting and transporting technology and the insight by accidental discovery that the seeds of edible wild grasses could be planted in the soil in the spring to produce a new edible plant in the fall, thus providing a renewable food source.

Dedication

We would like to dedicate this paper to Professor Dr. Klaus Schmidt, the discoverer of Göbekli Tepe's megalithic stone circles, who tragically passed away on 20 July 2014.

Conflicts of Interest

The authors declare no conflicts of interest regarding the publication of this paper.

References

Ames, K. M. (1994). The Northwest Coast: Complex Hunter-Gatherers, Ecology, and Social Evolution. *Annual Review of Anthropology, 23,* 209-229. https://doi.org/10.1146/annurev.an.23.100194.001233

Baines, J. (2004). The Earliest Egyptian Writing: Development, Context, Purpose. In S. D. Houston (Ed.), *The First Writing: Script Invention as History and Process* (pp. 150-189). Cambridge: Cambridge University Press.

Banning, E. B. (2011). So Fair a House: Göbekli Tepe and the Identification of Temples in the Pre-Pottery Neolithic in the Near East. *Current Anthropology, 52,* 619-660. https://doi.org/10.1086/661207

Bouckaert, R., Lemey, P., Dunn, M., Greenhill, S. J., Alekseyenko, A. V., Drummond, A. J., Gray. R. D., Suchard, M. A., & Atkinson, Q. D. (2012). Mapping the Origins and Expansion of the Indo-European Language Family. *Science, 337,* 957-960. https://doi.org/10.1126/science.1219669

Cauvin, J., (2000). *The Birth of the Gods and the Origins of Agriculture*. Cambridge, UK: Cambridge University Press. (English Translation by Trevor Watkins)

Cavalié, O., & Jónsson, S. (2013). Block-Like Plate Movements in Eastern Anatolia Observed by InSAR. *Geophysical Research Letters, 41,* 26-31. https://agupubs.onlinelibrary.wiley.com/doi/epdf/10.1002/2013GL058170 https://doi.org/10.1002/2013GL058170

Collins, A. (2014). *Göbekli Tepe-Genesis of the Gods, the Temple of the Watchers and the Discovery of Eden*. Rochester, VT: Bear & Company.

Collins, A. (2015). *First Pictorial Representation of Göbekli Tepe T-Pillars Found on Tiny Bone Plaque*. http://www.andrewcollins.com/page/articles/plaque.htm

Collins, A. (2017). *Göbekli Tepe's Vulture Stone: A Warning across Time or Signpost to the Land of the Dead? Putting into Perspective the Carved Imagery on Göbekli Tepe's Pillar 43 in Enclosure D*. http://www.andrewcollins.com/page/articles/sagittarius.htm

Damerow, P. (2006). The Origins of Writing as a Problem of Historical Epistemology. *Cuneiform Digital Library Journal, 2006,* 1.

De Lorenzis, A., & Orofino, V. (2015). New Possible Astronomic Alignments at the Megalithic Site of Göbekli Tepe, Turkey. *Archeological Discovery,* 3, 40-50. https://doi.org/10.4236/ad.2015.31005

Demiral, S. (2016). *Recent Researches in Interdisciplinary Sciences* (Chapter 10, pp. 130-138). Sofia: St. Kliment Ohridsky University Press. https://www.researchgate.net/publication/311400755_Domestication_of_Wheat_in_Anatolia_from_the_Neolithic_Period_to_the_Iron_Age

Ercan, M. (2015). *Signs of World's First Pictograph Found in Göbeklitepe*.

http://www.hurriyetdailynews.com/signs-of-worlds-first-pictograph-found-in-gobeklitepe--85438

Fenton, B. (2017). *A Global Aboriginal Australian Culture? The Proof at Göbekli Tepe*. New Dawn Magazine, 2017. http://ancientnews.net/2017/10/13/a-global-aboriginal-australian-culture-the-proof-at-gobekli-tepe/

Goedegebuure, P. (2016). *Luwian Hieroglyphs: An Indigenous Anatolian Syllabic Script*. Lecture Given at the Oriental Institute. https://www.youtube.com/watch?v=fOd_hodh7Mc

Goedegebuure, P. (2017). Hittite Anatolia Cornucopia of Cultures in Contact. *News & Notes Member Magazine, 234,* 4-9. https://oi.uchicago.edu/sites/oi.uchicago.edu/files/uploads/shared/docs/Publications/nn234.pdf

Goldwasser, O. (2016). The Birth of the Alphabet from Egyptian Hieroglyphs in the Sinai Desert. In D. Ben-Tor (Ed.), *Pharaoh in Canaan: The Untold Story* (pp. 166-170). Exhibition Catalogue. Jerusalem: Israel Museum. https://www.academia.edu/38014205/Goldwasser_O._2016._The_Birth_of_the_Alphabet_from_Egyptian_Hieroglyphs_in_the_Sinai_Desert_in_Daphna_Ben-Tor_ed._Pharaoh_in_Canaan_the_untold_story._Exhibition_catalogue._Jerusalem_Israel_Museum

Gresky, J., Haelm, J., & Clare, L. (2017). Modified Human Crania from Göbekli Tepe Provide Evidence for a New Form of Neolithic Cult. *Science Advances, 3,* e1700564. http://advances.sciencemag.org/content/3/6/e1700564/tab-pdf https://doi.org/10.1126/sciadv.1700564

Helck, W. (1987). *Untersuchungenzur Thinitenzeit*. Wiesbaden: Otto Harrassowitz Verlag.

Hodder, I. (2011). The Role of Religion in the Neolithic of the Middle East and Anatolia with Particular Reference to Çatalhöyük. *Paléorient, 37,* 111-122. https://doi.org/10.3406/paleo.2011.5442

Hodder, I. (2012). Çatalhöyük. A Summary of Recent Work Concerning Architecture. In B. Söğüt (Ed.), *Festschrift for Ahmet A. Tırpan* (pp. 303-314). İstanbul: Ege Yayınları. https://static1.squarespace.com/static/53568703e4b0feb619b78a93/t/53679823e4b0124f24031679/1399298083752/catalhoyuk-a-summary-of-recent-work-concerning-architecture.pdf

Hoskins, M., Hochsieder, P., & Knösel, D. (1990). The Orientation of the Taulas of Menorca (2): The Remaining Taulas. *Archeoastronomy, 21,* 37-48.

Laroche, E. (1960). *Les Hiéroglyphes Hittites*. Paris: Éditions du Centre National de la Recherche Scientifique (CNRS).

Lull, J., & Belmonte, J. A. (2009). *In Search of Cosmic Order*. Cairo: Supreme Council of Antiquities Press.

Magli, G. (2013). *Possible Astronomical References in the Project of the Megalithic Enclosures of Göbekli Tepe*. Cornell University Library Online.

Magli, G. (2016). Sirius and the Project of the Megalithic Enclosures at Gobekli Tepe. *Nexus Network Journal, 18,* 337-346. https://doi.org/10.1007/s00004-015-0277-1 https://doi.org/10.1007/s00004-015-0277-1d

Putney, A. (2014). *Resonance at Göbekli Tepe, Turkey*. http://www.human-resonance.org

Sandars, N. K. (1979). The Religious Development of Some Early Societies. In P. R. S. Moorey (Ed.), *The Origins of Civilization* (pp. 103-127). Oxford: Clarendon Press.

Schmidt, K. (2000). Göbekli Tepe, Southeastern Turkey. A Preliminary Report on the

1995-1999 Excavations. *Paléorient, 26,* 45-54. https://doi.org/10.3406/paleo.2000.4697

Schmidt, K. (2011). Göbekli Tepe: A Neolithic Site in Southeastern Anatolia. In S. R. Steadman, & G. McMahon (Eds.), *The Oxford Handbook of Ancient Anatolia* (pp. 917-933). Oxford: Oxford University Press.

Schmidt, K. (2012). *Lecture, Sanliurfa*. https://youtu.be/J1PDX0NjwsA

Schoch, R. (2012). *Forgotten Civilization: The Role of Solar Outbursts in Our Past and Future*. Rochester, VT: Inner Traditions.

Schoch, R. M. (2017). Controversies Concerning the End of the Last Ice Age. In R. M. Schoch, & R. Bauval (Eds.), *Origins of the Sphinx: Celestial Guardian of Pre-Pharaonic Civilization* (pp. 445-466). Rochester, VT: Inner Traditions.

Senner, W. (1991). *The Origin of Writing*. Lincoln: University of Nebraska Press.

Smith, M. (2009). V. Gordon Childe and the Urban Revolution: A Historical Perspective on a Revolution in Urban Studies. *Town Planning Review, 80,* 3-29. http://www.public.asu.edu/~mesmith9/1-CompleteSet/MES-09-Childe-TPR.pdf https://doi.org/10.3828/tpr.80.1.2a

Sweatman, M. B., & Tsikritsis, D. (2017). Decoding Göbekli Tepe with Archaeoastronomy: What Does the Fox Say? *Mediterranean Archaeology and Archaeometry, 17,* 233-250.

Waal, W. (2013). Writing in Anatolia. The Origins of the Anatolian Hieroglyphs and the Introduction of the Cuneiform Script. *Altorientalische Forschungen, 39,* 287-315.

Zangger, E. (2016). *The Luwians: A Lost Civilization Comes Back to Life*. Lecture at Klosters. https://youtu.be/1DNyA90f_aw

Archaeological Discovery, 2019, 7, 54-74
http://www.scirp.org/journal/ad
ISSN Online: 2331-1967
ISSN Print: 2331-1959

The Pillboxes of Lanzarote (Spain)

Giancarlo T. Tomezzoli

Etno-Archaeological Observatory, Munich, Germany
Email: gt21949@gmx.de

How to cite this paper: Tomezzoli, G. T. (2019). The Pillboxes of Lanzarote (Spain). *Archaeological Discovery, 7,* 54-74.
https://doi.org/10.4236/ad.2019.72004

Received: January 20, 2019
Accepted: February 19, 2019
Published: February 22, 2019

Abstract

The visit of Lanzarote took place on November 2018 and allowed to note that its defensive military structures were composed by pillboxes, truncated, pyramidal bases, ground emplacements and artillery bases. This article describes the Playa Blanca and Punta del Papagayo coastal defences and the artillery bases of Mirador del Rio for concluding that today, at about seventy years from the WWII end, they appear in good preservation state and their integrity not particularly menaced by possible further expansions of touristic and residential centres. In addition, their study provided examples of WWII Spanish military architecture and gave hints about the defence concepts involved in the WWII Lanzarote defence.

Keywords

WWII, Canary Islands, Lanzarote, Operation Pilgrim, Coastal Defences, Artillery, Pillbox, Bunkers, Spain

1. Introduction

The presence of bunkers in the Canary Islands comes to my attention through an article (Anonym, 2018) dedicated to the Operation *Pilgrim*. After having reminded the 10th June 1941 meeting between Hitler and the Spanish minister Serrano Suñer dedicated to the possible invasion of Gibraltar (Operation *Felix*) and summarized the strategic importance of Gibraltar for the British interests, the article introduced the Operation *Pilgrim*, to be accomplished on September 1941, concerning the British invasion of the Canaries in case of loss of Gibraltar. Suspecting such an invasion Hitler offered anti-aircraft guns and Stukas to be stationed to the islands and the dictator Franco sent concrete to build bunker systems. However, the German Operation *Barbarossa* and contrasts between Hitler and Franco caused Gibraltar to remain British and no invasion of the Canaries.

2. Historical Information

During the WWII and the years after, the Independent Artillery Group of Canaries (*Grupo de Artilleria Independiente de Canarias*) was present in the Canaries. It included a 1st artillery section in Tenerife, a 2nd artillery section in Gran Canaria, a Fono-localization group based on Belgian TEPA devices mod. D-20 already used by the Republican *Flak* during the Spanish Civil War. The 5th Field Group of the Artillery Regiment n. 7 (*V Grupo de Campaña del Regimiento de Artilleria n.* 7) based on 105/22 mm Vickers guns was present in Tenerife and La Palma. The artillery guns were protected against naval fire and bombardments by casemates resisting up to 200 kg bombs. On the islands were present machine guns as the 7 mm Hotchkiss mod. 1914, 8 mm Fiat mod. 1935, 6.5 mm Fiat mod. 1914, 8 mm Saint Etienne mod. 1907 and 7 mm Colt mod. 1914. Only the first two were suitable for both offensive and defensive actions, the heavier last two were suitable only for static defence. Lacking radars, air exploration and recognition units, the surveillance was based on observatories on the island elevations (Defensa, 2015).

The 12th Coastal Battery of the Artillery Regiment n. 7, based on 102/45 mm Ansaldo guns, was in Los Guinchos in Santa Cruz de la Palma. La Palma defence was completed by the 42nd and 131st Infantry battalions, the 231st and 331st Infantry battalions in case of total mobilisation, an artillery groups based on two 105/22 mm Vickers batteries, two 37 mm anti-tank guns and two 7.92 mm *Flack* guns. The request to Germany of a 150 mm battery, 5 field batteries, machine guns, projectors, radios and other materials remained unsatisfied. However, La Palma, which due to its orography offered only two possible landing areas, was judged not a defence priority. Much more important were the defence of Tenerife and Gran Canaria at West and Fuerteventura and Lanzarote, with their ports and air fields, at East. An artillery battery with command bunker was built in locality Matas Blancas, Pajara coast (Fuerteventura) (Defensa, 2015).

The allied secret services, formed by personnel members of British enterprises, of the British Las Palmas consulate, of the US Tenerife consulate and simple residents were active in acquiring information about the islands defences. The transit of workers and construction materials were monitored and communicated in different ways. For limiting their activities, large island coast portions were declared military zones with strict access interdiction to the nearby farmers and inhabitants. During the construction of a battery in Gran Canaria, the Guardia Civil reported foreign subjects engaged in espionage activities (Defensa, 2015).

In Lanzarote (29˚2'19"N, 13˚39'1"W) (**Figure 1**), a battery, today disappeared, was built on 1941 at Punta Limones in Playa Blanca. It included a command bunker and Arisaka guns, which crossed their fire with that of the 150 mm Ordoñez mod. 1885 guns of the Corralejo battery in Fuerteventura for controlling La Bocayna channel between the two islands. The 107 mm Arisaka Meiji mod. 38 gun was the Japanese modified version of the 100 mm Krupp mod. 1904 gun,

built on 1914 under licence by Arisaka in 120 exemplars for the Russian Army. During the Spanish Civil War 74 of these guns were used by the People's Republican Army (*Ejército Popular de la República*—EPR) and passed to the Spanish Army after the Civil War conclusion. Notwithstanding their range of 12 km, because of their rare calibre and their reduced number, they were destined to the coastal defence from the Canaries up to Fernando Poo Island. Another battery was already built at Mirador del Rio as consequence of the Hispano—American war of 1898, based on 150 mm Ordoñez mod. 1885 guns. It remained as reserve up to 1940 when the bad preservation state of its guns rendered problematic its reactivation. In this period various ameliorations were made including the construction of a command bunker (Defensa, 2015). According to another source (Axis, 2012) two batteries were present at Mirador del Rio at that time, the first provided with 2 × 76 mm guns and the second with 4 × 210 mm howitzers.

In Lanzarote the coastal artillery comprised 4 × 152 mm Putilov guns and 3 × 107 mm Arisaka guns. The Putilov guns were a Russian version of a Schneider gun. They were sent by the URSS to the EPR during the Civil War. They had a range of 15 km, but their reduced number, their not normalized calibre and the few ammunitions available caused them to be used for the coastal defence and retired in July 1942. In the island were built 75 bunkers, 25 double and 50 single, 56 machine gun nests and 5 casemates. The thick of the casemate walls were 80 cm up to 1 m for those much exposed to enemy landing (Defensa, 2015).

Figure 1. A Atlantic Ocean; B La Bocayna channel; L Lanzarote island; G La Graciosa island; 1 - 12 Playa Blanca coastal defences; 13 - 27 Punta del Papagayo coastal defences; 28 - 42 Mirador del Rio artillery bases (ZoomEarth).

The denomination "pillbox" applied to casemates and bunkers is current in literature (Pillbox Study Group, 2016-2018) although its meaning is uncertain. In this article it will be applied to small, camouflaged bunkers provided with one or more fire apertures, encountered during the visits.

3. Playa Blanca Coastal Defences

The visit took place on 25th November 2018 and, proceeding West to East; the identified military structures were the following.

A well preserved old lighthouse (1) (**Figure 2**) (28˚51'19.89"N, 13˚52'21.06"W), built in local, magmatic, black breeks, composed by a one floor, square building about 20 × 20 m, and a protruding cylindrical light tower, about 10 m high and 4 m in diameter. The south facade had one window at each side of the light tower, the west facade had two windows, the north facade had an entrance and a window and the east facade had two windows and an entrance. All the windows were closed by breeks and a layer of concrete. The entrance on the east façade was closed by breeks with a superimposed concrete layer and the entrance on the north facade was closed by a brown painted, wood door. The interior was inaccessible; therefore, the internal room organization remained unknown. Satellite images show an internal, central square court. The facade walls were covered by recent graffiti. The flat roof had a balustrade and a protruding chimney at the corner between the east and the south facades. At the top, the tower preserved a white painted top circular portion in which an exit gave access to a circular balcony, and, superimposed, the metallic rests of the lamp house. No defensive structures were identified around the old lighthouse.

A well preserved truncated, pyramidal base (2) (**Figure 3**), 0.5 m high, 1.5 m each side at the base, 1 m each side at the top, built by local, small magmatic pebbles mixed with concrete (Tomezzoli, 2015a). A thin concrete layer covered portions of the side surfaces. No cylindrical, metallic shaft was at the centre of the top surface.

A well preserved truncated, truncated, pyramidal base (3) (**Figure 4**), 0.5 m high, 1.5 m each side at the base, 1 m each side at the top, built by local, small magmatic pebbles mixed with concrete. A concrete thin layer covered the side

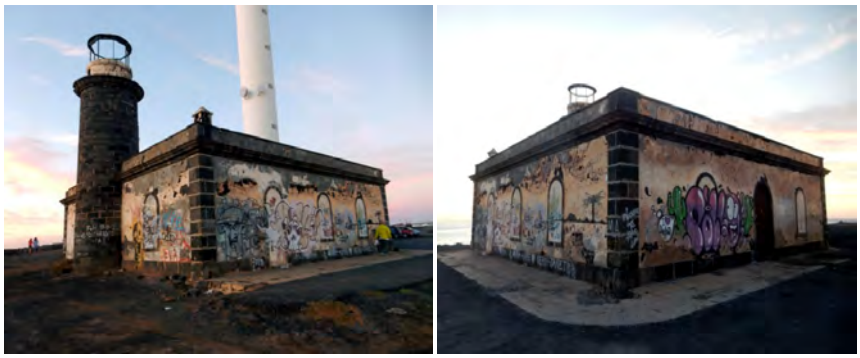

(a) (b)

Figure 2. Old lighthouse (1)—(a) South and east facade; (b) East and north facade.

(a) (b)

Figure 3. Truncated, pyramidal base (2)—(a) General view, on the foreground Playa Blanca; (b) Thin concrete layer covering portions of the side surfaces.

(a) (b)

Figure 4. Truncated, pyramidal base (3)—(a) General view, on the foreground, Lobos island in the middle and Fuerteventura island on the right; (b) Local, small magmatic pebbles mixed with concrete and cylindrical, metallic shaft at the centre of the square top surface.

surfaces letting visible traces of the construction formwork. A cylindrical, metallic shaft, about 5 cm in diameter with a central hole slightly protruded at the centre of the top surface.

A well preserved one floor, rectangular pillbox bunker (4) (28˚51'38.76"N, 13˚51'30.81"W) (**Figure 5**), about 8 × 5 m, 2.5 m high. Rather robust, it fallen from the cliff to the beach without structure damages. Its front facade had two fire apertures, about 30 × 40 cm, each with splinter guards and its rear facade had one entrance. The facades and the roof were covered by local, sea rounded magmatic stones. A single room formed its interior.

A quite well preserved truncated, pyramidal base (5) (**Figure 6(a)**), 0.5 m high, 1.2 m each side at the base, 1 m each side at the top, partially buried in the modern touristic promenade. It was built by local, small magmatic pebbles mixed with concrete. A thin concrete layer covered portions of the side surfaces. No cylindrical, metallic shaft was at the centre of the top surface.

A bad preserved truncated, pyramidal base (6) (**Figure 6(b)**), 0.5 m high, 1.5 m each side at the base, 1 m each side at the top, built by local, small magmatic pebbles mixed with concrete. Part of the top was lost letting visible internal bigger

(a)

(b)

(c)

Figure 5. Pillbox (4)—(a) General view; (b) Front side with two fire apertures provided with splinter guards; (c) Rear side with entrance.

(a)

(b)

Figure 6. (a) Truncated, pyramidal base (5) general view; (b) Truncated, pyramidal base (6) on the foreground left Punta del Papagayo coast.

local, magmatic stones mixed with the concrete. A cylindrical, metallic shaft, about 5 cm in diameter with a central hole slightly protruded at the centre of the top surface.

A well preserved two floors, bunker (7) (28˚51'22.84"N, 13˚50'25.5"W) (**Figure 7**) at Punta Limones. Its entrance on its rear side, on the touristic promenade, was closed by an iron gate letting the interior inaccessible. However, the entrance let visible an access stair toward an underground floor. Local, magmatic,

well placed black breeks were visible on the stair sides. The underground floor room organization remained unknown. Another stair from the underground floor gave access to the single room of its emerging portion, the floor of

(a)

(b)

(c)

(d)

(e)

(f)

(g)

(h)

Figure 7. Punta Limones bunker (7)—(a) General view; (b) Rear side with entrance closed by an iron gate; (c) Entrance stair; (d) Emerging portion; (e) Front aperture of the single room; (f) Entrance in the single room; (g) Single room floor; (h) Bunker front side.

which was partially invaded by trash and had no trace of a gun or projector basement. The single, 180˚ room aperture was closed by cylindrical shafts. The bunker interior preserved its original white painting. The emerging portion and its coverage were camouflaged with local, magmatic stones, but a collapsed, upper portion of the aperture let visible its armoured concrete structure. The possible rests of the battery of Punta Limones, if any, were buried or destroyed during the construction of a nearby, modern touristic apartment complex.

A ground emplacement (8) (28˚51'19.96"N, 13˚48'38.91"W) (**Figure 8**) located in front of the 1769 Castillo del Áquila (28˚51'21.12"N, 13˚48'38.68"W). It was formed by a trench about 6 m long, 2 m large connected to a circular cavity about 6 m in diameter.

A well preserved one floor, rectangular pillbox (9) (28˚51'28.03"N, 13˚47'55.67"W) (**Figure 9(a)**), about 5 × 4 m, partially buried in the terrain. The entrance and the single fire aperture were buried in the terrain, so that the inspection of its interior was not possible. Its facades and coverage were camouflaged with local, rounded magmatic stones, and a thin, horizontal concrete layer covered a portion of the front facade.

A well preserved one floor, rectangular pillbox (10) (28˚51'27.44"N, 13˚47'55.23"W) (**Figure 9(b)**), about 5 × 4 m, partially buried in the terrain. The entrance and the single fire aperture with splinter guards were buried in the terrain, so that the inspection of its interior was not possible. Its facades and coverage were camouflaged with local, rounded magmatic stones.

A possible, circular ground emplacement (11) (**Figure 9(c)**), about 3 m in diameter was on a side of the pillbox (10).

A well preserved truncated, pyramidal base (12) (**Figure 9(d)**), 0.5 m high, 1.5 m each side at the base, 1 m each side at the top, built by local, small magmatic pebbles mixed with concrete, letting visible traces of the construction formwork. A cylindrical, metallic shaft, about 5 cm in diameter with a central hole slightly protruded at the centre of the top surface.

(a) (b)

Figure 8. Ground emplacement (8)—(a) General view, on the foreground Castillo del Áquila on the left and Playa Blanca; (b) Access trench, on the foreground Lobos and Fuerteventura.

(a) (b)

(c) (d)

Figure 9. (a) Pillbox (9) front side; (b) Pillbox (10) front side with fire aperture provided with splinter guards; (c) Possible ground emplacement (11) on a side of the pillbox (10); (d) Truncated, pyramidal base (12).

4. Punta Del Papagayo Coastal Defences

The visit took place on 27th November 2018 and continuing toward East the identified military structures were the following.

A well preserved truncated, pyramidal base (13) (28˚51'25.1"N, 13˚47'54.46"W) (**Figure 10(a)**), 0.5 m high, 1.5 m each side at the base, 1 m each side at the top, built by local, small magmatic pebbles mixed with concrete, letting visible traces of the construction formwork. A scratch on one side let visible a portion of its internal armored concrete. A cylindrical, metallic shaft, about 5 cm in diameter

with a central hole slightly protruded at the centre of the top surface.

A ground emplacement (14) (28˚51'18.2"N, 13˚47'50.75"W) (Figures 10(b)-(d)) located at a cliff edge. It was formed by a two central, circular cavities about 5 m in diameter, each connected to an external, semi-circular trench following the cliff edge.

A well preserved truncated, pyramidal base (15) (Figure 10(e)), 0.5 m high, 1.5 m each side at the base, 1 m each side at the top, built by local, small magmatic pebbles mixed with concrete, letting visible traces of the construction formwork. A cylindrical, metallic shaft, about 5 cm in diameter with a central hole slightly protruded at the centre of the top surface.

A well preserved, white painted geodetic stone (16) (Figure 10(f)) formed by a cubic base with a superimposed cylinder. An oval, green plate on the base informed:

(a) (b) (c) (d) (e) (f)

Figure 10. (a) Truncated, pyramidal base (13) General view, in the foreground Playa Blanca and Castillo del Áquila; (b)-(d) Ground emplacement (14); (e) Truncated, pyramidal base (15), in the foreground Castillo del Áquila; (f) Geodetic stone (16).

INSTITUTO GEOGRAFICO NACIONAL VÉRTICE GEODESICO
LA DESTRUCCION DE EST ASEGNALESTA' PENADA POR LA LEY

without indication of the construction date.

A well preserved one floor, rectangular pillbox (17) (28˚51'16.77"N, 13˚47' 31.91"W) (Figure 11(a)), about 5 × 4 m, near Playa Mujeres. Its entrance was on a road and had a single fire aperture directed toward the beach. Its facades and coverage were camouflaged with local, rounded magmatic stones.

A well preserved truncated, pyramidal base (18) (Figure 11(b)), 0.5 m high, 1.5 m each side at the base, 1 m each side at the top, built by local, small magmatic pebbles mixed with concrete, letting visible traces of the construction formwork. No cylindrical, metallic shaft was at the centre of the top surface.

A well preserved one floor, rectangular pillbox (19) (28˚51'15.22"N, 13˚47'

(a) (b) (c) (d) (e) (f)

Figure 11. (a) Pillbox (17) near Playa Mujeres, general view; (b) Truncated, pyramidal base (18); (c)-(d) Pillbox (19) at Playa Mujeres near a middle-age guard tower; (e) Pillbox (20) at Playa Mujeres, general view; (f) Truncated, pyramidal base (21).

40.04"W) (Figure 11(c) & Figure 11(d)), about 8 × 5 m, 2.5 m high, at the East side of Playa Mujeres. Its front facade had two fire apertures about 30 × 40 cm, without splinter guards and its rear facade had one entrance. The facades and the coverage were camouflaged with local, sea rounded magmatic stones. A single room without furniture formed its interior.

A well preserved one floor, rectangular pillbox (20) (28˚51'5.26"N, 13˚47'30.75"W) (Figure 11(e)), about 8 × 5 m, 2.5 m high, at the West side of Playa Mujeres. Rather solid, it fallen from the cliff to the beach without structure damages. Its front facade had two fire apertures, about 30 × 40 cm, each with splinter guards, the rear façade was buried in the terrain. The facades and the coverage were camouflaged with local, sea rounded magmatic stones. A concrete layer was under the apertures.

A bad preserved truncated, pyramidal base (21) (Figure 11(f)), 0.5 m high, 1.5 m each side at the base, 1 m each side at the top, built by local, small magmatic pebbles mixed with concrete. Part of the top was lost. The sides were deeply eroded letting visible layers corresponding to the construction formwork. A cylindrical, metallic shaft, about 5 cm in diameter with a central hole slightly protruded at the centre of the top surface.

A well preserved one floor, rectangular pillbox (22) (28˚51'0.74"N, 13˚47'28.98"W) (Figures 12(a)-(c)), about 8 × 5 m, 2.5 m high, leaning against the cliff and partially buried in the sand. Its front facade had two fire apertures, about 30 × 40 cm, without splinter guards and its side facade had one entrance. The facades

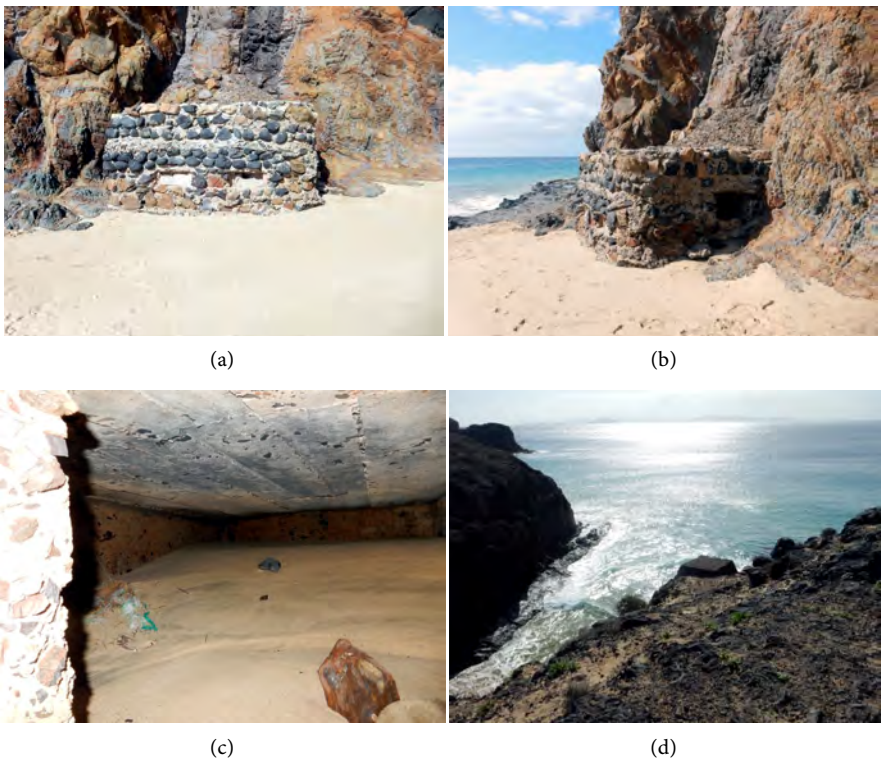

(a) (b) (c) (d)

Figure 12. (a) Pillbox (22) front side view; (b) Pillbox (22) rear side view; (c) Pillbox (22) interior view; (d) Truncated, pyramidal base (23).

and the coverage were camouflaged with local, sea rounded magmatic stones. The sand invaded the single room of its interior. The walls appeared orange coloured; on the ceiling the traces of the construction formwork were clearly visible.

A well preserved truncated, pyramidal base (23) (28˚50'58.59"N, 13˚47'27.26"W) (**Figure 12(d)**), 0.5 m high, 1.5 m each side at the base, 1 m each side at the top, built by local, small magmatic pebbles mixed with concrete. A cylindrical, metallic shaft, about 5 cm in diameter with a central hole slightly protruded at the centre of the top surface.

A well preserved one floor, rectangular pillbox (24) (28˚50'38.92"N, 13˚47' 20.21"W) (**Figures 13(a)** & **Figure 13(b)**), about 8 × 5 m, 2.5 m high leaning

(a)

(b)

(c)

(d)

(e)

Figure 13. (a) Pillbox (24) general view; (b) Pillbox (24) front view; (c) Truncated, pyramidal base (25); (d) Pillbox (26) general view; (e) Pillbox (26) front view.

against the cliff. Its front facade had two fire apertures, about 30 × 40 cm, without splinter guards. The facades and the coverage were camouflaged with local, sea rounded magmatic stones.

A well preserved truncated, pyramidal base (25) (**Figure 13(c)**), 0.5 m high, 1.5 m each side at the base, 1 m each side at the top, built by local, small magmatic pebbles mixed with concrete. A cylindrical, metallic shaft, about 5 cm in diameter with a central hole slightly protruded at the centre of the top surface.

A well preserved one floor, rectangular pillbox (26) (28˚50'37.11"N, 13˚46'48.17"W) (**Figure 13(d)** & **Figure 13(e)**), about 8 × 5 m, 2.5 m high. Its front facade was provided with two fire apertures, about 30 × 40 cm, without splinter guards. The facades and the coverage were camouflaged with local, sea rounded magmatic stones. An elongated, concrete layer was above the apertures.

A well preserved bunker (27) (28˚50'24.69"N, 13˚47'16.57"W) (**Figure 14**) completely buried in the terrain. Its entrance had an upper front side, formed by rounded magmatic stones allowing estimating at about 1 m the thickness of its coverage. A concrete, square pit, about 2 × 2 m was at one side of the entrance. Local, small magmatic pebbles mixed with concrete were visible on the entrance stair sides. The stair introduced in a 1st room with walls and ceiling formed by local, small magmatic pebbles mixed with concrete, letting visible traces of the construction formwork. A separation wall allowed entrance to a 2nd room with walls and ceiling formed by local, small magmatic pebbles mixed with concrete, letting visible traces of the construction formwork. On one side a square column protruded from a wall in correspondence with another protruding square column

(a)

(b)

(c)

(d)

(e)

(f)

(g)

(h)

Figure 14. (a) Bunker (27) general view toward south; (b) Square pit and access stair; (c) Access stair with upper front side formed by rounded magmatic stones; (d) 2nd room with protruding square columns and niche, in the middle, separation wall and access stair; (e) 2nd room, on the left wall three curved fixation for a disappeared support or device, in the middle separation wall; (f) Curved exit; (g) Exit ramp with protective walls; (h) Bunker (26) general view toward north.

and a niche on the opposed wall. On one wall three, curved fixations joints and on the opposite wall four holes indicated disappeared supports or devices. A separation wall provided the entrance to a 3rd room with walls and ceiling formed by local, small magmatic pebbles mixed with concrete, letting visible traces of the construction formwork. The 3rd room gave access to a curved passage towards a ramp about 30 m long with protective side walls made by local, magmatic stones. The ramp floor appeared not provided with rails. The bunker interior preserved its original white painting. All the original furniture disappeared and no trace

was visible of supports for an illumination system.

5. Mirador Del Rio Artillery Batteries

The visit took place on 29th November 2018, but, unfortunately, the Mirador del Rio military structures (Figure 15) were on a terrain with access interdiction; therefore they were only indirectly identified. Satellite images permitted to recognize a 1st battery (1) (29˚12'52.73"N, 13˚28'51.28"W) and a 2nd battery (2) (29˚12'52.73"N, 13˚28'51.28"W). The identified structures (Figure 16) of the 1startillery battery (1), near the modern Mirador del Rio parking, were the following.

A well preserved oval emplacement (28) (29˚12'51.89"N, 13˚28'51.64"W) (Figures 16(a)-(c)), about 10 × 8 m, 1.5 m deep. Its interior was partially covered by terrain and vegetation. On one side an entrance gave access to a corridor and an interior floor.

A buried rectangular bunker (29) (29˚12'52.33"N, 13˚28'51.45"W) (Figure 16(a), Figure 16(d)), about 10 × 6 m. Its coverage appeared in a good preservation state.

A well preserved bunker (30) (29˚12'52.51"N, 13˚28'51.15"W) (Figure 16(d)) similar to the bunker (7) (Figure 7) at Punta Limones. Its emerging portion had a single room with a single 180˚ aperture. The external surface of the emerging portion, except the rear side, and its coverage were camouflaged with local, magmatic stones. The presence of an underground floor was not possible to be ascertained.

A possible rectangular bunker (31) (29˚12'53.22"N, 13˚28'51.01"W) (Figure 16(a)), about 10 × 6 m, on the cliff edge. Its coverage appeared in a good preservation state.

The identified structures of the 2nd battery (Figure 17), about 300 m north from the 1st battery, were the following.

A circular artillery emplacement (32) (29˚12'57.13"N, 13˚28'42.93"W) about 10 m in diameter, having a single entrance, without protection, wall toward the Lanzarote interior and a support for a gun at its centre.

A circular artillery emplacement (33) (29˚12'57.68"N, 13˚28'42.46"W) about

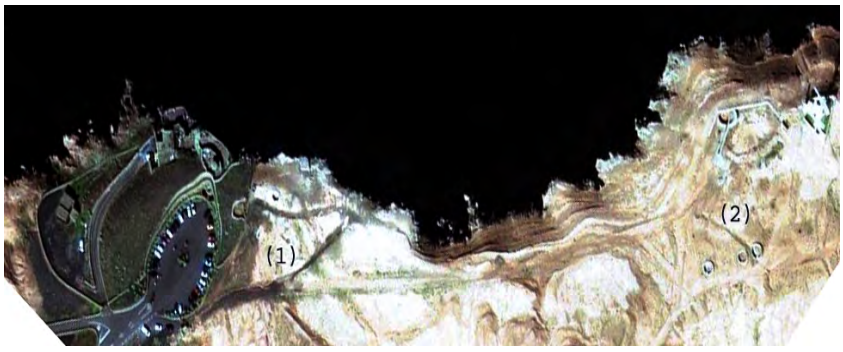

Figure 15. Mirador del Rio artillery batteries—(1) 1st artillery battery; (2) 2nd artillery battery (ZoomEarth).

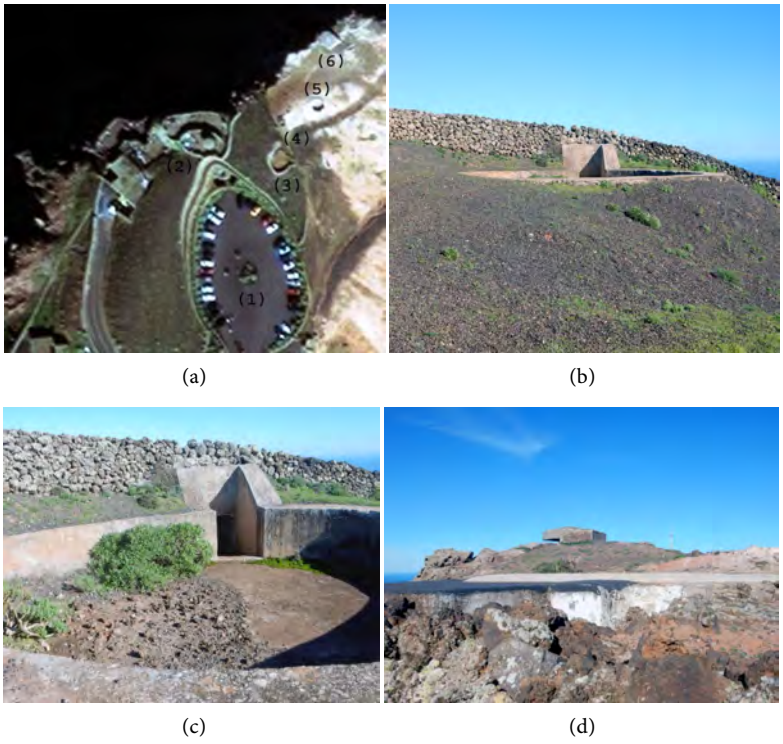

Figure 16. Mirador del Rio 1st artillery battery—(a) 1st artillery battery components (ZoomEarth): (1) parking, (2) Mirador del Rio restaurant, (3) oval emplacement (28), (4) buried rectangular bunker (29), (5) bunker (30), (6) possible rectangular bunker (31); (b)-(c) Oval emplacement (28) with entrance to the interior floor; (d) Buried rectangular bunker (29), in the foreground, bunker (30).

Figure 17. Mirador del Rio 2nd artillery base—(1) circular artillery emplacement (32); (2) circular artillery emplacement (33); (3) circular artillery emplacement (34); (4) embankment (35); (5) three sided barrier wall (36); (6) oval artillery emplacement (37); (7) trench (38); (8) buried bunker (39); (9) small construction (40); (10) cistern (41); fort or modern house (42) (ZoomEarth).

10 m in diameter, having a single entrance, without protection wall, toward the Lanzarote interior and a support for a gun at its centre.

A circular artillery emplacement (34) (29˚12'57.94"N, 13˚28'42.28"W) about 10 m in diameter, having a single entrance, without protection wall, toward the Lanzarote interior. It was located close to circular artillery emplacement (33) and a support for a gun at its centre was not clearly identifiable.

An arcuate embankment (35) (29˚12'52.33"N, 13˚28'51.45"W).

A three sided barrier wall (36) (29˚12'59.43"N, 13˚28'44.05"W) having a central portion about 40 m long on the cliff edge and two wings about 20 m long, each angled about 45˚ with respect to the central portion. The three sided barrier wall (36) together with the arcuate embankment (35) formed a closed area.

An oval artillery emplacement (37) (29˚12'59.1"N, 13˚28'44.24"W) about 15 × 10 m, leaning against the east side of the central portion of the three sided barrier wall (36), similar to the oval emplacement (28) but apparently without entrance to internal or underground rooms.

A trench (38) (29˚12'58.5"N, 13˚28'44.1"W) about 30 m long.

A buried bunker (39) (29˚12'52.33"N, 13˚28'43.87"W) about 10 × 5 m, similar to the bunkers (29), (31), connected by the trench (38) to the oval emplacement (37).

A small construction (40) (29˚12'58.27"N, 13˚28'43.68"W) about 5 × 3 m.

An open cistern (41) (29˚12'59.75"N, 13˚28'43.15"W) about 10 × 5 m.

A fort or modern house (42) (29˚13'0.27"N, 13˚28'42.82"W) contoured by a triangular wall about 30 m each side.

6. Discussion

The Lanzarote defences were composed mainly by pillboxes, truncated, pyramidal bases, ground emplacements and artillery bases.

The pillboxes were of simple project, easy and rapid to build. They were not built on island elevations from which dominate beaches and large spaces but letting them exposed and easy to identify. Rather, they were built low along the coasts or directly on the beaches. Normally, they were located at one side of short beaches, as pillboxes (22), (24), (26), or at both sides of longer beaches so as to cross their fire against landing forces, as the pillboxes (19)-(20) at the East and West sides of Playa Mujeres. The local, magmatic stones covering their surfaces reinforced the pillboxes structure and provided camouflage. This, combined with theirlocation increased their defensive effectiveness against landings and survival capacity. Their single, internal room functioned as close combat room and lodgement for a crew of at least an officer and three or four soldiers armed with personal, light machine guns. The pillboxes (9)-(10), (17), provided with a single fire aperture, correspond to single bunkers (Defensa, 2015). The pillboxes (4), (19)-(20), (22), (24), (26), provided with two fire apertures, correspond to double bunkers (Defensa, 2015). The recent construction formwork traces observed on the ceiling of pillbox (12) would indicate the pillbox con-

struction in the period of the WWII.

The truncated, pyramidal bases, as (2)-(3), (5)-(6), (12)-(13), (15), (18), (21), (23), (25), because of their low, difficult to identify structure, were instead located on relatively elevated positions from which dominate beaches and large spaces. They were generally close to pillboxes for supporting their fire. The bases hosted probably one offensive and defensive or static defence machinegun served by two or three soldiers. However the way in which a machine gun was mounted on a truncated pyramidal base and the machine guns designated for said bases remain unknown.

The ground emplacements were located in relatively elevated positions to dominate large spaces were the fire of machine guns on said bases was judged insufficient. They offered better protection to one or two officers and about five to ten soldiers armed with personal machine guns and one or more offensive and defensive or static defence machine guns. The ground emplacements (8), (11), (13) correspond to machine gun nests (Defensa, 2015).

The two floors, bunker (7) corresponds to the command bunker of the Punta Limones battery (Defensa, 2015). The cylindrical shafts on the 180˚ aperture were placed later after its construction. During the WWII the aperture was free, and the reduced room dimensions, the absence on its floor of a basement for a heavy gun or a projector suggests that it was mainly used for observation and fire direction of the battery. It probably hosted a telemeter although the presence of one or more defence machine gun mounted on its own bases for far and close defence cannot be excluded. Its armoured concrete structure confirms its construction during the WWII. The battery guns were field guns on their own carriage (Defensa, 2015), therefore they needed only circumstance places not necessarily artillery emplacements. The battery personnel lodged outside the bunker in disappeared barracks or tents.

The bunker (27) lodged personnel in the 1st and 2nd rooms and one or two guns mounted on wheeled support in the 3rd room to be conducted and placed outside through the ramp. The square pit (Tomezzoli, 2017) near the entrance was probably an open, drinking water cistern although the function of external observation post for the surveillance and protection of the bunker by one soldier cannot be ruled out. The absence of trace of a kitchen and latrines at the interior and a chimney at the exterior, indicate that the personnel lodged outside the bunker in disappeared barracks or tents and reached the bunker in case of alarms.

The bunkers (7), (27), (29)-(31), (39) correspond to casemates (Defensa, 2015).

The pillboxes and casemates of Lanzarote both for project and construction appear rather different with respect to the German *Regelbauten* (Rudi, 1998) and Italian bunkers (Tomezzoli, 2012, 2013, 2015b) and more similar to the British pillboxes type 22-28 (Pillbox Study Group, 2016-2018).

The old lighthouse was an excellent observation place for controlling the naval traffic in La Bocayna channel and in the open Atlantic Ocean. It was probably

operated by a small garrison.

The geodetic stone (15), of recent construction (Tomezzoli, 2017), certainly was not an original component of the Lanzarote defences.

The satellite images confirm that Mirador del Rio hosted two artillery batteries (1)-(2) (Axis, 2012). The 1st battery (1) comprised a command bunker (30), similar to the command bunker (7) of the artillery battery of Punta Limones, on the cliff edge for early discovery of objectives far in the ocean. The oval emplacement (28), retracted from the cliff edge probably hosted one or the two 77 mm guns (Axis, 2012). The rectangular bunkers (29), (31) hosted materials and personnel in service at the 1st battery (1). The 2nd artillery battery (2) apparently had no command bunker. Therefore, its fire was directed by the 1st artillery battery (1) command bunker (30). The three circular artillery emplacements (32)-(34) and the oval artillery emplacement (37) hosted three of the four 210 mm howitzers (Axis, 2012). The buried bunker (39), the small construction (40) and the possible fort (42) hosted materials and personnel in service at the 2nd battery (1). The trench (38) allowed protected access of the personnel from the buried bunker (39) to the gun in the oval emplacement (37). The closed area formed by the three sided barrier wall and the embankment (35) probably hosted disappeared barracks or tents for the personnel provided with drinking water through the open cistern (41).

7. Conclusion

Today, at about seventy years from the WWII end, to which they did not participated, the discovered Lanzarote military structures appear in good preservation state and, because of their location on the beaches, on the cliffs, and at Mirador del Rio, their integrity is not particularly menaced by possible further expansions of touristic and residential centres. In addition, their study provided examples of WWII Spanish military architecture and gave hints about the defence concepts involved in the WWII Lanzarote defence.

Acknowledgements

I thank very much Mr. L. Martinuzzi for having provided me with the article mentioning the presence of bunkers in Lanzarote and for having guided me to the discovery of said bunkers.

Conflicts of Interest

The author declares no conflicts of interest regarding the publication of this paper.

References

Anonym (2018). Churchill's Plan to Invade the Canaries. *Gazette Life, February 2018, 19*.

Axis History Forum (2012). https://forum.axishistory.com/viewtopic.php?t=194258

Defensa de Canarias (2015). *El Plan Pilgrim Foro El Gran Capitan*.

http://www.elgrancapitan.org/foro/viewtopic.php?p=765014

Pillbox Study Group (2016-2018). Types of Pillboxes. http://www.pillbox-study-group.org.uk/types-of-pillbox/

Rudi, R. (1998). *Typologie du Mur de l'Atlantique.* Beetsterwaag. NUGI 923.

Tomezzoli, G. (2012). Militärische Anlagen bei Verona. *DAWA Nachrichten, Ausgabe 59, 4-27.*

Tomezzoli, G. (2013). Der Bunker der Wehrmacht-Werkehrdirektion Italien in Verona. *DAWA Nachrichten, Ausgabe 62, 4-13.*

Tomezzoli, G. (2015a). The Ero Vili and the Atlantic Wall. *Advances in Anthropology, 5,* 183-204. https://doi.org/10.4236/aa.2015.54018

Tomezzoli, G. T. (2015b). A Small WWII Italian Bunker in Heraclea Minoa (Sicily). *Advances in Anthropology, 5, 144-151.* https://doi.org/10.4236/aa.2015.53013

Tomezzoli, G. T. (2017). The WW II German Stutzpunkt on the Menez-Hom (Finistere-FR). *Archaeological Discovery, 5, 224-237.* https://doi.org/10.4236/ad.2017.54013

Archaeological Discovery, 2019, 7, 75-83
http://www.scirp.org/journal/ad
ISSN Online: 2331-1967
ISSN Print: 2331-1959

The Monitoring Mast of the WWII German W/T Station Be-2

Giancarlo T. Tomezzoli

Etno-Archaeological Observatory, Munich, Germany
Email: gt21949@gmx.de

How to cite this paper: Tomezzoli, G. T. (2019). The Monitoring Mast of the WWII German W/T Station Be-2. *Archaeological Discovery, 7,* 75-83.
https://doi.org/10.4236/ad.2019.72005

Received: February 16, 2019
Accepted: March 29, 2019
Published: April 1, 2019

Abstract

A first visit on the site of the WWII German W/T station at Mont Saint-Michel de Brasparts (Brittany-FR), cover name Be-2, indicated sometime as either B 2 or B2, on 21st December 2009 allowed the identification of many components and to evaluate their preservation state. The secret Interpretation Report NO. G.590 of the No. 80 Wing RAF of 6th October 1942, dedicated to Be-2, mentioned a cable trench and a short mast may be for calibration purposes, not identified during the first visit, motivated the further visits on 13th - 14th May 2017 for searching their possible vestiges. This article presents the vestiges discovered, the feature of the mast and the reconstruction of Be-2.

Keywords

Atlantic Wall, France, Finistère, Saint-Michel, Brasparts, *Luftwaffe*, *FuSan* 724/725, Be-2, *Bernard*, Calibration, Monitoring Mast

1. Introduction

The WWII German W/T (Wireless/Transmission) station Be-2, indicated sometime as either B 2 or B2, at Mont Saint-Michel de Brasparts (Finistère-FR), was provided with an antenna *Telefunken FuSan* 724/725 *Bernard* for driving *Luftwaffe* bombardiers on their targets on Great Britain. The interest for this sophisticated and technologically advanced W/T station motivated a first visit for identifying the Be-2 surviving components and determining their preservation state.

2. First Be-2 Visit

The first visit of the Be-2 site (**Figure 1**) took place on 21st December 2009, following a suggestion of prof. Mevel of the Rennes University after a visit of the WWII German radar camp of Monterfil (Dupont et al., 2007), and permitted to identify the following Be-2 components (Tomezzoli & Dupont, 2011).

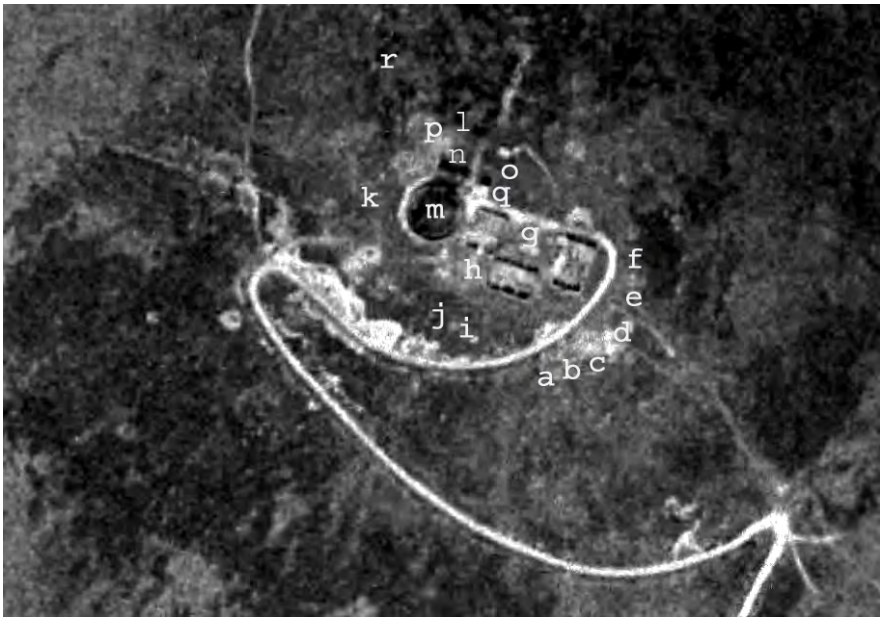

Figure 1. Be-2 site: (a) Concrete niches; (b) Emplacement for machine or *Flak* guns; (c) Possible stone bunker; (d) Emplacement for machine or *Flak* guns; (e) Emplacement for machine or *Flak* guns; (f) Emplacement for machine or *Flak* guns; (g) Barrack emplacement; (h) Cisterns; (i) Bunker; (j) Trench; (k) Bunker; (l) Two antenna cable anchorages; (m) *FuSan* 724/725 circular support; (n) 17th century Saint Michel chapel; (o) Ruins of a small construction; (p) Two antenna supports; (q) Transformer cabin; (r) Possible *Flak* emplacement.

Two well preserved concrete niches (a), about 1.5 × 1.0 × 0.6 m, one above the other on a side of the mount for storing ammunitions and/or materials for the nearby machine or *Flak* guns. On their vertical sides the joints for two closing wood doors were still visible.

A ground emplacement (b) in the terrain, probably for machine or *Flak* guns. Built by local stones, it was in a degraded preservation state and completely invaded by the vegetation.

A possible 5 × 3 m stone bunker (c), near the ground emplacement. Built by local stones, it was in a degraded preservation state. It cannot be excluded that originally it was an old country construction probably reused during the WWII as guardhouse or commandment place for the nearby machine or *Flak* guns.

A 2 × 2 m emplacement (d) for machine or *Flak* guns. Built by local stones it was in a degraded preservation state and completely invaded by the vegetation.

Two emplacement (e)-(f) for machine or *Flak* guns. Excavated directly in the terrain, they were in a degraded preservation state.

A barrack emplacement (g) for three barracks. The barracks were gone and only their traces and their concrete foundations were visible on the terrain.

Two well preserved 3 × 2 m open cisterns (h).

A possible bunker (i) buried in the terrain, having four 60 × 30 cm rectangular apertures on one side of its well preserved coverage, in correspondence with an aperture on one of its side walls. Probably it hosted an emergency electrical ge-

nerator and the apertures ensured its cooling. According to another interpretation (Tomezzoli & Dupont, 2011), it was the basis of a disappeared latrine barrack.

A degraded trench (j) still visible on the terrain, connecting the bunkers (i) and (k).

A bunker (k) (48˚21'00N, 003˚56'41W) about 9 × 4 m, buried in the terrain. The descending entrance, oriented toward the *FuSan* 724/725, was filled by terrain; therefore the inspection of the interior was not possible. It was probably a protection bunker for the personnel or for Be-2 instrumentation in case of attack.

Two antenna cable anchorage supports (l) at their places on the terrain.

The *FuSan* 724/725 support (m) formed by a concrete, circular ring about 20 m in diameter and 1.5 m in width, with a circular, concrete construction about 4 m in diameter at its centre, slightly emerging from the terrain. The internal room of the construction was completely filled by terrain; therefore the inspection of the interior was not possible. The circular rail on the ring for the rotation of the *FuSan* 724/725 disappeared and only its fixation joints emerged from a light concrete layer covering the ring.

The well preserved 17th cen. Saint Michel chapel (n) having a short bell tower superimposed on its front facade. One of its doors was open, but surprisingly its interior was not vandalized or disfigured by modern graffiti. The chapel and its bell tower evidently have not interfered with the *FuSan* 724/725 radio emissions.

The ruins of a small construction (o), still intact in the year 1991, probably hosting a transmission centre.

Two antenna supports (p) at their places on the terrain.

A possible emplacement (r) for a *Flak* gun, excavated on a mount side.

At that time, the vestiges of the transformer cabin (q) (**Figure 1**) were not recognized and because of the lack of information, the vestiges of the cable trench (b) and the monitoring mast (d) (**Figure 2**) were not searched at all.

Figure 2. Be-2 site—(a) Mont Saint-Michel de Brasparts; (b) Cable trench; (c) Stone straight alignment; (d) Monitoring mast concrete support.
C3639-0431_1948_MISSIONBETAGNE9_0168, n˚168, Argentique, 16/04/1948.

3. Interpretation Report NO. G.590

The secret Interpretation Report NO. G.590 of the No. 80 Wing RAF of 6th October 1942 (Dörenberg, 2019b) based on photographs taken on 24th September 1942 during the Sortie Q/21, at the Contact Scale: 1:30,000 (F.L.12"), in the Locality: Morlaix, described a W/T station on the Mount St. Michel de Brasparts in the following terms:

1) Map Reference: (a) pinpoint: 48˚21'03"N. 3˚56'46"W.

2) Position: On the summit of Mt. St. Michel, of the Montagne D'Arret, 1282 ft. a.s.l.

3) Description:

a) the installation consists of a low circular wall, about 98 ft. external diam., 4 ft. thick upon which was mounted diametrically a framework superstructure similar in appearance to the one at the W/T station at le Bois Julien, near Desvres. The two principal points of similarity are the heavy appearance of the superstructure, and the fact that it does not extend at either end beyond the circle.

b) The superstructure is presumably rotatable, as what appears to be trolley wheels visible at each end of it.

c) From the site a cable trench leads off on a bearing of 284°, for a distance of about 950 ft., terminating at a short mast, also in common with le Bois Julien, which may be for calibration purposes.

d) The installation appears to be still under construction and operating quarters, etc. have either not yet been constructed or may be underground and possibly covered with camouflage.

SECRET	DISTRIBUTION	Reports	Photos.
…	…	…	…

The operating quarters mentioned in the rapport are visible in an after war French air reconnaissance image of Be-2 (**Figure 1**) and correspond to the components (a)-(r) identified in the first visit.

The mention of a cable trench and a calibration mast (**Figure 2**) not identified during the first Be-2 visit motivated the further visits on the Be-2 site.

4. Second Be-2 Visit

The second Be-2 visit, in the light of the Interpretation Report NO. G.590 information, took place on 13th May 2017. The weather initially rainy and windy permitted to ascertain that the Be-2 components (a)-(p), (r) remained in the preservation state evaluated in the first visit. But the following storm did not permitted the identification of cable trench vestiges and consequently to arrive to possible mast vestiges (**Figure 2**).

5. Third Be-2 Visit

The third Be-2 visit took place on 14th May 2017 with good weather. It was possible to recognize on the terrain the traces of the foundations of the transformer cabin (q) close to the chapel (n) and to ascertain that the cable trench (b)

(Figure 2) was no longer identifiable.

To arrive to the mast vestiges (d), I followed a stone straight alignment (c) visible on the terrain, which passed in proximity of their position (Figure 2 & Figure 3). The stones were posed directly on the terrain with no trace of excavation. Search for possible rests of cables or other military devices between or under the stones gave no result.

The mast concrete support (48˚21'7.86"N, 3˚57'28.14"W) (Figure 4) was at about 915 m from the chapel along the stones straight alignment, displaced about 43 m south from it. The support was formed by a square concrete foundation about 3 × 3 meters just emerging from the terrain and a square mast metallic fixing frame. A thick concrete layer covered the foundation surface and the fixing frame. A failure on two sides of the concrete layer let visible part of the fixing frame. Originally, it was formed by four 2 m long, 20 cm high, L-shaped riveted metal beams fixed by bolts to the foundation. Only two beams were actually in place on the foundation, buried in the concrete layer. Three mast leg rests were in place on the fixing frame and emerged from the concrete layer. Two leg rests, along a fixing frame diagonal, appeared sawn. In particular, one of them (Figure 4(e) & Figure 4(f)), free from the concrete layer, showed the rivets securing it to the fixing frame near a bolt securing the fixing frame to the foundation. The third leg rest (Figure 4(a)), at a corner of the fixing structure, appeared not only sawn, but also broken along a vertical line and curved toward the exterior of the foundation. The pebbles of the EroVili (Tomezzoli & Marzin, 2015) mixed to the foundation concrete and the concrete layer were clearly visible.

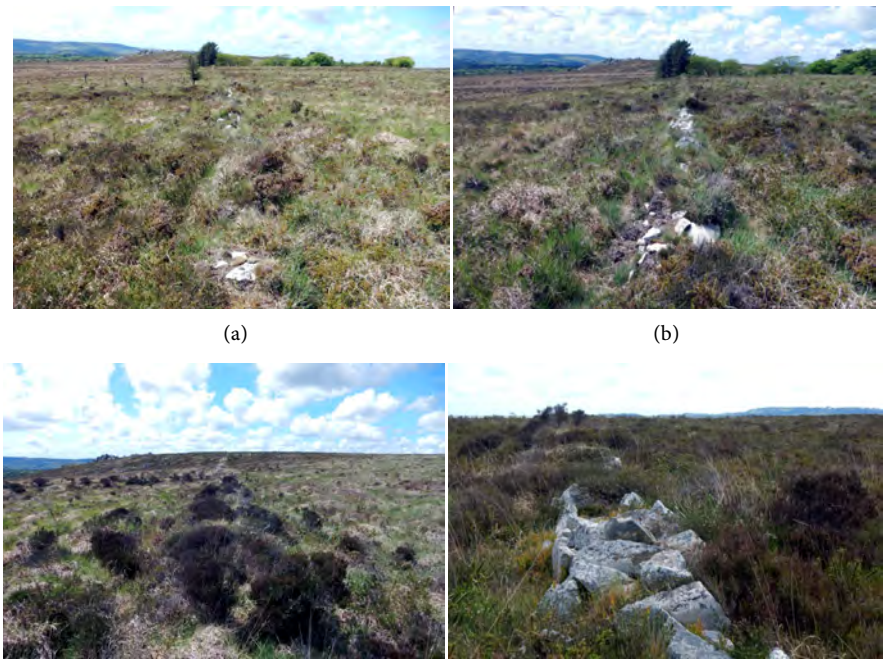

(a) (b)

(c) (d)

Figure 3. Third Be-2 visit—(a)-(d) stone straight alignment.

(a) (b)

(c) (d)

(e) (f)

Figure 4. Mast vestiges—(a) Mast support, north vision; (b) Mast support, east vision, on the background the 17th cen. Saint Michel chapel (n) on Mont Saint Michel de Brasparts; (c) Mast support, south vision, on the background group of basaltic blocks emerging from the terrain; (d) Mast support, west vision; (e) Mast fixing structure, thick concrete layer with EroVili pebbles; (f) Mast fixing structure, rivets and fixing bolt.

6. Discussion

The secret Interpretation Report NO. G.590 informs that on 6th October 1942, i.e. well after the conclusion of the Battle of Britain, Be-2 was under construction, but the cable trench and the mast were already in place.

The mast was about 921 meters distant from the centre of the Be-2 ring, i.e. not about 950 ft. (289.5 m) from the site as written in the Report. The mast distance is the longest compared to those of the other W/T German Be stations. The mast distance was selected for avoiding radio interferences from other Be-2 devices, allowing measuring the *FuSan* 724/725 radiation pattern cleanly and avoiding saturation of the mast receiver (Dörenberg, 2019a). The cable trench

disappeared either because both it was covered by terrain and vegetation, in which case the cable, probably an Erdkabel RLM with external insulation and four conductors (Dörenberg, 2019a), would be still in place, or was filled up by terrain after the cable removal.

The fixing portion beams and the sawn legs indicate that the mast was a metal, square and four legs truss mast. Thus, it was similar at least to the masts of Be-0 at Trebbing/Glau (Germany), Be-3 at Le-Bois-Julien (France), Be-10 at Hundborg (Denmark) and Be-11 at Trzebnica (Poland), this last preserving (2014) (Dörenberg, 2019a) the mast still in place. The mast was therefore 20 m high (Dörenberg, 2019a) and manufactured according to a common, normalized project, by the same company *Hein, Lehman & Co* which manufactured the other masts and, under *Telefunken* licence, the antennae *FuSan* 724/725 (Dörenberg, 2019a).

The mast therefore comprised a lightning protection, a remote, tunable diode receiver near the base and a vertical 2.6 meters high antenna on the top (Dörenberg, 2019a). The *FuSan* 724/725 was thus calibrated by emitting its signals toward the mast antenna from where the signals collected by the receiver, through the trench cable, reached the concrete construction of the *FuSan* 724/725 support (m) where they were analysed for deducting and eventually correcting the features of the emitted signals. The mast also monitored (Dörenberg, 2019a) the *FuSan* 724/725 emitted signals during its normal functioning.

The concrete foundation was similar in dimensions to the foundations of Be-0, Be-9, Be-10, Be-11 and Be-13 at Buke (Germany), but it was the only one in which the foundation surface and the mast fixing structure were covered by a concrete layer. The purpose of this layer was to insulate the mast fixing structure from corrosion due to the weather. Differences in the construction technics indicate that the foundations were manufactured by local companies or artisans under the supervision of personnel of the *Organization Todt*.

The failure of the concrete layer on two sides, the absence of the corresponding two fixing frame beams and the third mast leg rest sawn but also broken and curved toward the exterior of the foundation, indicate that during the mast removal, at least three legs were sawn and the mast fall in the direction of the third leg. The fall of the mast on the terrain broken and curved the third leg rest. During the fall, the fourth leg tore up the two missing fixing frame beams which caused the observed failure of the thick concrete layer. The mast, and may be the cable, was removed between the 1946, when the antenna *FuSan* 724/725 was sold for demolition, and the 16th April 1948 date to which it is no longer visible in the air reconnaissance image C3639-0431_1948_MISSIONBETAGNE9_0168 (**Figure 2**).

The transformer cabin (q) was a classical transformer cabin connected to the local/regional electrical system (Dörenberg, 2019a). It was completely demolished after the WWII because un-useful after the *FuSan* 724/725 removal and anti-aesthetically close to the chapel (n).

The absence of rests of cables or other military devices along the stone straight alignment indicates that it was simply a stone border between two adjacent pri-

vate estates.

The now available information permits to reconstruct Be-2 as it was during the WWII and as seen by the personnel in service (Figures 5-7).

7. Conclusion

The information in the secret Interpretation Report NO. G.590 allowed the

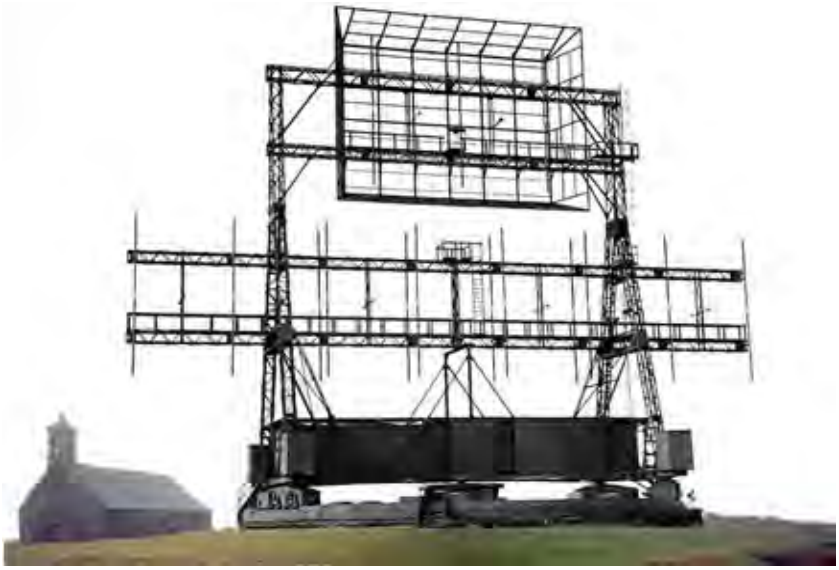

Figure 5. Be-2 reconstruction—*FuSan* 724/725 during normal functioning, on the left the 17th cen. chapel (n) on the top of Mount Saint Michel de Brasparts.

Figure 6. Be-2 reconstruction—*FuSan* 724/725 during calibration, seen from the base of the monitoring mast.

Figure 7. Be-2 reconstruction—monitoring mast seen from the base of the *FuSan* 724/725.

identification of Be-2 components not identified in the first Be-2 site visit, to clarify details of the *FuSan* 724/725 calibration and monitoring and to proceed to the Be-2 reconstruction at more than seventy years after the WWII end. I hope that this article would stimulate the interest of archaeologists, scholars and a large public for the German sophisticated and technologically advanced structures mixed with the defence structures of the Atlantic Wall.

Acknowledgements

I desired to thank prof. Mevel F. for his suggestion to visit the Be-2 site and Mr. Dörenberg F. for his permission to insert in this article information coming from his website and for his revision of the present article.

Conflicts of Interest

The author declares no conflicts of interest regarding the publication of this paper.

References

Dörenberg, F. (2019a). Hellschreiber-FuSan 724/725 "Bernard" Radio Navigation Ground Station. https://www.nonstopsystems.com/radio/hellschreiber-modes-other-hell-statns.htm#top-of-page

Dörenberg, F. (2019b). Interpretation Report NO.G.590. https://www.nonstopsystems.com/radio/pdf-hell/article-hell-NA123-NA126-127.pdf

Dupont, Ph., Fresil, Y., & Tomezzoli, G. (2007). *Deutsche Militärbauten bei Rennes, DAWA Nachrichten* (Ausgabe 49, pp. 56-66). Köln: Verlag Harry Lippmann.

Tomezzoli, G., & Dupont, Ph. (2011). *Die Drehfunkfeueranlage Bernhard auf dem Mont Saint-Michel de Brasparts* (DAWA Nachrichten, Ausgabe 57, pp. 4-15). Köln: Verlag Harry Lippmann.

Tomezzoli, G., & Marzin, Y. (2015). The EroVili and the Atlantic Wall. *Advances in Anthropology, 5, 183-204*. https://doi.org/10.4236/aa.2015.54018

Archaeological Discovery, 2019, 7, 84-91
http://www.scirp.org/journal/ad
ISSN Online: 2331-1967
ISSN Print: 2331-1959

Evidence of Bat Sacrifice in Ancient Maya Cave Ritual

James E. Brady

Department of Anthropology, California State University Los Angeles, Los Angeles, CA, USA
Email: jbrady@calstatela.edu

How to cite this paper: Brady, J. E. (2019). Evidence of Bat Sacrifice in Ancient Maya Cave Ritual. *Archaeological Discovery, 7,* 84-91.
https://doi.org/10.4236/ad.2019.72006

Received: February 11, 2019
Accepted: March 29, 2019
Published: April 1, 2019

Abstract

Excavations conducted in Naj Tunich, Petén, Guatemala encountered a number of slabs of speleothem curtains that were used as altars. Two of these contained bat skeletons suggesting that bats had been sacrificed as part of ceremonies carried out in the cave. A review of the archaeological literature documents that remains of bats has been reported in burials, caches, and constructions. Naj Tunich, however, is the first instance of sacrifice occurring in a cave which raises the problem of distinguishing between cultural as opposed to natural deposition. A series of propositions are advanced for dealing with the issue.

Keywords

Maya, Cave, Bat, Sacrifice, Ritual, Naj Tunich

1. Introduction

Maya cave archaeology as a self-conscious area of investigation dates only to the end of the last millennium (Scott, 2012). The rapid expansion of the field since that time has produced an impressive corpus of data concerning Maya ritual and, in the process, field archaeologists involved in cave studies have begun to more critically examine their artifact assemblages. Classes of material not previously collected have been shown to have ritual significance (Brady et al., 1997; Brady & Prufer, 1999; Brady & Rissolo, 2006; Halperin et al., 2003). A similar situation appears to be the case with animal bones where cave investigators, with the notable exception of David Pendergast (1969, 1971, 1974), have tended not to save and analyze faunal remains. Even where samples have been saved, however, the bones of species that inhabit or frequent caves are often not given close consideration since one cannot rule out their being naturally deposited (Luther, 1974: p. 63; Pohl, 1983: p. 90; Pollock & Ray, 1957: p. 642; Savage, 1971: p. 83).

While it is recognized that natural deposition is a problem, attention needs to be focused on the implications of overlooking locally occurring species from the analysis of ritual sites. It may be that species inhabiting ritual sites are precisely those selected for utilization. Lévy-Bruhl (quoted in Eliade, 1958: p. 367) observes that, "To these natives, a sacred spot never presents itself to the mind in isolation. It is always part of a complexus of things which includes the plant or animal species which flourished there at various seasons...". This very point has been documented in the ethnographic record for the Maya area where plants and animals found near cenotes [a cave feature] are associated with the rain god and the plants are those preferentially selected for ritual use (Redfield, 1941: p. 117). The problem for cave archaeologists is that their field or analytical procedures might tend to exclude from consideration the remains of those species which are potentially most intimately associated with cave ritual. This paper will offer evidence that this is the case with respect to bat remains.

2. Bat Utilization at Naj Tunich

Naj Tunich, a large cave site located in southern Peten, Guatemala, was first reported in 1980 (**Figure 1**). Archaeological investigation was carried out between 1981 and 1989 (Brady, 1989). Clear evidence of bat utilization was recovered during stratigraphic excavations conducted in 1988 on the Balcony, a highly modified area of the cave entrance. By filling and leveling behind several dozen retaining walls, the Maya created a two-tiered platform that served as the cave's central ceremonial stage (**Figure 2**). In one excavation at the base of the retaining walls, a large slab of stalagmitic curtain was found set on top of a number of rocks to form an altar. The horizontally set piece of formation was flat except for a naturally occurring trough which ran the length of the stone. This trough was completely filled with charcoal, presumably from burning copal. While not containing faunal remains, this find was important in establishing the use of this type of formation as an altar top and, therefore, special care was taken when similar pieces were found in an excavation on the second level of the Balcony. An excavation unit opened in the cave floor just below Structure 1 found a piece of that formation with the headless skeleton of a bat in the trough (**Figure 3**). To recover all of the bones, the formation was removed and the dirt from the trough was carefully passed through a fine sieve. While the location of the bones in the trough is suggestive of cultural utilization, the possibility, however unlikely, was recognized that the bat could have died of natural causes and fallen into the trough.

The removal of the formation uncovered a second, similar piece with the trough facing downward. When this formation was removed, a second, complete, bat skeleton was revealed in the soil impressed along the trough. While the first skeleton might have been a highly unusual example of natural deposition, the second in the downward-facing trough removes any doubt of its cultural origin.

Figure 1. Map of Central America showing the location of Naj Tunich in Guatemala.

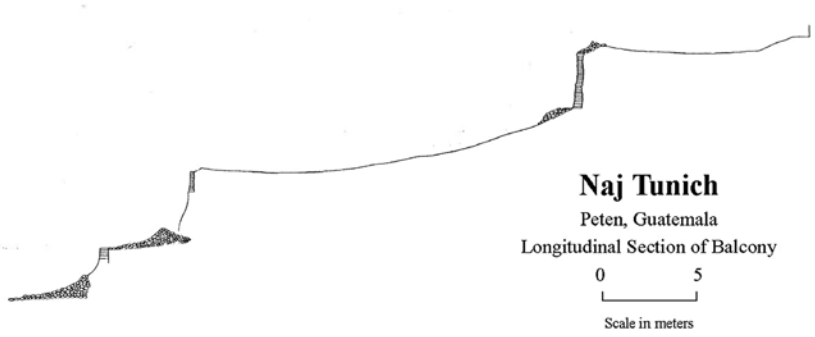

Figure 2. Cros section view of the balcony.

Figure 3. The bat skeletons were found in excavation on the floor below Structure 1.

Actually, these discoveries culminated several days of discussion over the possibility of a cultural use of bats engendered by the recovery of a far larger quan-

tity of bat bone along use-floors than in pre-cultural levels in another excavation unit. This is exactly the opposite of what one would expect. On our initial visit to Naj Tunich, it was noted that our presence scared away bats living in the tunnels and they did not return the subsequent day. The posting of a guard shortly after this was enough to keep the bats from returning. Thus, even a moderate use of the cave in ancient times should have been sufficient to cause the bats to relocate.

During ceremonies conducted in Naj Tunich by Q'eqchi' Maya in 1988 and 1989, huge quantities of copal incense were burned, filling the entire entrance chamber with clouds of thick black smoke. Such burning appears to be a common feature of Maya ceremonies, so much so, that the K'iche' refer to rituals as "burnings" (Cook, 1986: p. 139). During the archaeological survey at the site, it was noted that many of the ceiling formations had been smoke blackened in ancient times so it is suspected that ancient ceremonies would have regularly filled the entrance in the same way as modern ceremonies. Once again, it is unlikely that bats would have remained in the presence of such pollution. Finally, the ceilings above our excavations were checked for evidence of bat marking which might indicate that the area had been used for perching since most naturally occurring skeletons would be deposited below such an area. None were found and it should be noted that all the bats encountered on our first visit had been roosting in the tunnels rather than the entrance. For all these reasons, the presence of large quantities of bat bones along use-floors appears anomalous and suggests cultural utilization.

3. Archaeological Distribution of Bat Remains

Although bat remains are infrequently reported, they are not unknown in the archaeological literature. Large quantities of bones from two species of bat and several species of rat were found in the excavation of a series of altars in Temple E-II at Uaxactun (Ricketson & Ricketson, 1937: p. 55). Mixed with the bones were over 70 fragments of jade as well as flint and shell in a matrix of fine black soil. Associated with the altars was Cist C-8 containing two ceramic vessels placed lip to lip inside of which were to two obsidian lancets that the authors suggest were used for sacrificing the animals. A vampire bat skull was found in Burial A33 (Smith, 1950: p. 98) at the same site along with the bones of a rat, mouse, shrew and a small bird. Skull fragments of an unidentified specie of bat was also recovered in Burial E4 along with bones of a bird and the skull of a rodent (Ricketson & Ricketson, 1937: p. 141).

The skull of a leaf-nosed bat was found in Cache C5 beneath a bench at San Jose, Belize (Thompson, 1939: pp. 189-190). The cache contained a tubular bone ornament, a jade pebble, a pottery spindle whorl and a human tooth. The bones of bats and birds were also found in a cache at Palenque (Fernandez, 1943: p. 55). The bones were deposited in two cylindrical vessels with sherd lids so these are clearly not intrusive. In addition to the bones were fragments of jade and

"anthropoid extremities". Two bat skulls were recovered from a burial at San Gervasio but these were treated as intrusive (Hamblin, 1984: p. 162). Ignacio Bernal (1949: p. 95) investigated a number of tombs in Coixtlahuaca, Oaxaca that were so well sealed that there was no dust on the floors. He found quantities of bat skeletons in vessels that had been left as funerary offerings.

Willian Coe (1990: p. 673) discovered bat bones along will bones of deer, dog, cottontail, toad, lizard, snake, tortoise and 150 bird bones in a Preclassic chultun in the bedrock located beneath the centerline of several later structures in Tikal's North Acropolis. In addition, 200 Pomacea and 400 animal teeth were recovered. Twenty-five human bones were also found. Based on the unusual assemblage Coe (1990: p. 674) suspected that the chultun may have had an "esoteric" function.

Kitty Emery (2004) lists bat remains from the Cueva de los Quetzales among the "sacred animals" found in the faunal assemblage. Although she acknowledges that the species may have been utilized outside the cave and deposited there only at the conclusion of the ritual, her analysis frequently mentions the "underworld" association of the species in attempting to link them to the cave context. The archaeologists who excavated the site, however, clearly see all the material from the deposit as being utilized in rituals conducted in the central plaza of the site of Las Pacayas before being dropped down an opening in the plaza into the cave below (Brady & Rodas, 1995: pp. 30-31).

4. Discussion and Conclusion

While the proposal that bats were utilized for ritual purposes is not new, the idea does not appear to be widely accepted. Based on the cases available to him, Coe (1959: p. 64) states that, "The practice of sacrificing birds (and bats) and subsequently depositing them as votive offering evidently was established widely and persistently among the Maya". Given the fact that Coe produced fewer examples of bat offerings than cited above, his assertion was more provocative than convincing. Pohl (1983: p. 85) also raises the possibility that bats, along with rats and birds that live in caves, were used in ritual because of their cave association. Our data support the proposition that bats were considered by the ancient Maya to be a ritual fauna and suggest that they may have played an important role in cave ritual.

Brady and Coltman (2016) have recently discussed the meaning of bat depictions in Maya iconography, ethnohistory and ethnography. While the range of possible meanings is interesting, none show a bat actually being sacrificed and so do not provide direct information about the role of bats in the rituals documented at Naj Tunich. Lopez Medel's *Relación* of 1612 mentions that a woman to be sacrificed in the Sacred Cenote at Chichen Itza was instructed in what to ask for when meeting the gods (Tozzer, 1941: p. 223). In this way, the victim was both an offering to the gods and a messenger from the society. We find this to be a very reasonable model to apply to bat sacrifice. Brady and Coltman (2016: pp.

231-233) see bats as frequently being in the role of messengers for earth deities. Tozzer (1941: p. 180, note 948) notes that sacrifice is particularly prominent in petitions for rain and the Maya consider rain to be a terrestrial phenomenon produced in caves (Morris, 1986: p. 57; Vogt, 1969: p. 302). Thus, bats become the ideal sacrifice/messenger for rituals carried out in caves because of the animal's ability to navigate cave passages in complete darkness.

The bat remains previously documented in archaeological contexts tend to be recovered from caches, burials and constructions. They were noted simply because they were so "out of place". The current work is the first to offer solid evidence of utilization within caves. Utilization of bats within caves presents an obvious problem for archaeologists excavating in caves and analysts dealing with cave faunal assemblages who must now attempt to determine when or to what extent the remains are natural or cultural. At a minimum, archaeologists need to make a detailed examination of the physical location of excavation units in relation to current bat traffic and roosting areas. The presence or absence of bat bone on the surface should also be noted before excavation is begun. Such steps will provide data which will allow analysts to eliminate the most obvious cases of naturally deposited bone. Most importantly, careful control of archaeological context during excavation is essential.

The problem for the analyst is even more difficult. Certain areas may reflect natural deposition while others cultural utilization, so analyses which fail to separate one unit from another may obscure potentially significant patterns. On the other hand, dealing with individual lots generally reduces bone counts to the point where the numbers are not statistically significant and a methodology which allows the analyst to consider certain lots while excluding others opens the door to all kinds of bias. There will be no simple solution to the problem. The best remedy is for excavators and analysts to work closely. Excavators should, based on cave context, rate each lot on its potential for containing naturally deposited bones so that lots likely to contain non-cultural material can be eliminated before analysis is undertaken. In the end, the best results may be obtained by focusing attention on only those lots that offer particularly good opportunities for providing uncontaminated samples, such as those directly off use-surfaces.

Finally, we have noted that studies of Maya ritual fauna have tended to focus on very restricted samples recovered from special contexts such as burials and caches (Carr, 1985: pp. 126-129; Moholy-Nagy, 1985). As archaeologists and analysts increasingly venture out into "natural places" (Bradley, 2000), they need to adopt the perspective of the ritual specialist who realizes that species naturally associated with these landmarks may be the most likely to have been utilized in ritual.

Acknowledgements

Fieldwork was carried out while the author was on a Fulbright-Hays Training

Fellowship from the US Department of Education. The project was financed in part by a National Science Foundation Dissertation Improvement Grant (BNF-8800946). The authors would like to thank Betty Benson for her encouragement in looking more deeply into bats and Kitty Emery for her always constructive critiques of this work.

Conflicts of Interest

The author declares no conflicts of interest regarding the publication of this paper.

References

Bernal, I. (1949). Murciélagos. *Tlatoani, 3,* 95.

Bradley, R. (2000). *The Archaeology of Natural Places*. London: Routledge.

Brady, J. E. (1989). *An Investigation of Maya Ritual Cave Use with Special Reference to Naj Tunich, Peten, Guatemala*. PhD Dissertation, Los Angeles, CA: Archaeology Program, University of California.

Brady, J. E., & Coltman, J. D. (2016). Bats and the Camazotz: Correcting a Century of Mistaken Identity. *Latin American Antiquity, 27,* 227-237. https://doi.org/10.7183/1045-6635.27.2.227

Brady, J. E., & Prufer, K. (1999). Caves and Crystalmancy: Evidence for the Use of Crystals in Ancient Maya Religion. *Journal of Anthropological Research, 55,* 129-144. https://doi.org/10.1086/jar.55.1.3630980

Brady, J. E., & Rissolo, D. (2006). A Reappraisal of Ancient Maya Cave Mining. *Journal of Anthropological Research, 62,* 471-490. https://doi.org/10.3998/jar.0521004.0062.402

Brady, J. E., & Rodas, I. (1995). Maya Ritual Cave Deposits: Recent Insights from the Cueva de los Quetzales. *Institute of Maya Studies Journal, 1,* 17-25.

Brady, J. E., Scott, A., Neff, H., & Glascock, M. (1997). Speleothem Breakage, Movement, Removal and Caching: An Unreported Aspect of Ancient Maya Cave Modification. *Geoarchaeology, 12,* 725-750. https://doi.org/10.1002/(SICI)1520-6548(199709)12:6<725::AID-GEA10>3.0.CO;2-D

Carr, H. S. (1985). Subsistence and Ceremony: Faunal Utilization in a Late Preclassic Community at Cerros, Belize. In M. Pohl (Ed.), *Prehistoric Lowland Maya Environment and Subsistence Economy* (pp. 115-132). Papers of the Peabody Museum of Archaeology and Ethnology, Vol. 77, Cambridge: Peabody Museum, Harvard University.

Coe, W. R. (1959). *Piedras Negras Archaeology: Artifacts, Caches, and Burials*. Philadelphia, PA: The University Museum, University of Pennsylvania.

Coe, W. R. (1990). *Excavations in the Great Plaza, North Terrace and North Acropolois of Tikal*. Tikal Report No. 14. Philadelphia, PA: The University Museum, University of Pennsylvania.

Cook, G. (1986). Quichean Folk Theology and Southern Maya Supernaturalism. In G. H. Gossen (Ed.), *Symbol and Meaning Beyond the Closed Community: Essays in Mesoamerican Ideas* (pp. 139-153). Albany: Institute of Mesoamerican Studies, State University of New York, Albany.

Eliade, M. (1958). *Patterns in Comparative Religion*. New York: Sheed and Ward.

Emery, K. F. (2004) Animals from the Maya Underworld: Reconstructing Elite Maya Ritual at the Cueva de los Quetzales, Guatemala. In S. Jones O'Day, W. Van Neer, & A.

Ervynck (Eds.), *Behaviour Behind Bones: The Zooarchaeology of Ritual, Religion, Status and Identity* (pp. 101-113). Oxford: Oxbow Books.

Fernandez, M. A. (1943). New Discoveries in the Temple of the Sun in Palenque. *Dyn, No. 4-5,* 55-58.

Halperin, C. T., Garza, S., Prufer, K., & Brady, J. E. (2003). Caves and Ancient Maya Ritual Use of Jute. *Latin American Antiquity, 14,* 207-219. https://doi.org/10.2307/3557596

Hamblin, N. L. (1984). *Animal Use by the Cozumel Maya*. Tucson: University of Arizan Press.

Luther, E. (1974). Faunal Material. In D. M. Pendergast (Ed.), *Excavations at Actun Polbilche, Belize* (pp. 62-80). Monograph 1. Toranto: Royal Ontario Museum.

Moholy-Nagy, H. (1985). The Social and Ceremonial Uses of Marine Molluscs at Tikal. In M. Pohl (Ed.), *Prehistoric Lowland Maya Environment and Subsistence Economy* (pp. 147-158). Papers of the Peabody Museum of Archaeology and Ethnology, Vol. 77, Cambridge: Peabody Museum, Harvard University.

Morris, W. F. Jr. (1986). Maya Time Warps. *Archaeology, 39,* 52-59.

Pendergast, D. M. (1969). *The Prehistory of Actun Balam, British Honduras*. Art and Archaeology Occasional Paper 16, Toranto: Royal Ontario Museum.

Pendergast, D. M. (1971). *Excavations at Eduardo Quiroz Cave, British Honduras* (Belize). Art and Archaeology Occasional Paper 21, Toranto: Royal Ontario Museum.

Pendergast, D. M. (1974). *Excavations at Actun Polbilche, Belize*. Monograph 1. Toranto: Royal Ontario Museum.

Pohl, M. (1983). Maya Ritual Faunas: Vertebrate Remains from Burials, Caches, Caves, and Cenotes in the Maya Lowlands. In R. M. Leventhal, & A. L. Kolata (Eds.), *Civilizations in the Ancient Americas* (pp. 55-103). Albuquerque: University of New Mexico Press.

Pollock, H. E. D., & Ray, C. E. (1957). *Notes on Vertebrate Animal Remains from Mayapan*. Department of Archaeology, Current Reports No. 41, Washington DC: Carnegie Institution of Washington.

Redfield, R. (1941). *The Folk Culture of Yucatan*. Chicago: University of Chicago Press.

Ricketson, O. G. Jr., & Ricketson, E. B. (1937). *Uaxactun, Guatemala: Group E 1926-1931*. Washington DC: Carnegie Institution of Washington.

Savage, H. G. (1971). Faunal Material. In D. M. Pendergast (Ed.), *Excavations at Eduardo Quiroz Cave, British Honduras (Belize)* (pp. 78-111). Royal Ontario Museum Art and Archaeology Occasional Paper 21, Toranto.

Scott, A. M. (2012). The Historical Context of the Founding of Maya Cave Archaeology. In J. E. Brady (Ed.), *Heart of Earth: Studies in Maya Ritual Cave Use* (pp. 9-15). Austin: Association for Mexican Cave Studies.

Smith, A. L. (1950). *Uaxactun, Guatemala: Excavations of 1931-1937*. Carnegie Institution of Washington Publication 588, Washington DC.

Thompson, J. E. S. (1939). *Excavations at San Jose, British Honduras*. Washington DC: Carnegie Institution of Washington.

Tozzer, A. M. (1941). *Landa's Relacion de las Cosas de Yucatan*. Papers of the Peabody Museum of American Archaeology and Ethnology, Vol. XVIII, Cambridge: Harvard University.

Vogt, E. Z. (1969). *Zinacantan: A Maya Community in the Highlands of Chiapas*. Cambridge, MA: Harvard University Press.

Archaeological Discovery, 2019, 7, 92-126
http://www.scirp.org/journal/ad
ISSN Online: 2331-1967
ISSN Print: 2331-1959

Ales Stones in Southern Sweden: A Remarkable Monument of the Sun Cult and Advanced Astronomy in the Bronze Age

Nils-Axel Mörner*, Bob G. Lind

Paleogeophysics & Geodynamics, Stockholm, Sweden
Email: *morner@pog.nu

How to cite this paper: Mörner, N.-A., & Lind, B. G. (2019). Ales Stones in Southern Sweden: A Remarkable Monument of the Sun Cult and Advanced Astronomy in the Bronze Age. *Archaeological Discovery, 7,* 92-126.
https://doi.org/10.4236/ad.2019.72007

Received: March 28, 2019
Accepted: April 22, 2019
Published: April 25, 2019

Abstract

Ales Stones is a famous stone ship in southern Sweden. Besides its size (69 m) and location right beside the shore of the Baltic, it is a remarkable monument of the Sun Cult and very advanced knowledge of astronomy by the Bronze Age people. This paper summarizes the findings, and puts it into the context of other monuments in southern Sweden. Also presented are a new time-correction of the sunrise at Winter solstice 700 BC and a remarkable sun-wheel on the Island of Bornholm of astronomical dimensions almost identical to those of the Ales Stones monument: the Madsebakke Sun-wheel. It all provides a congruent picture of intensive Sun Cult activity and close connections between of southeast Sweden and the Island of Bornholm.

Keywords

Ales Stones, Astronomy, Solar Alignment, Late Bronze Age 700 BC, Stratigraphy, Sand Drift, Quarrying, Sun Cult, Rock-Carvings, Madsebakke Sun-Wheel

1. Introduction

Despite the fact that thousands of stone ships were built in Scandinavia in the period 1000-4000 BP, there are no traces anywhere of a stone ship comparable to Ales Stones. It is unique. The stone ship of Ales Stones is 69 m long and 19 m wide, and it is strictly aligned with respect to the sunrise at Winter solstice in the SE and the sunset at Summer solstice in the NW (**Figure 1**). Radiocarbon dates indicate that the stones were in position by about 500 AD, at the latest. Stratigraphy indicates that the monument was erected before the major sand-drift period dated at 600-400 BC (Mörner, 2015). Cup marks are indicative of the

Bronze Age (1750-500 BC). Finally, the list of archaeological finds in the vicinity (Table 1) includes numerous finds from the Bronze Age, but zero finds from the Neolithic and Iron Age. Converging facts seem to indicate that Ales Stones was erected in the Bronze Age (Lind, 2004, 2005; Lind & Mörner, 2010; Mörner, 2015).

Figure 1. Ales Stones: a stone ship strictly aligned with respect to the Sun's annual and daily motions over the sky with the bow in the NW where the Sun sets at summer solstice, and the stern in the SE where the Sun rises at winter solstice.

The ship consists of 57 stones (originally 58 stones). The bow and stern stones are two monoliths of quartzite, quarried at Brantevik 20 km to the NE (Mörner, 2015). There is also a "rudder stone" and an "altar-stone" of quartzite. Today, the so-called "altar-stone" lies inside the ship, thrown there by the farmer from its original position in front of the bow stone. Therefore, this stone must have originally marked the ram of the ship. The ram (in its original position) and the so-called "rudder stone" are likely to represent the extended keel stern typical for ancient Greek ships and the ships found in Swedish rock carvings (Figure 2). On a drawing from 1777 (Hilfeling, 1777), the stone ship is drawn in great details (Figure 3) and there is no stone drawn where the "altar stone" is lying today.

Figure 2. Ship on a rock carving from the Bronze Age (located at Simris 2 km north of Brantevik). The keel stern is extended into rams both in the bow and the stern of the ship.

Figure 3. The drawing by Hilfeling from 1777. Note that the "altar stone" is not present inside the ship and that the stern stones are in firm positions (whilst the bow stone is tilted).

Figure 4. Ales Stones has a very strict SE-NW orientation with respect to the stern stone in the SE just where the Sun rises at Winter solstice (left) and with the bow stone in the NW just where the Sun sets at Summer solstice (right).

The strict solar alignment of the ship is illustrated in Figure 4. At Winter solstice, the Sun is rising just beside the stern stone, and at Summer solstice, it is setting right behind the bow stone. As evident from the drawing by Hilfeling (Figure 3), the stern stone was standing upright in its original position in 1777 (whilst the bow stone was half fallen). In a photography from 1916 (Lind & Mörner, 2010), the 3 stern stones are still in original position, whilst the bow stone is lying down. This implies that strict calculations of the solar alignment can only be done with respect to the stern stone. In Figure 4, the Sun rises just to the left of the stern stone. The tiny deviation in alignment (about 15 - 17 cm) is a measure of the time elapsed since the erection of the stern stone (see below).

With this description of the general shape and organization of the Ales Stones magnificent stone ship, we turn to the dating and the interpretations of the function of the monument (cf. Lind, 2004; Lind & Mörner, 2010; Mörner, 2015).

2. Dating the Erection of the Ship

There are five main means of shedding light on the time of the erection of the Ales Stone monument, viz. 1) the age of archeological finds in the vicinity of the ship, 2) C14-dates of finds inside the ship, 3) the exact solar alignment with respect to the sunrise at Winter solstice over the stern stone, 4) stratigraphy and C14-dates at Ales Stones, and 5) the time of the quarrying and shipping of the 4 quartzite blocks (Section 3).

2.1. Archaeological Finds at and around Ales Stones

Table 1 lists all the archaeological finds in the vicinity of Ales Stones. Whilst there are lots of finds of tools and objects from the Bronze Age, especially the Late Bronze Age, there are no finds at all of objects from the Neolithic and the Iron Age (except for a number of charcoal dates as listed in Table 1). This seems quite significant for the age of the activity at Ales Stones. This was also the conclusion drawn at the excavation in 2011 (Mörner, 2011; Duczko, 2011).

From the Neolithic, there are two C14-dates of charcoal. One from a hearth just in front of the bow stone of Ales Stones, collected and dated by Lind (Lind & Mörner, 2010; Mörner, 2015). The age is 3175 ± 375 cal. yrs BC, which implies that humans were present in the area at least 5000 years ago. There is also a charcoal date of 2525 ± 36 cal. yrs BC from a depression in the old till surface

(Andersson et al., 2013).

Table 1. List of archaeological finds and dates in the vicinity of Ales Stones (AS).

Neolithic (N):
1) Hearth in front of AS dated at 3175 ± 375 cal. yrs BC (a)
2) Charcoal from a depression dated at 2525 ± 36 cal. yrs BC (a, b)
3) Some tools of flint (b)
Bronze Age (B.A.):
1) Cup marks in the form of the Swan constellation on stone 1 in the NW (**Figure 7**)
2) Three cup marks on stone 8 in the W strictly aligned to the sunrise at winter solstice (**Figure 8(a)**)
3) Four cup marks on stone 8 in the E strictly aligned to the annual solar motions (**Figure 8(b)**)
4) Razor from the Late B.A. found in the 30's 50 m to the E of AS (c)
5) Hollow axe from the Late B.A. found in the 30's close to AS (c)
6) Knife of bronze from the Late B.A. found 50 m to the E of AS (c)
7) Neck ring of bronze from the Late B.A. found in 1937 40 m to the E of AS (c)
8) Eight arrow points of bronze from the Late B.A. found in 1937 15 - 20 m to the S of AS (e)
9) Bronze dagger, 30 cm long, from the Late B.A. found in 1937 10 m from AS (e)
10) Loop button of bronze from the Late B.A. found in 1988 close to AS (c)
11) Stone in the form of a foot with cup marks found in 1994 10 m from AS (e)
12) Amber owl found in 1953 40 m E of AS (e)
13) Eleven pieces of flint found in 2011 (in excavation pit E) 30 m from AS (f)
14) Imprint of removed block (1.0 × 2.5 m) covered by eolian sand dated at 600 cal. yrs BC (f)
15) Charcoal in shore cliff dated at 785 ± 20 and 775 ± 35 cal. yrs BC (a)
Iron Age (I.A.):
1) Hearth in the shore cliff dated at 385 ± 35 cal. yrs BC (a)
2) Urn buried in eolian sand in the ship dated at 400 ± 150 and 525 ± 105 cal. yrs AD (a, b)
3) Charcoal of birch beside stone 24 in the E dated at 525 ± 105 cal. yrs AD (a, b)
4) Charcoal from oak and hazel dated at 675 ± 275 and 665 ± 105 cal. yrs AD (a, b)
5) A flywheel of red sandstone from the Late Iron Age to Viking time (b)
6) Charcoal of beech at the centre of AS dated at 905 ± 145 cal. yrs AD (a, b)
Mound with bones at the shore cliff dated at 985 ± 45 cal. yrs AD (a, f)

(a) Mörner, 2015, **Table 1** (with additional information), (b) Söderberg et al., 2012, (c) Lund Historical Museum, (d) Ystad Museum, (e) Bob Lind's collection, (f) Mörner, 2011.

There are a lot of finds of tools and objects found in direct association with Ales Stones (**Table 1**). There are also cup marks and hearth dates. Most of the finds can be assigned to the Late Bronze Age. This is a strong argument in favor of a dating of Ales Stones to the Late Bronze Age. Stratigraphically, the Bronze Age ends with the deposition of a widespread layer of eolian sand dated at 600-400 BC (Mörner, 2015).

The Early Iron Age is represented by a hearth in the cliff section dated at 385 ± 35 cal. yrs BC. It overlies the first generation of eolian drift and underlies the second generation of eolian drift (Mörner, 2015).

The Middle Iron Age (the Migration period in Sweden, 375-550 AD) is represented by an urn buried in the eolian sand inside the ship, and charcoal found close beside one of the stones (at the outer side of stone N24). The age, 525 ± 105 cal. yrs AD, is identical to the age of food left in the urn. Because it was found at the side of one of the big blocks, it implies that Ales Stones must have been erected well before this age (Mörner, 2015); i.e. well before 500 AD.

From the Viking time, there is a charcoal date from the center of the ship. Its implication is not clear, however. From the shore at Kåseberga, there is a mound

(about 0.5 m high and 10 m wide) full of bones (mainly from pigs) and scorched stones. Its surface is covered by stones placed in position by humans (Mörner, 2011, 2015). It provides firm evidence that people have lived in the vicinity during the Viking time.

2.2. Dates of Objects inside the Ship

The original surface upon which Ales Stones once was built has a sandy-silty humus soil. It is covered by eolian sand deposited in three main sand drift generations. There was a major gap with soil formation in the period at about 400-1100 AD. The urn and charcoal dated 525 ± 105 cal. yrs AD belongs to this soil formation period. Obviously, the finds were buried in the previously deposited eolian sand. The dates indicate that the erection of Ales Stones must be older than 500 AD. There are also some dates of charred wood (**Table 1**), which may signify a growth of trees on the moraine plateau.

2.3. Date from the Exact Solar Alignment at Winter Solstice

Today, the Sun is rising not exactly behind or at the edge of the stern stone, but at about 15 - 17 cm to the left of the stone (edge to edge) when observing the sunrise at Winter solstice from the center of the ship (**Figure 5**). From this deviation, Lind calculated that the stones must have been erected at about 700 BC (Lind, 2004, 2005; Lind & Mörner, 2010). This age fits very well with stratigraphical data and new C14-dates (Mörner, 2015). The deviation observed implies a northward displacement of the Sun's path by 0.77˚ in 2700 years.

Astronomer Göran Henriksson has kindly undertaken a high-precision astronomical recalculation of the data (**Figure 6**). The time when the Sun rose in perfect alignment with the stern stone is 700 BC. This lends strong support (not to say final conclusion) to a Late Bronze Age time for the erection of the Ales Stones monument.

Figure 6 is a novel contribution to the discussion of the true age of the Ales Stones monument. It is a very important contribution because it implies that we now have the time quite well locked in the Late Bronze Age. Earlier, there were "greater than" dates but not really any limiting chrono-stratigraphic limit back in time (Mörner, 2015). With the **Figure 6** image, the time of the erection of the Ales Stones monument seems to be limited to a fairly narrow time-window at about 700 BC, which is 200 years before the end of the Scandinavian Bronze Age.

2.4. The Occurrence of Cup Marks on Ales Stones

Cup marks (small round depressions) were predominantly carved into the bedrock in the Bronze Age, but may also occur on carvings from the Neolithic and Early Iron Age. On the outer surface of the stone just to the east of the bow stone, there are cup marks, which form the Swan star constellation (**Figure 7**) (Lind & Mörner, 2010). This implies a deep knowledge of and interest in astronomy, typical for the Bronze Age (Mörner & Lind, 2018; Kristensen, 2010; Bröndsted, 1938; Montelius, 1911).

Figure 5. The sunrise at Winter solstice on December 22, 2002 (photo: Bob Lind). The photo was taken from the center of the ship, and the Sun rose 15 - 17 cm to the left of the stern stone.

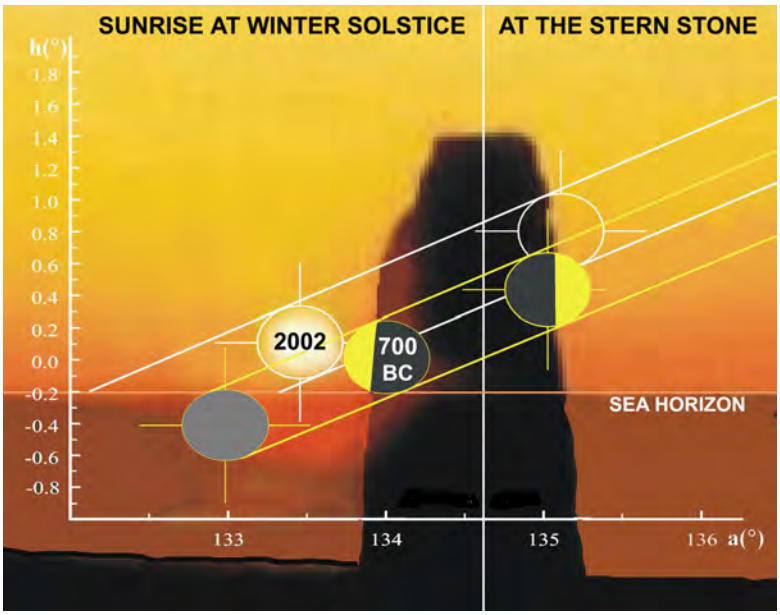

Figure 6. Astronomical high-precision calculation by Henriksson of the deviation between the present sunrise and a sunrise with perfect alignment to the edge of the stern stone (the symmetry axis of the stern stone is given by the white vertical line at 134.6˚). This alignment occurred 700 BC, and it is here proposed to provide a reliable age for the erection of the monument.

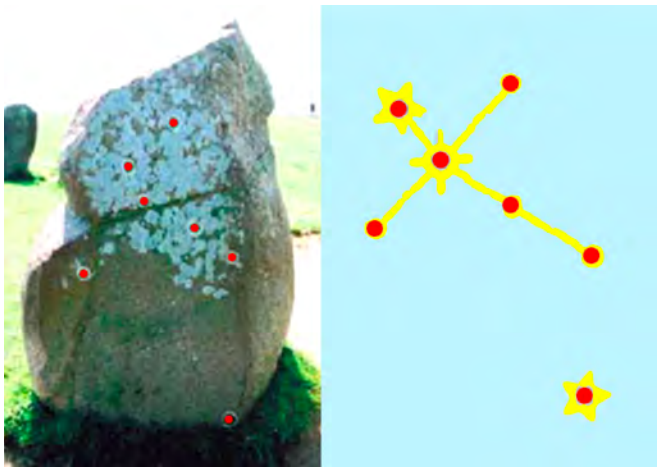

Figure 7. Cup marks on the side of one of the stones in Ales Stones in the form of the Swan constellation (left) and the same constellation as seen in the sky (right).

Cup marks exist on the top of two stones (the so-called stones 8^1 and 8^2); one of 3 cup marks in perfect alignment with the sunrise at Winter solstice (**Figure 8(a)**), and one of 4 cup marks like a mini ship with perfect alignment to the sunrises at Winter and Summer solstice and the sunset at Summer and Winter solstice (**Figure 8(b)**).

Cup marks in the form of a star constellation (**Figure 7**) and cup mark signs in perfect alignment with the sunrise at Winter solstice (**Figure 8**) are quite clear indications of a Bronze Age construction of the Ale Stones monument.

Figure 8. Cup marks on the top of two side stones (number 8 in the SE and number 8 in the NW); one in the form of an aim of 3 marks (a) where the Sun rises right in the aim at Winter solstice, and one in the form of a mini-ship of 4 marks (b) where the Sun rises right along the long-axis of the "ship" at Winter solstice.

2.5. Stratigraphy and C14-Dates at Ales Stones

Strömberg, who undertook all the original excavations of Ale Stones, seems to have been focused on finding objects and graves. Therefore, stratigraphic observations are virtually lacking in her reports (Strömberg, 1990, 1992, 1997), like later summaries of her reports (Söderberg et al., 2012). Notions of 60 and 85 cm of topsoil or humus soil (Swed: "*matjord*"), of course, represent inadequate sediment identifications.

There are fundamental stratigraphical facts that must be considered, however. This applies both from the moraine hill around the ship and from the shore sections below (Mörner, 2011, 2015). The reference sites are marked in **Figure 9**.

Figure 9. Ales Stones on top of the moraine hill and the shore sections at Kåseberga and other reference sites discussed: red dots at the ship and sites A, L and D (from Mörner, 2015).

Figure 10. The exposed till surface with a hearth dated at 3175 ± 375 cal yrs BC (point L in **Figure 9**) from an excavation in 1995 (photo: Lind, 1995). The till surface is covered by about 90 cm of eolian sand. It is easy to identify a strong humus soil developed in the top of the till surface (of boulder clay) and a second strong soil separating two units of eolian sand.

2.5.1. The Moraine Hill

The hill, upon which Ales Stones are located, is an interlobate moraine of boulder clay and glacifluvial material. The age of the moraine is about 14,000 BP. On top of the moraine, there is a soil from an exposed land period lasting from about 12,000 to 600 BC. The Ales Stones monument is built on this surface. All the tools and objects from the Bronze Age (**Table 1**, nos. 4 - 13) and the two charcoal dates from the Neolithic (**Table 1**, nos. 1 - 2; **Figure 9**, points L and A) are found on this surface.

This ancient soil surface is covered by eolian sand deposited in a succession of phases and interrupted by non-depositional intervals. At one of the non-depositional intervals, there was quite a strong soil formation (**Figure 10**). This soil is very well expressed in the shore section (below; Mörner, 2015). It seems to have lasted from the Roman Iron Age up to the end of the Viking time or from about 200 up to 1100 AD. This implies quite a long time with an exposed land surface with soil formation and growth of trees and shrubs. The urn was buried in the sand below this surface (**Figure 11**). The urn is standing on the soil surface of the boulder till. It includes food remains dated at 525 ± 105 cal. yrs AD and charcoal dated 400 ± 150 cal. yrs AD (providing minimum ages of the onset of the second soil horizon). Finds of birch (525 ± 105 AD), oak 675 ± 275 AD), hazel (665 ± 105 AD) and beech (905 ± 145 AD) have been dated to this period (**Table 1**, Iron Age, nos. 2 - 5), which implies that the soil formation period was also a period with trees and shrubs covering the hill. Furthermore, there are several finds of depressions in this surface, which represent the removal of stones and blocks for the construction of the monument (Mörner, 2011).

Figure 11. The urn from inside the ship. It is buried in the eoliand sand below the second soil horizon, and placed in standing position on the old till surface. The two dates (400 ± 150 and 525 ± 105 cal yrs AD) provide a minimum age of the second soil horizon.

The depth of the eolian sand deposits covering the old till surface is on the order of 60 - 90 cm in the ship itself. It includes one very distinct soil horizon (Figure 10). The covering eolian sand is from the periods of intensive sanddrift in medieval time and from the period of deforestation and plowing starting in the 19th century. The plowing lead to intensive sand drift and the monument acted as a trap where large quantities of sand accumulated, calling for major sand clearing in1956 (Lind, 2018).

In 2011, we undertook excavations on the plane to the east of Ales Stones (Figure 9, site D), where several of the objects from the Late Bronze Age had been found (Table 1, Bronze Age, nos. 4, 6, 7 and 12). In the five excavation pits (A-E), we only found pieces of flint, all of which had a touch-up typical for the Late Bronze Age (E. Jonsson in Mörner, 2011).

Figure 12. Stratigraphy exposed at our 2011 excavation at Ales Stones (Mörner, 2011). (a) The usual stratigraphy: 25 cm of plow-stirred humus soil directly covering the old till surface (a stony boulder clay, often weathered into a brownish-yellowish colour); (b) 30 cm sediment cover with a 12 cm topsoil in eolian sand.

Figure 13. Two of several artifacts found when plowing down to the till surface (**Table 1**). (a) An owl of amber found in 1953 (now co-owned by Mörner & Lind); and (b) A neck-ring of bronze found in 1937 (now at Ystad Museum).

On the plane east of Ales Stones, the old till surface is covered by only about 20 - 40 cm of eolian sand (except for depressions where the cover may go up to 40 - 60 cm). In most places the stirring by plowing has reached all the way down to the till surface exposing a black humus soil from the ground surface down to the till surface (**Figure 12(a)**). In a few places the ground has remained undisturbed and there is a normal humus soil of about 12 cm in the top of the eolian sand (**Figure 12(b)**).

Most of the artifacts found on the plane surrounding Ales Stones were found by the farmers when plowing the fields (**Figure 13**). Predominantly, they all belong to the Late Bronze Age (**Table 1**).

At our excavation in 2011, Mörner (2011) observed that there was an imprint in the bounder clay from a big block of about 3 m in length and 1 m in width (**Figure 14**). Obviously it had been broken-up out of the till surface by the builders of Ales Stones. There were even marks in the ground from the process of breaking it out of the till.

The depression is filled with eolian sand from the period of extensive sand drift 600-400 BC (Mörner et al., 2009; Mörner, 2011, 2015). As there were no sediments in the depression, it is likely that the removal of the block occurred shortly before the sand drift starting in 600 BC.

In **Figure 15** we compare the size of the imprint with stone S26 (the second on the south side from the stern stone). The agreement is reasonably good. Even other blocks could be considered, however. The height of the stone is 1.5 m, and this level is marked with a green bar in **Figure 15**. When the stones were put in place the ground level was about 60 - 70 cm lower as marked with the blue line, implying that about 1 m of the block was rooted in the till (and fixed in place by foot stones pounded into the boulder clay).

It is of great importance that the big boulder was bent out of position in the surface of the till by humans for the obvious purpose of using it for the building of Ales Stones. Because the imprint in excavation pits D and B (**Figure 14** & **Figure 15**) was filled by eolian sand dated 600-500 BC, the building of Ales Stones must be older than 600 BC.

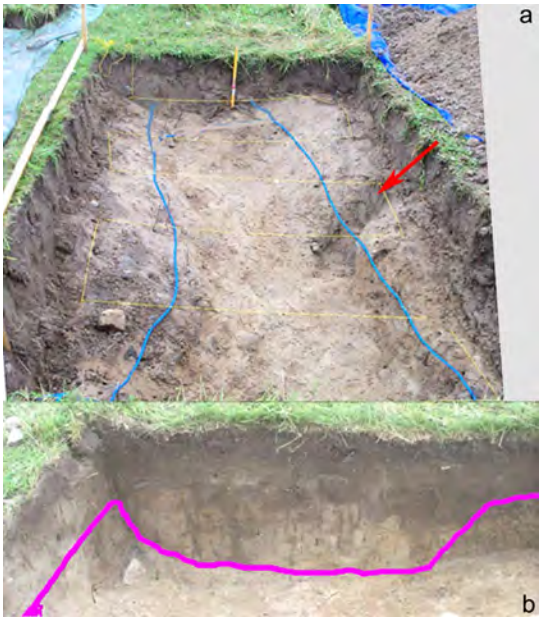

Figure 14. Imprint of a huge block (3 × 1 m) in the boulder clay surface (purple line marking a 0.5 m deep and 1 m wide depression in the till). Arrow shows the mark of a rod pushed down to bend the block out of the ground. The imprint was filled by eolian sand from the sand drift period 600-400 BC. Consequently, the removal of the block must have occurred before 600 BC. (a) Refers to excavation pit D with the blue rope marking the edges of the imprint; (b) The perpendicular section of the imprint (observed in excavation pit B) with a sediment depth of 95 cm consisting of two sedimentary cycles: the upper 35 cm with the present top soil and the lower 60 cm of post-600 BC eoliand sand with a weak top soil.

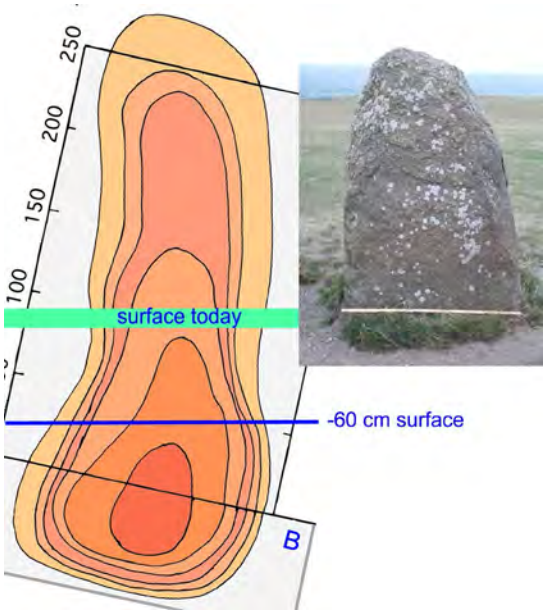

Figure 15. The imprint documented in excavation pits B and D (Mörner, 2011, 2015) compared to Block S26 (the second block on the southern side from the stern stone). The green bar across the imprint marks the present ground surface. The blue line gives the approximate position of the ground surface when the ship was built, implying that about 2 m of the block was sticking up, and about 1 m was rooted in the boulder clay.

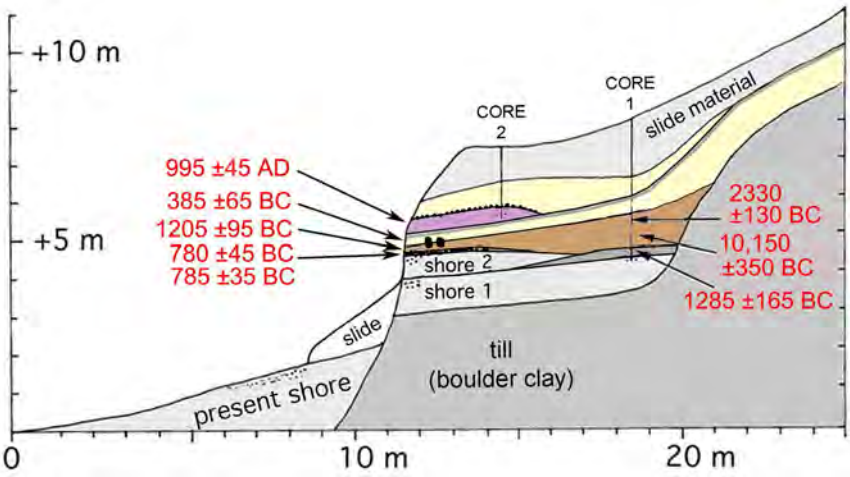

Figure 16. Stratigraphy and C14-dates from the shore section at Kåseberga, downhill of Ales Stones (form Mörner, 2011, 2015). Black layer = fire surface, brown layer = earthquake layer, and purple layer = mound with bones and burned stones from the Viking time.

2.5.2. The Shore Cliff

In the shore cliff to the west of Kåseberga and just downhill from Ales Stones (**Figure 9**), there is an excellent stratigraphic record covered by profiles along the cliff and perpendicular to the cliff (Mörner, 2011, 2015). A total of 8 C14-dates were obtained in this section, which led to the establishment of a very clear stratigraphy (**Figure 16**).

At the base, there is a boulder clay from the deglaciation period, with an erosional unconformity covered by shore 1 from around 2600 BC.

Shore-2 has a known age of 1000-750 BC. It is underlain by a humus soil C14-dated at 1285 ± 165 cal. yrs BC, and overlain by a black layer of humus and burned remains (a fire surface) C14-dated at 785 ± 35 and 780 ± 45 cal. yrs BC.

It is covered by an earthquake layer (Mörner, 2014, 2015) with re-deposited material as indicated by older C14-dates: 1205 ± 95 (bone), 2330 ± 130 (gastropod) and 10,150 ± 350 (marine shells) cal. yrs BC.

Directly above this layer lies eolian sand. This represents a well-known period of general sand-drift at the Sub-Boreal/Sub-Atlantic boundary at about 500 BC. In Mörner et al. (2009) this first general sand drift (Sand-Drift-1) is bracketed by two C14-dates: 467 ± 45 and 604 ± 126 cal. yrs. BC (providing a firm age of this sand drift period of 600-450 BC). It is covered by a weak soil with a heath dated at 385 ± 65 cal. yrs BC.

A second eolian unit follows, which ends in an extensive soil horizon, representing most of the Late Iron Age and the Viking time. On this soil horizon there is a mound (or midden) of about 0.5 m in height and 5 m in diameter. It is full of bones (mainly of young pigs) and stones affected by burning. The surface consists of stones placed in position by people (Mörner, 2011, 2015). A bone was C14-dated at 995 ± 45 cal. yrs AD, implying the Viking time.

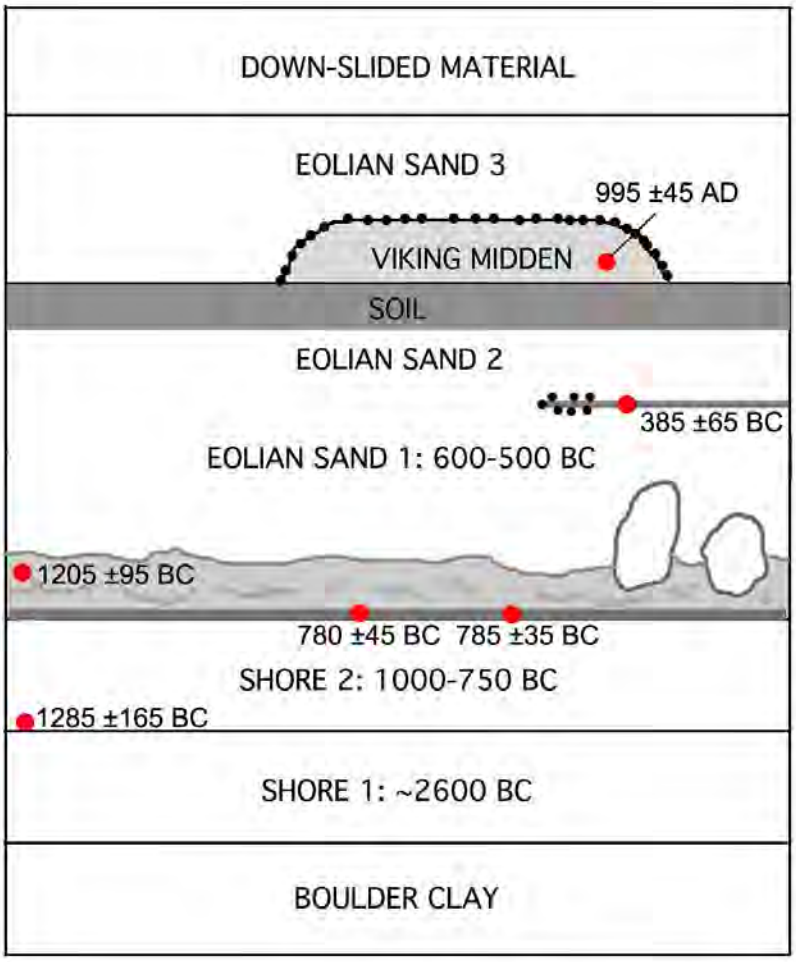

Figure 17. Composed stratigraphy and C14-dates from the shore section at Kåseberga.

The soil horizon and Viking mound (midden) are covered by a third layer of eolian drift. Obviously, it dates from medieval time. At Vitemölle, Mörner et al. (2009) dated the onset of this period of general sand drift (Sand-Drift-2) at 1345 ± 38 and 1415 ± 12 cal. yrs AD. Finally, there is a layer of down-slide material, which belongs to the last century's human and animal activity.

Figure 17 summarizes the stratigraphy in the shore section. It has a fundamental bearing on the interpretation of the stratigraphy and chronology of the building of Ales Stones. The main eolian drift covering the original ground floor in Ales Stones (**Figure 10**) and the imprint of the block (**Figure 14**) have to be identical to the "eolian sand 1" unit in **Figure 17** with an onset of deposition at 600 BC. The strong soil horizon in the shore section must be an equivalent to the buried soil at Ales Stones (**Figure 10**). It represents a hiatus of considerable time: at least 600 years from 400 to 1000 AD, but probably about double that time, from about 0 to 1350 AD.

During this interval, the urn (**Figure 11**) was buried inside the ship and the charcoal and bone fragments just outside stone N24. Trees and shrubs (birch, oak, hazel, etc.) grew on the exposed land surface. During the Viking time, it

seems that the centre of the stoneship was used as a firebox. The beech wood dated at 905 ± 145 cal. yrs AD is an excellent firewood. In combination with the midden (or mound) dated at 995 ± 45 cal. yrs. AD (Mörner, 2011, 2015; **Figure 17**) it indicates that the area hosted intense activity by people during the Viking time. This was an activity linked to a re-use of the existing old ship monument, and has nothing to do with the time of construction.

3. The 4 Quartzite Blocks: Quarrying and Shipping

Ales Stones has 4 blocks consisting of quartzite: the two huge megaliths erected as bow stone and stern stone, and the two extended ram stones termed the altar stone and the rudder stone. These four blocks have sharp angular edges and fracture marks indicating that they have not been transported to the region by the land ice (as all the other blocks in Ales Stones have), but must have been quarried from an *in situ* quartzite bedrock. This was already proposed by Bergström et al. (1988), and they pointed out the coastal area between Gislövshammar and Simrishamn.

We claim that we have found the exact place from where the four blocks originate; viz. Branteträsk in Brantevik (between Gislövshammar and Simrishamn), some 20 km to the northeast of Ales Stones (Mörner, 2012b, 2014, 2015, 2017a).

In 2009, we found fractured quartzite blocks in a forested area at Brantevik. After extensive cleaning, it became obvious that a large area of quartzite bedrock had been fractured up in large angular pieces by an earthquake (**Figure 18**).

Figure 18. A quartzite bedrock fractured into angular blocks with knife-sharp edges. The surface is weathered and glacially scoured. The origin is a seismic deformation 750 BC (Mörner, 2014).

The bedrock surface at Branteträsk (the name of the site of quartzite bedrock deformation and quarrying) is heavily fractured into blocks (**Figure 18**). The original fracturing can only have originated from a major earthquake generating extensional forces in two perpendicular directions (Mörner, 2012b, 2014; Mörner & Lind, 2013). Traces of this earthquake have been recorded over an area of about 70 × 20 km and include post-carving fracturing of petroglyphs from the Bronze Age (Mörner, 2012a, 2012b, 2014). The magnitude was estimated at about 6.3 - 6.8 (Mörner, 2014). This earthquake was dated at about 780 BC (Mörner, 2014).

After the earthquake fracturing, people must have turned the site (well prepared with its bedrock surface fractured up into loose individual blocks) into an "industrial" quarry. This quarrying is evident from the removal of flat quartzite discs from the bedrock blocks, and from a block piled up in inclined position ready to be transported away (**Figure 19**).

Figure 19. The pieces of deformed quartzite bedrock have undergone a second deformation by people breaking-off large discs (i.e. using the blocks for quarrying). In the background, there is a piled-up bedrock (1) and in the quartzite surface one can identify the removal of large discs (2, 3).

The grain size and internal bedding of the quartzite at Branteträsk are identical to that of the bow and stern stones in Ales Stones (**Figure 20**, arrow 2). The surface structures of the old bedrock surface at Branteträsk is strongly weathered and traversed by glacial scouring structures identical to the old surface of the bow stone in Ales Stones (**Figure 19**, arrow 1). Therefore, we are quite sure that the quartzite blocks in Ales Stones were quarried at Branteträsk and transported to Ales Stones by rafts or boats (**Figure 21**).

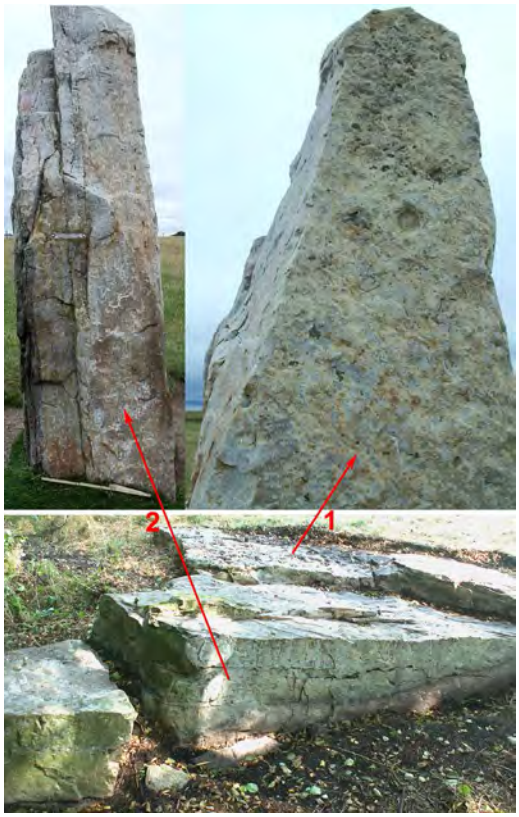

Figure 20. Comparison between the surface weathering pattern (1) and the internal bedding pattern (2) of the stern and bow stones in Ales Stones (above) and the blocks at Branteträsk (below). The similarities are very close, not to say identical, lending strong support to our proposition that this was the place of the quarrying of the quartzite blocks now being the bow stone and the stern stone plus the two ram stones (i.e. the rudder stone and the altar stone) in Ales Stones.

Figure 21. The transport route of the 4 quartzite blocks from their quarrying at Branteträsk via rafts or boats from Brantevik to Kåseberga up to their erection in the stone ship of Ales Stones (a distance of 30 km). Dotted areas represent the occurrence of Cambrian quartzite bedrock *in situ*.

The fracturing of the quartzite bedrock surface (**Figure 18**) is dominated by extension forces in the E-W, NNE-SSW and NW-SE directions (Mörner, 2014). This fracture opening can never have been achieved by human activity and can only be understood in terms of a significant seismic event. Paleoseismic criteria (bedrock fracturing at 13 sites, fracturing of rock-carvings from the Bronze Age at 7 sites and liquefaction at two sites 43 km apart) indicate a seismic magnitude of about M 6.3 - 6.8 (and intensity VIII-IX) with the epicenter at Glimmingehallar 3 km to the west. The dating of the event (by radiocarbon, archaeology and sea level history) seemed well established at 780-750 BC.

Subsequent studies and C14-dating have revealed that there were, in fact, two earthquakes: one at around 3000 BC and one (as previously described) at 780-750 BC. It does not change the timing of the quarrying at Branteträsk and transport of the blocks to Ales Stones, however.

At Brantevik, there was a grave, known as Brantarör, from the Late Bronze Age (Lind, 2011). It included some bronze objects, a rock-carving of a sun-symbol (typical for the Bronze Age) and an urn dated at 800-300 BC (**Figure 22**). It also included some 75 huge blocks of quartzite, indicating intensive quarrying at around 700 BC (Mörner, 2015).

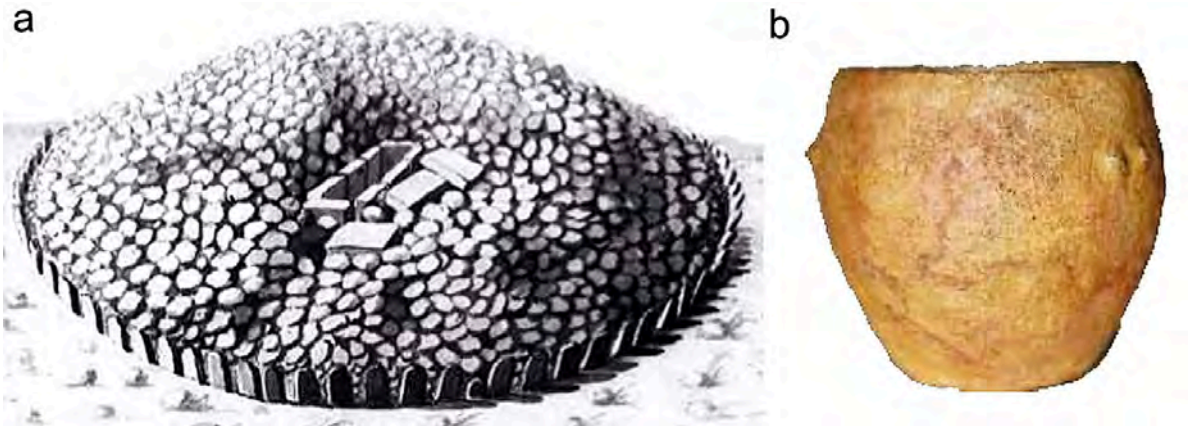

Figure 22. (a) The Brantarör grave as drawn by Hilfeling (1777). The sarcophagus included a hilt of bronze and an urn (b), and a sun symbol was cut in one of the stones. This indicates that the grave belongs to the Bronze Age. The urn is quite unique and was dated at 800-500 BC; i.e. the Late Bronze Age (Lind, 2011; Mörner, 2015).

The Brantarör grave (**Figure 22(a)**) is surrounded by about 60 curbstones and the sarcophagus consists of 14 big blocks. All of these blocks are flat quartzite blocks that must have been quarried in the close vicinity. The obvious place of a quarry of nearly industrial dimensions is Branteträsk, 600 m to the SW (**Figure 23**), and we see a logical chain of events: 1) a seismic fracturing of the quartzite bedrock, 2) a human utilization of the site for quarrying flat quartzite blocks, 3) a transport of blocks to be used in the building of the Brantarör grave (about 74 blocks) and 4) a shipping of four blocks to be erected in Ales Stones (the bow and stern monoliths, plus the altar stone and the rudder stone) as illustrated in **Figure 23** (Mörner, 2015, 2017a).

Figure 23. The quartzite blocks quarried at Branteträsk were transported 600 m to the NE partly for the building of the Brantarör grave (74 blocks) and partly for transport to Ales Stones (4 blocks) via the natural harbour when sea level was at +2.1 m in the period 1000-750 BC and sea transport as shown in **Figure 21** (from Mörner, 2015).

Obviously, the Brantarör grave dates from the Late Bronze Age (Lind, 2011; Mörner, 2015; Mörner, 2017a). There are a number of graves at Brantevik (Lind, 2011). It seems significant that they exhibit an alignment with respect to the Sun (Lind, 2011). The "southern grave" lies 1.2 km to the SW of the Brantarör grave. At Summer solstice, the Sun rises right over the Brantarör grave when viewed from the southern grave (Lind, 2011). This is another factor linking the Brantevik area to the Ales Stones monument and its erection in the Late Bronze Age (Mörner, 2015).

4. The Function of the Ales Stones and Related Monuments

We have reviewed the dating of Ales Stones, indicating a time of erection of the monument of about 750-700 BC, and it is now time to review the function of the monument. Lind (2004, 2005) showed that the monument must have worked as a sophisticated astronomical calendar in good agreement with earlier proposals (Alfredson & Meurling, 1976; Lind, 1977; Carter & Malmström, 1979; Roslund, 1979) and later verifications (Lind & Mörner, 2010; Mörner & Lind, 2012, 2013; Mörner, 2015).

4.1. Ales Stones as a Calendar

The 69 m long stone ship was erected on the top of the Kåseberga hill with a remarkable view over the sea (**Figure 1**). The position of the individual stones (57 plus 1 missing) is arranged in a very close (not to say exact) relation to the Sun's annual and daily motions over the sky (Lind & Mörner, 2010, p. 96 and 98, respectively).

The construction of the stone ship is shown in **Figure 24**. Every stone has a number beginning with number 1 in the bow stone in the NW and 1 in the stern stone in the SE. The following main solar alignments are recorded of the Sun's annual motions:

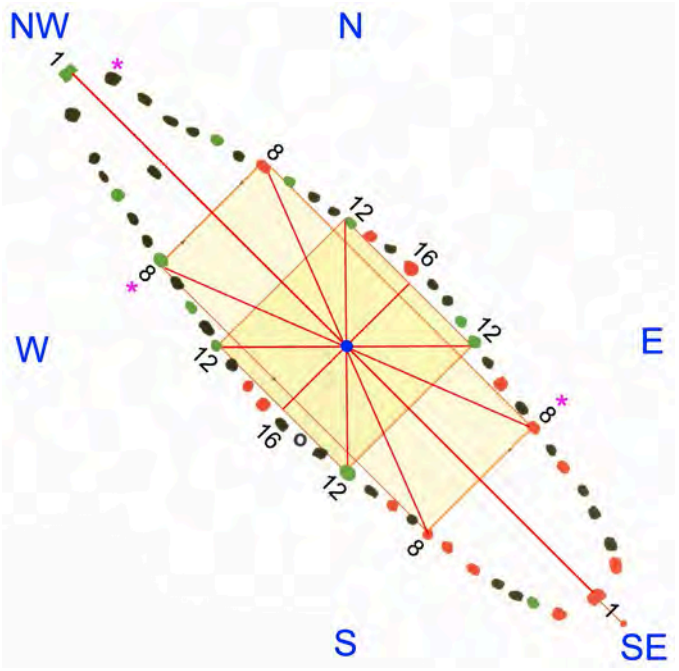

Figure 24. The geometry, position of stones and geographic orientation of Ales Stones. The long-axis is in NW-SE with sunrise at Winter solstice at the stern stone in the SE and the sunset at Summer solstice at the bow stone in the NW. Stone colouring: red = in place, green = tilted, black = fallen before restauration in 1916 (Lind, 2018). Asterix signs denote cup marks. Basic geometric concepts: the NW-SE long-axis, the stone 8 rectangle, the stone 12 square and the central point (blue dot). The arrangement of stones gives a sophisticated astronomical annual calendar and sundial (Lind, 2005; Lind & Mörner, 2010) as further discussed below.

- Sunrise at Winter solstice over stone 1 in the SE (**Figure 4**).
- Sunset at Winter solstice over stone 16 in the SW.
- Sunrise at Spring Equinox over stone 12 in the E.
- Sunset at Spring Equinox over stone 12 in the W.
- Sunrise at Summer solstice over stone 16 in the NE.
- Sunset at Summer solstice over stone 1 in the NW (**Figures 4-6**).
- Sunrise at Spring Equinox over stone 12 in the E.
- Sunset at Spring Equinox over stone 12 in the W.

On the top of stones 8 in the SE and stone 8 in the NW, there are cup marks (**Figure 25**) as shown and discussed in Lind & Mörner (2010), Mörner (2015, Figure 18) and Lind (2017, Figure 3 and Figure 5). The cup marks in a triangle on top of stone 8 in the SE give a perfect alignment to the sunrise at Winter solstice (**Figure 8(a)**). The cup marks as a ship on top of stone 8 in the NW record the 4 solar turning-points during a year (**Figure 8(b)**).

The fact that the cup mark signs and the main ship itself (**Figure 25**) give exactly the same alignments with respect to the Sun's main annual positions indicates beyond doubt that we are dealing with sophisticated astronomical calendar alignments (it is, of course, impossible that these perfect solar alignments would have been achieved by coincidence).

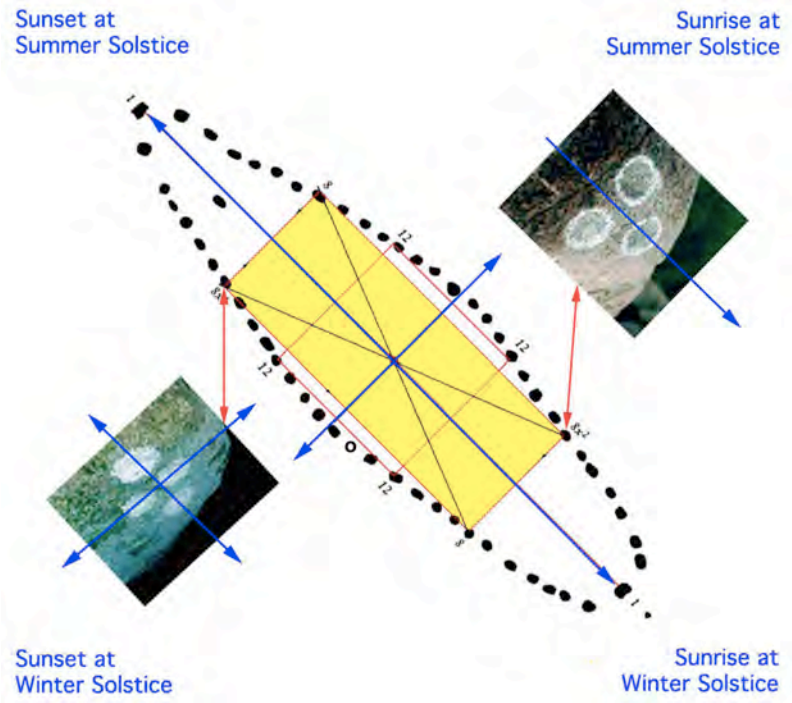

Figure 25. The 4 main solstice positions (blue arrows) of alignments of the ship itself and the two cup mark figures (from Mörner, 2015).

There is also a monthly organization of Ales Stones (**Figure 26**; cf. Lind, 2005; Lind & Mörner, 2010: p. 97). After the sunrise at Winter solstice over stone 1 in the SE, the point of sunrise moves in steps of 30 days (i.e. 1 month) to the southwest to stone 3 (January 23), stone 9 (February 22), stone 12 (March 24), stone 14 (April 23), stone 15 (May 23) and then stone 16 (June 22 at the Summer solstice). The next half calendar year continues with the position of the sunset at Summer solstice over stone 1 in the NW moving to the southeast to stone 3 (July 27, making this month 35 days long), stone 9 (August 26), stone 12 (September 25), stone 14 (October 25), stone 15 (November 24) and then stone 16 (December 24 at the Winter solstice). This completes one circuit around Ales Stones and one calendar year consisting of 11 months of 30 days and 1 month of 35 days (the June-July 35 days month) giving a full year of 365 days. This is why there is a larger gap between stones 2 and 3 in the NW. All the 14 sunrise and sunset positions have been documented by Lind (Lind & Mörner, 2010: p. 94).

Ales Stones also works as a huge sundial (**Figure 27**; cf. Lind, 2005; Lind & Mörner, 2010). The stone ship can be divided up in 16 segments each representing 1.5 hours making a full day of 24 hours. Placing a long rod in the centrum point (with a dip to the north of about 25˚), its shadow will move as follows:

- On stone 16 in the SW at 03.00 o'clock (sunrise at Summer solstice).
- On stone 14 in the WSW at 04.30 o'clock.
- On stone 12 in the W at 06.00 o'clock at (sunrise at the Equinoxes).
- On stone 8 in the WNW at 07.30 o'clock.
- On stone 1 in the NW at 09.00 o'clock at (sunrise at the Winter solstice).

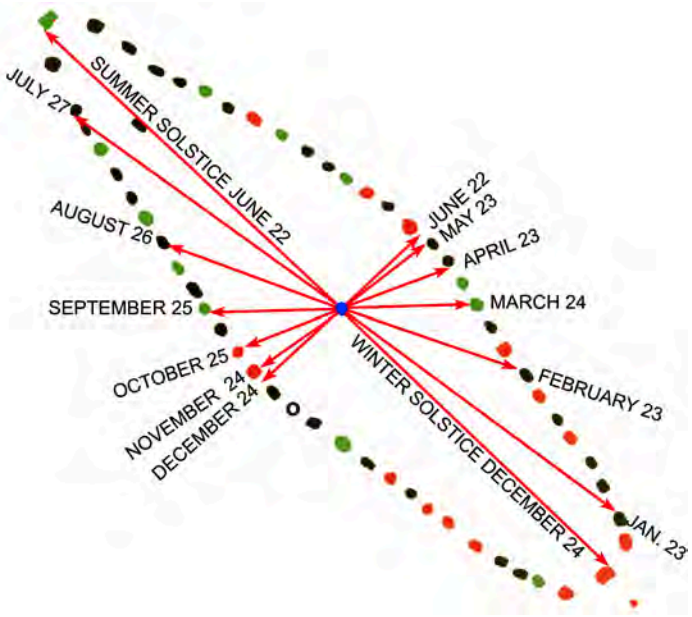

Figure 26. The monthly sunrise (the SE-sector) and sunset (the NW-sector) positions with respect to the individual stones. All months consist of 30 days except for July which includes 35 days giving a full year of 365 days.

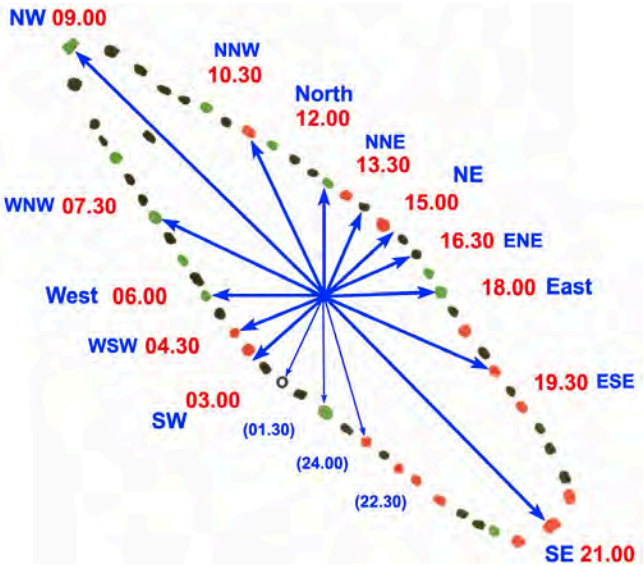

Figure 27. Ales Stones as a large sundial. With a tall rod in the centrum (inclined at ~25˚ to the north) the shadow will move as shown by the blue arrows with the hourly time in front. The day is composed of 16 segments each with a duration of 1 hour and 30 minutes.

- On stone 8 in the NNW at 10.30 o'clock.
- On stone 12 in the N at 12.00 o'clock (noontime).
- On stone 14 in the NNE at 13.30 o'clock.
- On stone 16 in the NE at 15.00 o'clock (sunset at Winter solstice).
- On stone 14 in the ENE at 16.30 o'clock.
- On stone 12 in the E at 18.00 o'clock (sunset at Equinoxes).

- On stone 8 in the ESE at 19.30 o'clock.
- On stone 1 in the SE at 21.00 o'clock (sunset at Summer solstice).

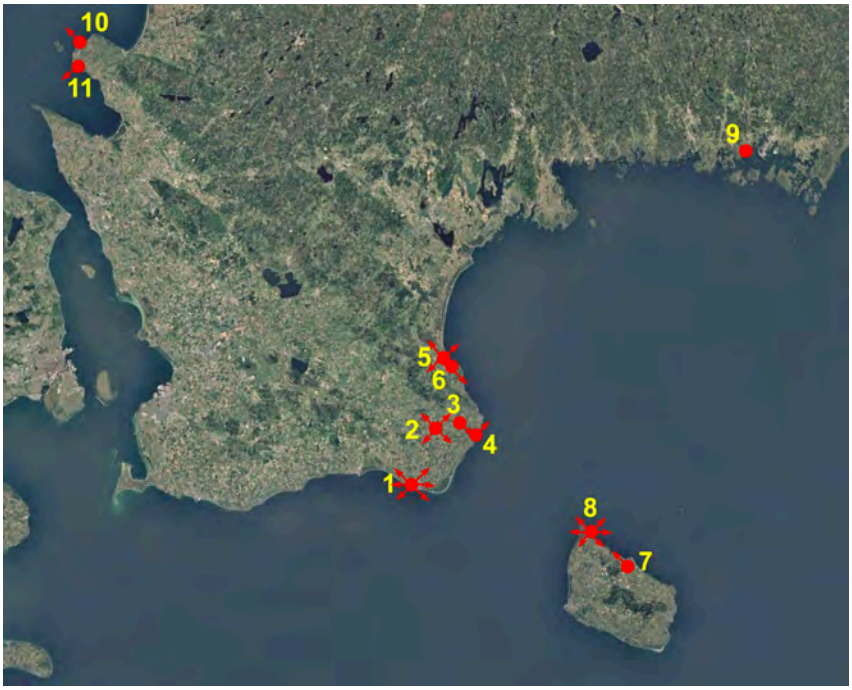

Figure 28. Some Bronze Age sites of solar alignments (illustrated by red arrows) in southern Sweden and the Island of Bornholm: (1) Ales Stones, (2) Stenhed, (3) Järrestad, (4) Brantevik, (5) Heimdall's Stones, (6) the Kivik grave, (7) Lensbjer, (8) Madsebakke, (9) the Golden Sky Dome from Mjövik, (10) Gröthögarna, (11) Dagshög.

In conclusion, the stone ship of Ales Stones records the 4 main solstice positions (**Figure 25**), the 12 monthly positions with a full year of 365 days (**Figure 26**), and 16 daily sundial positions with 1.5 hour's intervals (**Figure 27**). This provides full evidence of a sophisticated insight into astronomy of the Bronze Age people (Lind & Mörner, 2010; Mörner & Lind, 2013, 2018; Mörner, 2015; Mörner et al., 2018). There is no mathematical possibility what so ever that all these perfect alignments could have been obtained just by chance.

Furthermore, solar symbols and solar alignments are recorded at several other sites in southern Sweden (**Figure 28**). Obviously, there are numerous archaeological objects in southern Sweden that are constructed with solar alignment (e.g. Mörner, 2015). We will select a few sites for special analysis below. From the Island of Bornholm, we add two exceptionally interesting and important sites, especially site 8 with the "*Madsebakke Sun-wheel*" of almost identical astronomical calendar functions as those in Ales Stones.

4.2. The Stone Ship at Stenhed

Stenhed is another stone ship, 50 m long and 14 m wide and consisting of 30 blocks. Its long-axis is in the NW-SE. The annual Sun motions are record in steps of 11 months of 30 days and one month of 35 days (just as in Ales Stones;

Figure 26). The Sun's daily movements record sixteen 1.5 hours segments (just as in Ales Stones; Figure 27).

Stenhed has an interesting geographic position right in the middle between Ales Stones and the remarkable Kivik grave (Lind & Mörner, 2010; Mörner & Lind, 2013).

4.3. The Winter Solstice Festival at Järrestad

Järrestad refers to a site of extensive rock-carvings west of Simrishamn (Althin, 1945; Lind & Mörner, 2010: p. 86). Mörner (2012a) showed that most of the images exhibit strict solar alignments. A central figure is "the Dancer". She is oriented strictly facing the SE; i.e. the alignment of the sunrise at Winter solstice (Figure 29). There are 69 feet and 11 pair of feet carved into the bedrock: 75% of those point to the sunrise at Winter solstice. There are also 19 pairs of shoes and 45 single shoes carved into the bedrock; 95.3% of them point to the sunrise at Winter solstice.

Obviously, "the return of light" at Winter solstice was a key event for the people living in southern Sweden in the Bronze Age. The Järrestad rock-carvings show an important manifestation of this: "the Dancer" faces the sunrise and 84% of all 144 feet and shoes are watching the event in the same alignment (Figure 29).

There is also a mini-ship oriented just as Ales Stones (Lind & Mörner, 2010: p. 88; Mörner, 2012a). Many of the rock-carving pictures are fractured by a post-carving earthquake (Mörner, 2012b, 2014).

Figure 29. Part of the Järrestad rock-carving site (Mörner, 2012a). All the pictures (shoes, feet, sun wheal and the Dancer) are aligned with respect to the sunrise at Winter solstice in the SE. This was *the Mid-Winter Festival* and "*the return of the Sun*".

4.4. Solar Alignment at Heimdall's Stones

Heimdall's Stones refer to a 30 m wide circular astronomical calendar (Mörner et al., 2009). There are numerous rock-carvings in the stones; cup marks, an omega sign, a delta sign, sun symbols, etc. The ground surface of the monument is covered by eolian sand from the sand drift dated 600-500 BC; hence the mo-

nument must be older than 600 BC.

Figure 30. At Winter solstice, the Sun rises right in the notch in the slope of Stenshuvud when viewed from the centre of Heimdall's Stones over the block in the SE (from Mörner et al., 2009). In 4 minutes, the Sun will be at the peak of Stenshuvud. From Bornholm 70 km on the other side, there is an opposed sightline of the sunset at Summer solstice (Kaul, 2005).

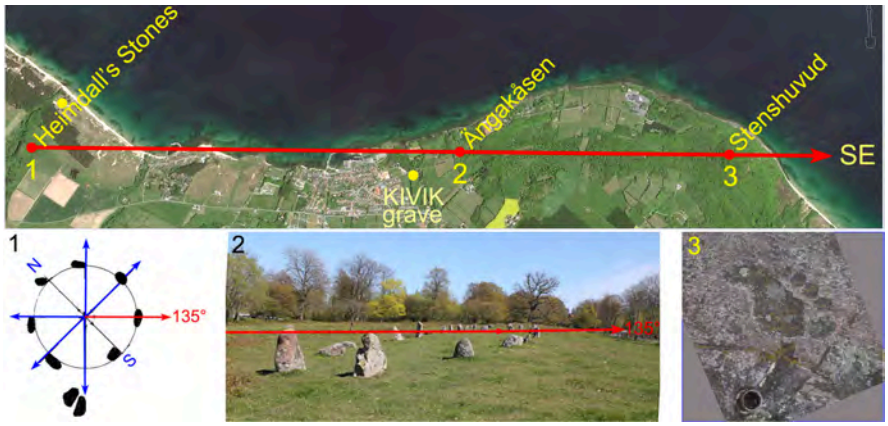

Figure 31. The sightline from Heimdall's Stones (1) via the Ängakåsen stone ship (2) to the peak of Stenshuvud (3) where there is a benchmark (+97 m) and a rock carving of a foot. At Winter solstice, the Sun rises in the SE right along this line (Mörner et al., 2009).

The Heimdall's Stones monument includes sightlines of the sunrise and sunset at Winter solstice, of the sunrise and sunset at the Equinoxes and of the sunrise and sunset at Summer solstice (Mörner et al., 2009, Figures 1-3). Most important is the alignment of the sunrise at Winter solstice, which passes directly over the hillside of Stenshuvud (**Figure 30**). **Figure 31** gives the sightline of the sunrise at Winter solstice from the archaeo-astronomical observatory of Heimdall's Stones (1) straight over the Ängakåsen stone ship (2) to the top of Stenshuvud (3) where there is a rock-carving of the front part of a foot pointing to the SE (just as the majority of feet and shoes at Järrestad; **Figure 29**). From the Island of Bornholm there is an opposed sightline to Stenshuvudon the sunset at Summer solstice (**Figure 32**; cf. Kaul, 2005; Mörner et al., 2009).

The Kivik grave indicates close contacts with the cultures in the East Mediterranean. The area may even have worked as a trading center from the onset of the Scandinavian Bronze Age at about 1750 BC (Lind & Mörner, 2010; Mörner &

Lind, 2013, 2015).

Figure 32. The sightline from Lensbjer to the sunset at Summer solstice over Hammer Odde and Stenshuvud in the NW (i.e. the opposed direction to that documented in **Figure 31**). The ship (white) has a form dating from 900-1000 BC. It sails towards the sunset. At Madsebakke (Allinge) there is a sun-wheel with the same astronomical function as that of Ales Stones. A ship (red) comes from the west; i.e. from the Ales Stones-Brantevik area in Sweden. This ship has a form dating from around 700 BC (just the age of Ales Stones).

4.5. Solar Alignment from the Island of Bornholm

More than 100 rock-carving images are documented on the Island of Bornholm (Kaul, 1998, 2005, 2006). The boat images are dated at about 900-500 BC (Kaul, 2006; Cole, 2011). They exhibit close similarity to the boat images in the Simrishamn area indicating communications and cultural linkage (Cole, 2011).

At Lensbjer (at Lensgård), 3 km SW of Gudhjem, Kaul (2001, 2005, 2006) found a site with six ships. Two of the ships points to the peak of Hammer Odde in the NW and further over the sea to Stenshuvud, and Kaul (2005, 2006) noted that the Sun sets along the same alignment at Summer solstice (**Figure 32**). The ship is 60 cm long. It is drawn with the bow in the direction to the sunset in the NW. Its shape suggests an age of 900-1000 BC (e.g. Cole, 2011).

At Madsebakke in Allinge on northwest Bornholm, there is a rock-carving with multiple images of shapes indicating ages ranging between 1000 and 500 BC (Kaul, 2005; Cole, 2011).

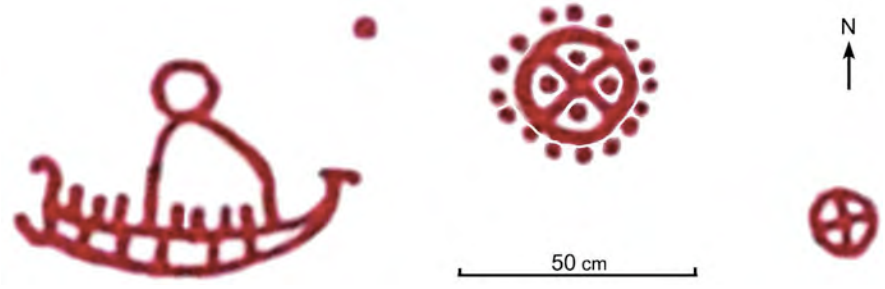

Figure 33. Segment of the Madsebakke rock-carving showing a ship of 700 BC characteristics sailing from the west to the east, and a sun-wheel of a perfect compass design (**Figure 34**) implying that it may have been used as a sundial and annual calendar.

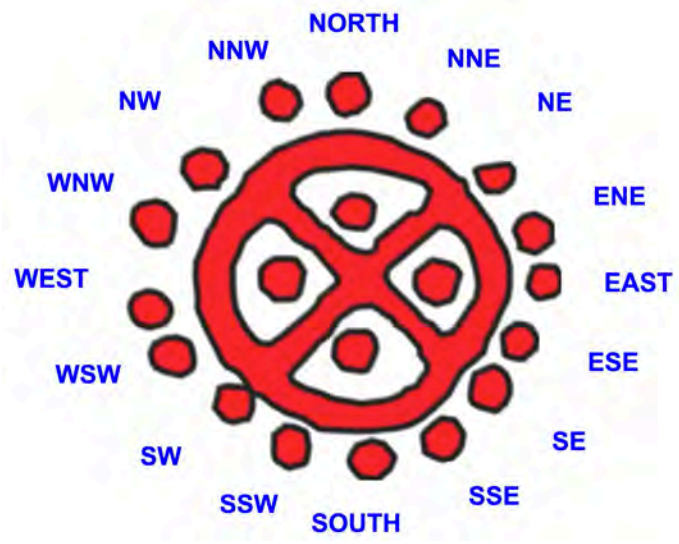

Figure 34. The Madsebakke sun-wheel has a design revealing a basic function as a compass implying that it can be used to document the daily and the annual motions of the Sun over the sky. This indicates very close, not to say identical, functions as the astronomical functions of the Ales Stones monument (**Figures 24-27**).

4.6. The "*Madsebakke Sun-Wheel*" on the Island of Bornholm

The Madsebakke rock-carving site includes the image of a sun-wheel: a sun-wheel divided in four segments and surrounded by 16 cup marks (**Figure 33**). We have undertaken a close field documentation of the exact geographic orientation of the sun-wheel (**Figure 34**). At Spring Equinox (March 21, 2019), we also documented the sunrise and sunset with respect to the sun-wheel, indicating perfect East/West alignments (**Figure 35**).

This enables us now to claim that the sun-wheel must have worked both as a sundial and as a compass or solar calendar (**Figure 34**). This implies an almost identical astronomical set-up and function as those documented in Ales Stones (**Figures 24-27**). The ship close by (**Figure 33**) has a form dating the rock-carving to 700 BC (Cole, 2011), i.e. the same age as Ales Stones.

The set-up as a sundial is illustrated in **Figure 36** (left image): 16 segments each of which corresponds to 1 hour and 30 minutes (some irregularities are noted in the figure). The set-up as an astronomical calendar is illustrated in **Figure 36** (right image): the alignments to the four main solar turning points. The alignment to the sunrise and sunset at Spring Equinox are documented in **Figure 35**. On a whole, this indicates that the "*Madsebakke Sun-wheel*" has identical functions to those recorded in Ales Stones (**Figure 27** and **Figure 25**). Judging from the design of the nearby ship (**Figure 33**), the age of the rock-carving seems to be about 700 BC (Cole, 2011), indicating that it is contemporary with Ales Stones, too.

The Madsebakke Sun-wheel provides a remarkable and novel record of the close connections existing in the Late Bronze Age between the Island of Bornholm and the Ales Stones-Järrestad-Brantevik-Kivik area in SE Sweden.

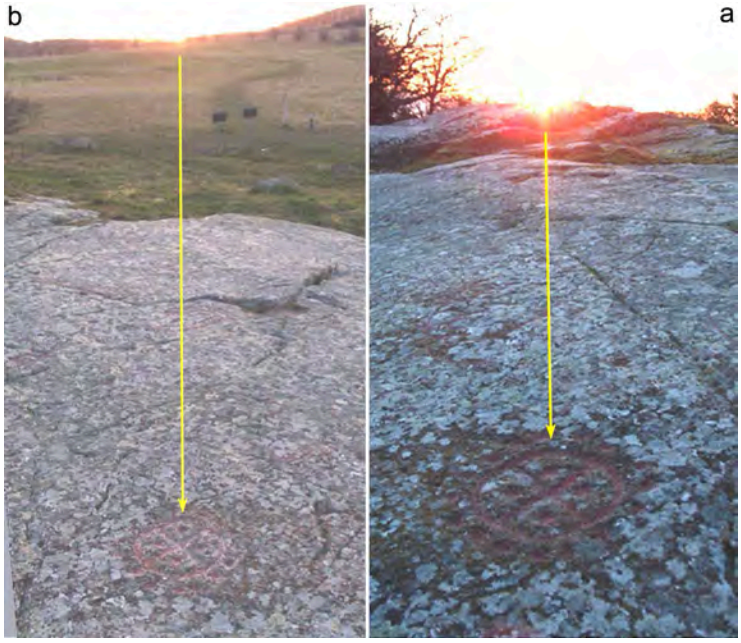

Figure 35. Documentation of the solar alignments at Spring Equinox (March 21, 2019) to the sunrise in the East (a) and the sunset in the West (b). Yellow arrows indicate the sunlight in relation to the sun-wheel; (a) the first light at sunrise and (b) the last light at sunset.

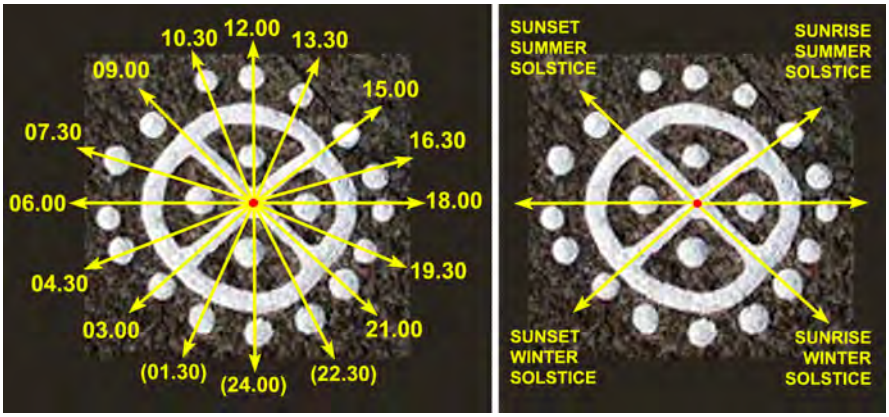

Figure 36. The Madsebakke sun-wheel with interpretations as a sundial (left) and as a compass with an annual calendar function (right). This implies very close, not to say identical, functions as the Ales Stones astronomical functions (Figures 24-27).

4.7. Some Other Sites of Sun Cult Relevance in Southern Sweden

We have addressed the questions of long-distance travel and trading (Lind & Mörner, 2010; Mörner & Lind, 2010, 2013, 2015) and the advanced astronomy and sun cult in the Bronze Age (Lind & Mörner, 2010; Mörner, 2015; Mörner & Lind, 2018). In this section, we will highlight a few facts of the Sun Cult flourishing in Southern Scandinavia in the Bronze Age (e.g. Montelius, 1911; Almgren, 1927; Bröndsted, 1938; Kristensen, 2010; Mörner & Lind, 2018) with respect to some other sites in Southern Sweden (Figure 28).

The Kivik grave (site 6 in Figure 28) is a remarkable place as noted above

(**Figure 31**). It has been further discussed in Lind & Mörner (2010) and Mörner & Lind (2013, 2015) and exhibits obvious links with the cultures of the East Mediterranean.

At Mjövik (site 9 in **Figure 28**) a golden urn was found in 1847. In 2017, we turned it up-side-down and found that we, in fact, were dealing with "sky dome" with 12 sun symbols, 12 moons and a 6-spoke sexagesimal system (Mörner & Lind, 2018; Mörner et al., 2018). This bears testimony of an advanced and widespread Sun Cult during the Bronze Age.

The Bjäre Peninsula has numerous mounds from the Bronze Age and some sites with clear solar alignment (Mörner, 2015, **Figure 19**). We will here limit the discussion to two sites with clear solar alignments (sites 10 and 11 in **Figure 28**).

At Gråthögarna (site 10) there is man-made "road" leading out to a group of 8 stone mounds from the Bronze Age (**Figure 37**). At Summer solstice, the Sun sets right over one mound in the straight elongation of the "road" (**Figure 38**).

Figure 37. The Gråthögarna shore site. Yellow lines mark man-made "road" out to the field of 8 stone mounds from the Bronze Age. The sea levels of 3800, 2600 and 850 cal. yrs BC are marked. White arrow shows the sightline of **Figure 38** of the sunset at the Summer solstice.

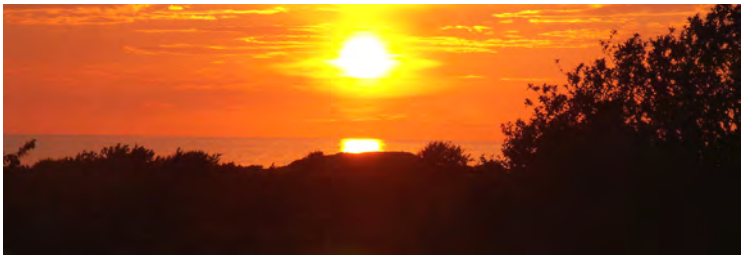

Figure 38. The sunset at Summer solstice right over one of the grave mounds in the same alignment as the man-made "road" shown in **Figure 37**.

Dagshög (site 11) is a 35 m wide grave mound from the Bronze Age. The mound lies between two lines set by large stones: one in the NE-SW and one in WNW-ESE (Figure 39). At Winter solstice, Sun sets right along the line pointing to the tip of the Kullen Peninsula 14 km to the SW (Figure 40). The other line points to the sunset at about August 26 in the WNW, probably marking an important time of the year like harvest time.

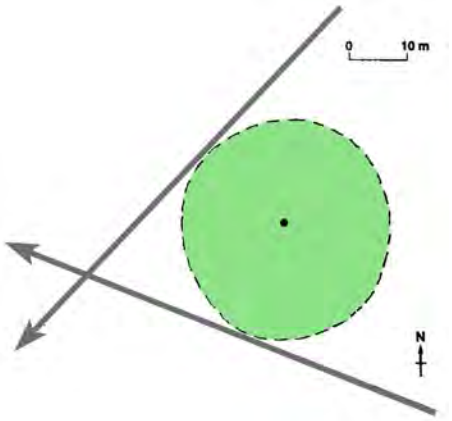

Figure 39. The Daghög grave (green) and stone-set lines (arrows).

Figure 40. The sunset at Winter solstice along the stone-set line NW of Dagshög pointing right at the tip of the Kullen Peninsula in the SW.

5. Conclusions

After this long review of Ales Stones and related documents on an advanced Sun Cult and deep knowledge of astronomy during the Bronze Age, we limit our conclusions to the following main points.

1) Ales Stones was built at about 750-700 BC. This is indicated by multiple criteria:

- Today, the sunrise at Winter solstice occurs 15 - 17 cm to the left of the stern stone. The deviation from a perfect alignment is due to astronomical variables (precession and tilt). In Figure 6, we have compensated for those va-

riables, providing a perfect fit at 700 BC. This lends very strong support to an age of construction of 700 BC.

- Stratigraphic facts indicate that the ship was built shortly before the general sand drift dated at 600-500 BC (**Figure 14**, **Figure 17**).
- Stratigraphy also shows that the monument is likely to have been constructed shortly after the earthquake occurring at about 780-750 BC (**Figure 17**).
- The quarrying of the 4 quartzite blocks in Ales Stones (like the block used in the Brantarör grave) must have occurred shortly after the earthquake dated at 780-750 BC and fracturing the bedrock (**Figure 18**, **Figure 19**).
- The shipping from the natural harbour at Brantevik to the coast at Kåseberga (just downhill of Ales Stones), is likely to have occurred at around 750 BC when sea level was still high and the harbour conditions favorable (**Figure 21**, **Figure 23**).
- All available facts taken together seem to give converging indications of an age of the erection of Ales Stones of 750-700 BC.
- The solar alignment between Heimdall's Stones and the mountain peak of Stenshuvud, and the opposed alignment between the direction of rock-carved ships at Lensbjer and Stenshuvud indicate a cultural connection (**Figure 32**). Close cultural connection is also indicated by the design of the ships found in rock-carvings on Bornholm and in the Simrishamn area. The Bornholm carvings are assigned an age of 900-500 BC (Kaul, 2006; Cole, 2011) in full agreement with our findings of high Sun Cult activity at Ales Stones and in Österlen in general.
- The Madsebakke Sun-wheel provides remarkable functional and temporal similarities with Ales Stones, and the other monuments and rock-carvings in southeastern Sweden (**Figure 28**).

2) Ales stones were built as a sophisticated astronomical calendar:

- The long-axis of the ship and the position of the individual stones are built with strict alignment to the solar movements over the sky during the year and throughout the day (**Figure 24**).
- The 4 main directions at Summer and Winter solstices are also recorded by the cup mark figures on the top of stones 8 in the SE and NW (**Figure 25**).
- The monthly sunrises from December to June move from stone to stone with an interval of 30 days. The monthly sunsets from June to December also move from stone to stone with an interval of 35 days for the first month and 30 days for the remaining 5 months. This gives a full year of 365 days (**Figure 26**).
- The ship also works as a huge sundial of 16 segments each covering 1 hour and 30 minutes (**Figure 27**).
- This implies overwhelming facts that the Ales Stones monument was built as astronomical calendar of remarkable skill and practical dimensions.
- This builds on to previous knowledge of an intensive Sun Cult in southern Scandinavia during the Bronze Age (e.g. Montelius, 1911; Almgren, 1927; Bröndsted, 1938; Kristensen, 2010; Lind & Mörner, 2010; Mörner & Lind,

2018).

- The Madsebakke Sun-wheel exhibits sophisticated astronomical functions almost identical to those recorded in Ales Stones.

3) Märta Strömberg (1997) described her project at Ales Stones in terms of three questions to be addressed: a) when was it built, b) what was the purpose, and c) what happened after. I think we have answered all three questions:

- It was built 750-700 BC as indicated by overwhelming facts highlighted in the text and summarized above under point 1.
- The purpose was the establishment of a sophisticated astronomical calendar giving the main solar turning points, the 12 months, the 365 days and the daily hours.
- Only limited activity can be recorded for the period 500 BC to 800 AD. In the Viking time there must have been intense activity, however, judging from the mound found in the shore section (Mörner, 2011, 2015), which is full of bones and burned stones and dated at 995 ± 45 cal. yrs BP.

4) Finally, we stress the remarkable functional and temporal correlations here established between Ales Stones and the Madsebakke Sun-wheel.

Acknowledgements

We acknowledge the kind recalculation by Göran Henriksson (Associate Professor in Astronomy at Uppsala University) of the true timing of sunrise at Winter solstice with respect to the stern stone of Ales Stones (**Figure 6**). We are indebted to Ingvar Kullberg, who assisted us in the field, made independent measurements and took excellent photographs for us (**Figure 35**), to Conny Klang, who assisted us in communications and various practical matters, to archaeologists Hans Ekerow and Esbjörn Jonson, who took part in the excavations in 2011 and correct presentation of Ales Stones at site, to Marie Schram, Lind's field assistant for many years, and to Pamela Matlack-Klein for her kind linguistic check. All our C14-dates (21 by now) were done by Göran Possnert at the Uppsala C14-laboratory. As a curiosity, we note that it was Nils Lind (a close ancestor to one of us), who discovered the Madsebakke rock-carvings in 1884. Finally we acknowledge a kind, sharp and very useful anonymous review.

Conflicts of Interest

The authors declare no conflicts of interest regarding the publication of this paper.

References

Alfredson, H., & Meurling, K. (1976). *Bästa vägen till Muckle Flugga: Notiser kring en resa till Island, Färöarna, Orkney och Shetland* (192 p.). Stockholm: Wahlström & Widstrand.

Almgren, O. (1927). Hällristningar och kultbruk. *Kungl. Vitterhets Hist. Antikv. Akad. Handlingar, 35,* 23-31.

Althin, C. A. (1945). *Studium zu Bronzezeitlichen Felszeichnungen*. Gleerups.

Andersson, M., Knarrström, A., Söderberg, B., & Wallebom, B. (2013). *Ales stenar i nytt ljus* (p. 80). Swedish Nat. Heritage Board, UV Rapport 2013.

Bergström, J., Daniel, E., Herner, E., Kornfält, K.-E., & Wikman, H. (1988). Ales stenar stenarnas historia. *Ale, 4,* 1-13.

Bröndsted, J. (1938). *Bronzealderens soldyrkelse*. København: Gyldendal.

Carter, J. J., & Malmström, V. J. (1979). Stenålderskalendrar i Sverige? *Forskning och Framsteg, 5,* 1-5.

Cole, A. J. (2011). A Social Semiotic Foray of Boat Images in Rock Art: Communication between Two Local Scandinavian Communities. In *XXIV Valcamonica Symposium: Art and Communication in Pre-Literate Societies* (pp. 130-136). Milano: Jaca Book.

Duczko, W. (2011). *Utanför skeppet. Rapport från arkeologisk undersökning inom fornlämningsområde Ales stenar, Skåne, Sverige*.

Hilfeling, C. G. G. (1777). *Skånska teckningar*. Köpenhamn.

Kaul, F. (1998). *Ships on Bronzes: A Study in Bronze Age Religion and Iconography*. Copenhagen: Danish National Museum.

Kaul, F. (2001). *Flere nye hellristningsfund*. Adoranten.

Kaul, F. (2005). *Hellristninger. Bilder fra Bornholms Bronzealder*. Rönne: Bornholms Museum.

Kaul, F. (2006). *Udgravninger vid hellristninger* (pp. 28-49, 50-63). Adoranten.

Kristensen, K. (2010). Rock-Art and Religion: The Sun Journey in Indo-European Mythology and Bronze Age Rock Art. In A. F. F. Criado Boado (Ed.), *From Representation and Communication: Creating an Archaeological Matrix of Late Prehistoric Rock Art* (pp. 93-115). Oxford: Oxbow.

Lind, B. G. (2004). *Ales stenar ur ett arkeoastronomiskt perspektiv*. Malmö: Stjärnljusets Förlag.

Lind, B. G. (2005). Ales stenar som sol kalender. *Ale, 3,* 27-33.

Lind, B. G. (2011). *Från Brantarör till Brantevik*. Malmö: Stjärnljustets Förlag.

Lind, B. G. (2017). *Ales Stenar: Dateringen* (16 p.). Malmö: Stjärnljusets Förlag.

Lind, B. G. (2018). *Ales Stenar: Restaureringen 1916* (16 p.). Malmö: Stjärnljusets Förlag.

Lind, B. G., & Mörner, N.-A. (2010). *Mykenska och Feniciska spår på Österlen*. Malmö: Stjärnljusets Förlag.

Lind, G. (1977). Har skeppssättningen haft en astronomisk funktion? *Elementa, 60,* 76-77.

Montelius, O. (1911). *Solguden och hans dyrkan. Nord. Tidskrift*.

Mörner, N.-A. (2011). *Rapport över sommarens arkeologiska utgrävningar vid Ales Stenar. Del 2: Geologiska Arbeten. Rapport till RAÄ Länsstyrelsen i Skåne* (24 p.).

Mörner, N.-A. (2012a). Strict Solar Alignment of Bronze Age Rock Carvings in SW Sweden. *Journal of Archaeological Science, 39,* 3301-3305. https://doi.org/10.1016/j.jas.2012.05.027

Mörner, N.-A. (2012b). Paleoseismic Fracturing of Rock Carvings 1000 BC in SE Sweden. In *Paleoseismology & Archaeoseismology* (pp. 127-130). Morelia: Paleoseismology & Archaeoseismology.

Mörner, N.-A. (2014). An M > 6 Earthquake ~750 BC in SE Sweden. *Open Journal of Earthquake Research, 3,* 66-81. https://doi.org/10.4236/ojer.2014.32008

Mörner, N.-A. (2015). Ales Stones in SE Sweden: A Solar Calendar from the Late Bronze Age. *Journal of Archaeological Science: Reports, 2,* 437-448. https://doi.org/10.1016/j.jasrep.2015.04.002

Mörner, N.-A. (2017a). *Ales Stenar: Stenbrottet* (16 p.). Malmö: Stjärnljusets förlag.

Mörner, N.-A. (2017b). *Comments on "New Light on Ale's Stones" by B. Söderberg & A Knarrström*.

Mörner, N.-A., & Lind, B. G. (2010). A Mediterranean Trading Centre in SE Sweden. In S. P. Paraminopolos (Ed.), *The Atlantis Hypotesis—Commentary 2008* (pp. 685-699). Athens: Heliotopos Publications.

Mörner, N.-A., & Lind, B. G. (2012). Stonehenge Has Got a Younger Sister. Ales Stones Decoded. *International Journal of Astronomy and Astrophysics, 2,* 23-27. https://doi.org/10.4236/ijaa.2012.21004

Mörner, N.-A., & Lind, B. G. (2013). The Bronze Age in SE Sweden: Evidence of Long-Distance Travel and Advanced Sun Cult. *Journal of Geography and Geology, 5,* 78-91. https://doi.org/10.5539/jgg.v5n1p78

Mörner, N.-A., & Lind, B. G. (2015). Long-Distance Travel and Trading in the Bronze Age. *Archaeological Discovery, 3,* 129-139. https://doi.org/10.4236/ad.2015.34012

Mörner, N.-A., & Lind, B. G. (2018). Astronomy and Sun Cult in the Swedish Bronze Age. *International Journal of Astronomy and Astrophysics, 8,* 143-162. https://doi.org/10.4236/ijaa.2018.82010

Mörner, N.-A., Jonsson, E., Ekerow, H., Henriksson, G., & Lind, B. G. (2012). *Vi utvärderar och underkänner: RAÄ Rapport 2012:21 Ales Stenar: Fördjupat kunskapsunderlag författad av Bengt Söderberg, Annika Knarrström & Kennet Stark. Skrivelse till Länsstyrelsens I Skåne Kulturmiljösektion och Riksantikvarieämbetet*.

Mörner, N.-A., Lind, B. G., & Henriksson, G. (2018). A Golden Calendar from the Bronze Age. *Archaeological Discovery, 6,* 53-61. https://doi.org/10.4236/ad.2018.62004

Mörner, N.-A., Lind, B. G., & Possnert, G. (2009). Heimdall's Stones at Vitemölla in SE Sweden and the Chronology and Stratigraphy of the Surroundings. *Geografiska Annaler, 91,* 205-213. https://doi.org/10.1111/j.1468-0459.2009.00364.x

Roslund, C. (1979). *Ale forntidsmatematiker och astronom* (p. 5)? Forskning och Framsteg.

Söderberg, B., & Knarrström, A. (2015). New Light on Ale's Stones. *Lund Archaeological Review, 21,* 87-106.

Söderberg, B., Knarrström, A., & Stark, K. (2012). *Ales Stenar: Fördjupar kunskapsunderlag*. RAÄ Rapport 2012:21.

Strömberg, M. (1990). *Vikingamonument eller maktsymbol i bronsåldersbygd*? Ystad: Ystads Fornminnesförening.

Strömberg, M. (1992). *Fortsatta fältstudiervid Ales stenar. Österlen 1992: Årsbok från den samlade hembygdsrörelsen på Österlen, Simrishamn*.

Strömberg, M. (1997). C14-dateringar vid Ales stenar. *Ale, 1,* 9-21.

Appendix

In order not to "contaminate" our main paper with negative discussions of unfortunate misunderstandings with respect to Ales Stones, we put these perspectives under this separate additional note.

It all goes back to a very strange excavation in 1996. Strömberg intended to try to find datable material underneath one of the stones, in order to get a final date of the erection of the monument. She selected stone N24 (the 5th stone on the northern side from the stern stone). She put two men to dig and sample any organic matter, but left for a private meeting (though this was her most important excavation). A pit was dug on the outer side of the stone, and when the men reached "the stone foot" (i.e. the circle of stones that had been hit into the bounder clay to keep the big block in position) they stopped at a depth of about 60 - 70 cm. In the lowermost 10 cm they found some black lumps, which they put into a plastic bag and backfilled the pit. When Strömberg returned she got the sample bag. On the bag she wrote: "*Ales stenar, beside block N*24*, ca* 70 *cm below surface, juni*-96" (see, Mörner, 2015, Figure 16). A piece of charcoal of birch was C14-dated at 525 ± 105 cal. yrs AD (Strömberg, 1997; Mörner et al., 2012; Mörner, 2015).

Here started the controversy about the age and function of Ales Stones. Strömberg (1997) unfortunately wrote that the sample came from *beneath* Stone N24, adding: *"if we can trust the excavators"*, which sounds like she was not sure herself.

We found the original sample bag, on which it is clearly written *"beside* (*Swedish: invid*) *block N24"*. "Beside" and "beneath" refer to two totally different positions. "Beside" the block implies that the erection of Ales Stones must be older than 525 ± 105 cal.yrs AD (our opinion: e.g. Lind & Mörner, 2010; Mörner, 2015). "Beneath" the block implies that Ales Stones must be younger (Strömberg, 1997; Söderberg et al., 2012; Söderberg & Knarrström, 2015).

The recovery of the original sample-bag (by Mörner on March 14, 2012) was a great thing for us realizing that something was wrong because of the same age of the charcoal claimed to come from beneath the block and from the food remains from inside the urn (**Figure 41**). Photos of the text on the sample-bag were published (Mörner et al., 2012; Mörner, 2015; below **Figure 41(C)**). One of the men who actually undertook the excavation was interviewed. He was quite sure that they had dug down to the stone-foot some 60 - 70 cm below surface, retrieved the samples in the lower part of the section, backfilled the pit and handed over a plastic bag with the samples to Strömberg, when she returned (certainly they had never gone below the stone).

In this situation, we are convinced that there can only be one true story, and this must be that the dated sample came from beside the stone, not below the stone. Therefore, Ales Stones must be older—not younger—than the 500 AD date.

Obviously, Strömberg (1997) herself was not sure. The more sure were her successors, however (Söderberg et al., 2012; Andersson et al., 2013; Söderberg & Knarrström, 2015). In a special report (Mörner et al., 2012), we objected to the

handling of the review of Ales Stenar by Söderberg et al. (2012). Mörner (2017b) objected to the story by Söderberg & Knarrström (2015).

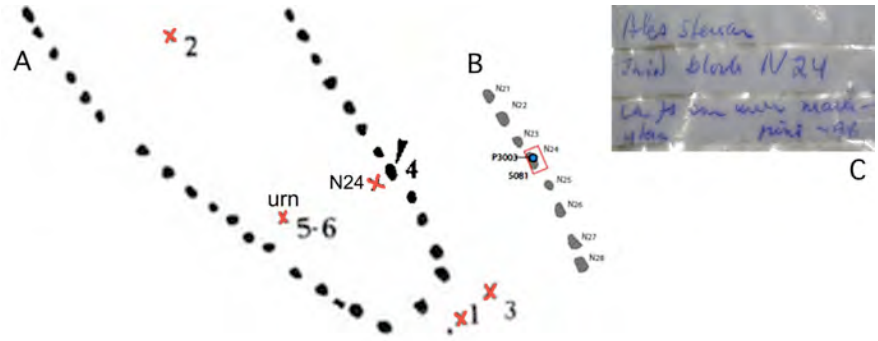

Figure 41. A: the original drawing by Strömberg (1997) with sites of C14-dates (1-6), the urn and excavation pit (4) beside block N24. B: the segment with the block N24 now with the sampling site wrongly sifted to a position below the block by Söderberg et al. (2012). C: photo of the original sampling-bag saying that the sample was taken beside (not below) bock N24 (from Mörner, 2015).

Besides the illusion of the correct position of the dated sample (beside not below block N24) just discussed, the proponents of a date of Ales Stones of about 500-1000 AD claim that the building of huge stone ships is typical for the Late Iron Age to Viking Age (Söderberg et al., 2012; Söderberg & Knarrström, 2015). Lind (2017) replied to this that all the ships built in the Late Iron Age and Viking Age have smoothly curved sides and sharp bows and sterns (**Figure 42**) contrary to Ales Stones, which has a truncated stern and an extended keel with rams typical for Greece ships in the Bronze Age.

Figure 42. The Anund ships at Västerås from the Viking period. The sides are smoothly curved and the bow and stern are pointed (from Lind, 2017) contrary to the Ales Stones ship which has a truncated stern and a keel extended into rams, just as the Greece ships of the Bronze Age had.

In conclusion, there seems to be no valid argument for claiming that Ales Stones was built in the period* 500-1000 *AD. On the other hand, there seems to be overwhelming evidence of a Late Bronze Age time of the erection of the monument.

Archaeological Discovery, 2019, 7, 127-154
http://www.scirp.org/journal/ad
ISSN Online: 2331-1967
ISSN Print: 2331-1959

Paleomagnetic Results from Archaeological Sites in Argentinean Patagonia: Evidence for the Holocene Geomagnetic Excursions in Southern South America and Its Chronostratigraphic Implications

Hugo G. Nami

Department of Geological Sciences, Laboratory of Geophysics "Daniel A. Valencio", CONICET-IGEBA, FCEN, UBA, Buenos Aires, Argentina
Email: hgnami@fulbrightmail.org

How to cite this paper: Nami, H. G. (2019). Paleomagnetic Results from Archaeological Sites in Argentinean Patagonia: Evidence for the Holocene Geomagnetic Excursions in Southern South America and Its Chronostratigraphic Implications. *Archaeological Discovery, 7,* 127-154.
https://doi.org/10.4236/ad.2019.72008

Received: March 21, 2019
Accepted: April 25, 2019
Published: April 28, 2019

Abstract

Detailed palaeomagnetic research performed in archaeological and paleontological sites in southern South America yielded a number of highly fluctuating paleosecular variation records with geomagnetic field excursion(s) during the Holocene. To assess this topic a variety of sections of recent sediments were sampled. In the case presented here they belong from diverse continental sedimentary sequences formed in coastal marine and cave's environments. Paleomagnetic samplings were performed in several deposits in San Blas Bay and Pali Aike areas, respectively located in the northern and southern parts of Argentinean Patagonia region. To collect samples, cylindrical plastic containers 2.5 cm long and 2 cm diameter were carefully pushed into the sections, overlying each other by about 50 percent. Their strike and dip were measured using a Brunton compass and inclinometer; they were consolidated with sodium silicate after removal and numbered from top to bottom. All samples were subjected to progressive AF demagnetization in steps of 3, 6, 9, 12, 15, 20, 25, 30, 40 and 60 mT in a 3-axis static degausser attached to a 2 G cryogenic magnetometer. Additional steps from 80 to 120 mT were used in some samples. Characteristic remnant magnetization was calculated using principal-components analysis, with the best-fitting line going to the origin in the Zijderveld diagrams. In general, maximum angular deviations were generally within low values. Some samples had univectorial behavior, while some showed two or three components. Most of the sections show normal and intermediate polarity directions far from the present GF, while reversed polarities were recorded at San Blas 2, La Serranita 1 and Punta Rubia 2 sites in San

Blas Bay as well Saenz cave in the Pali Aike area. They show similar directions observed in nearby sites from southern Patagonia in Argentina and Chile. In fact, previous results obtained at Mylodon, Cueva del Medio, Don Ariel and Las Buitreras caves yielded remanence directions corresponding to obliquely normal, obliquely reversed and reversed field polarity directions with similar VGPs. This situation strengthens the hypothesis of the existence of the Mylodon excursion in southern Patagonia. On the other hand, the presence of intermediate and reverse VGPs in San Blas records and other sites also supports its regional extent in the southern cone of South America. If the presented paleomagnetic features are true GMF behavior, the remarkably PSV record can serve to correlate regional stratigraphies, and to determine relative and absolute chronologies. Besides, if the anomalous directions represent excursions, they may be also used as dating devices, becoming excellent magnetostratigraphic markers for the time-span covered by the paleomagnetic record of the sites presented in this paper.

Keywords

Paleomagnetism, Geomagnetic Excursions, Archaeological Sites, Holocene, South America, Argentina

1. Introduction

Shared by the Republics of Argentina and Chile, Patagonia is a large geographic region of ~1,000,000 m^2 located in the southern end of South America. The Argentine portion of Patagonia is placed south of Colorado River and includes the provinces of Neuquén, Río Negro, Chubut and Santa Cruz, as well as the eastern portion of Tierra del Fuego Island and the southernmost part of Buenos Aires province. The Chilean part is located south of Bío Bío River and comprises the southern provinces and regions of Aisén and Magallanes, including the west of Tierra del Fuego and Cape Horn, and Palena Province in Los Lagos Region.

For a long time, this region was subjected to a significant number of Cenozoic palaeomagnetic investigations (Ré et al., 2008). Specific research on terminal Pleistocene and Holocene paleosecular variations records obtained at sedimentary lacustrine deposits in Argentina has been a topic since the early eighties (e.g., Creer et al., 1983; Gogorza et al., 1998, 2000; Sinito & Nuñez, 1997; Sylwan, 1989; Valencio et al., 1985). Detailed studies performed in archaeological and paleontological sites in Patagonia have yielded a number of results with stable and unstable records that showed intermediate and reverse geomagnetic field (GF) directions during the last ~11/10 ky, suggesting that GF excursion(s) occurred at different times through the Holocene (Nami, 1995a, 1999a, 2011, 2012; Nami & Sinito, 1991, 1993, 1995; Nami et al., 2017; Sinito et al., 2001). The possibility of an anomalous GF behavior during the more recent epoch seems to be an interesting palaeomagnetic subject, with important geomagnetic implications. The identification and definition of geomagnetic excursions have several re-

quirements (Laj & Channell, 2007; Roberts, 2008); one of the main ones in its distinction is the recording of similar behavior of the GF feature in diverse types of materials, such as lava flows, lacustrine sediments, and continental sedimentary deposits. Specifically, results obtained from the latter ones must belong to several sites and preferably in different environments (Thouveny et al., 1985; Verosub & Banerjee, 1977; Watkins, 1972). Hence, to assess this topic a variety of sections of recent sediments were sampled. Resulting from their study, this paper reports the results of a detailed palaeomagnetic research performed in archaeological and geological sections corresponding to Holocene deposits. They belong from diverse continental sedimentary sequences mainly formed in coastal marine and cave's environments. Paleomagnetic samplings were carried out in San Blas Bay and Pali Aike, which are areas located at the northern and southern portions of Argentine Patagonia, respectively.

2. Sampling Sites and Age of Deposits

To check results previously obtained, samplings were carried out in sections of fine sediments corresponding to the epoch under consideration. They were performed in the northern coast of Patagonia (Patagones Department) SE Buenos Aires province; also at the Gallegos-Chico River basin (Güer Aike Department), southern Santa Cruz province (**Figure 1**). Sampling sites were as follows:

1) San Blas 2 (SB2) (40˚33.39'S, 62˚14.35'W) is placed at San Blas village, Jabalí Island, in the Atlantic Ocean coast. The sampling (n = 36) was carried out in a section exposed on the entrance road to the village. It showed five stratigraphic levels; three of them are fine sediments (numbered I to III) while the other ones, are two gravel layers, named as I and II. Gravel I is located under the vegetation and gravel II of about 16 cm thick, is between 0.94 - 1.10 m below the surface. Layer I is sandy brown pale sediment, II is a more compacted sandy gray level and III is reddish sand, located below gravel II. The samples were taken as follows: In level I (samples SB2 1 to SB2 18), level II (SB2 19 to SB2 26) and the upper portion of level III (SB2 27 to SB2 36). A sample of re-deposited shell coming from gravel II yielded an uncalibrated ^{14}C date of 9720 ± 220 years before present (BP) (LP-1006); other ^{14}C dates on gravel deposits from Jabalí Island yielded ages of ~5.3 ky BP (Trebino, 1987). The gravel layer was probably formed at the time of the Holocene marine ingression that exhibited the maximum level between 6 and 5 ky BP in the eastern coast of South America in general (Pirazzolli, 1996), particularly in the Buenos Aires province (Violante et al., 2001).

2) Punta Rubia 2 (PR2) (40˚46.0'S, 62˚16.02'W) is situated on the Atlantic Ocean shoreline at ~20 km south of SB2. Over the coastal cliff there are a number of archaeological shell mounds that were impacted by diverse natural process, mainly the wind erosion. There, a number of sites were sampled for paleomagnetic research; one of them is an eroded shell midden called here PR2. A test pit of 1 m^2 by 1 m depth was performed for archaeological purposes. It showed three stratigraphic levels: I was formed by sand, layer II is reddish brown

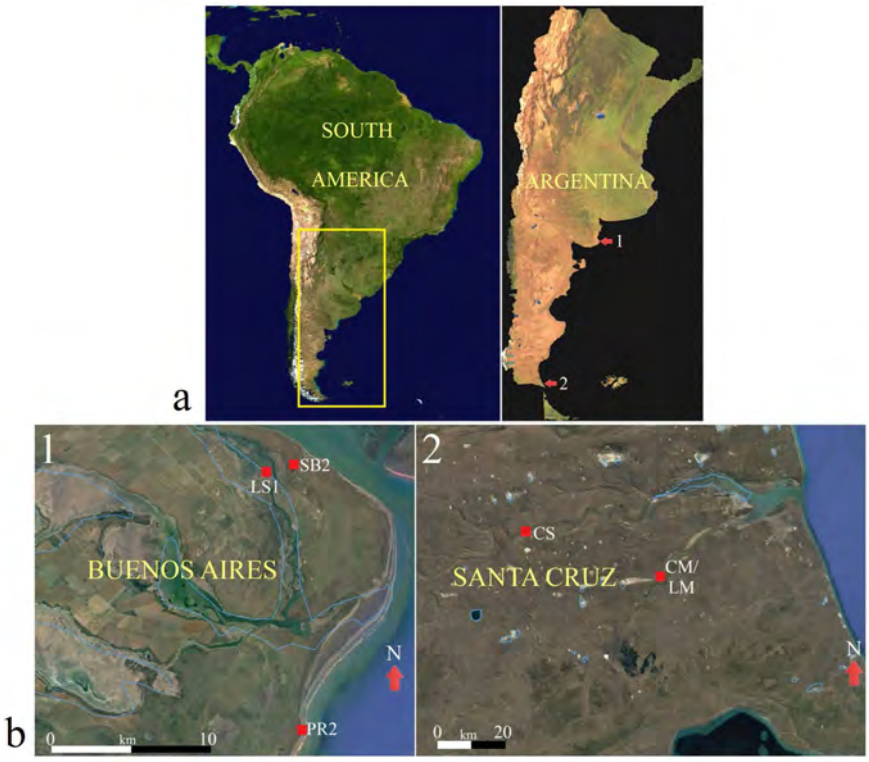

Figure 1. Geographical location of the sites reported in this paper. (a) Map of South America showing the location of Argentina Republic (denoted with a rectangle) indicating with numbers the place of the sampled sites; (b) Localities and sites showed in the general map: 1) San Blas bay in Buenos Aires province, 2) Pali Aike region in the Santa Cruz province (modified after Google maps).

clayed sediment and III is gray clay. Archaeological artifacts corresponding to the Late Holocene were found in the surface and the upper part of level II. A vertical sampling (n = 39) along the section of the test pit was carried out. Samples PR2 1 to PR2 16 belongs from level I, PR2 17 to PR2 34 from level II and PR2 35 to PR2 39 from level III.

3) La Serranita 1 (LS1) (40˚33.02'S, 62˚38.16'W) is located ~3 km to the West of San Blas village on a chain of sand dunes overlying a gravel deposit indicating a Middle Holocene coastal line dated ~6.0 ky BP (Trebino, 1987). At La Serranita locality, a number of archaeological shell middens are exposed with remains over the surface and partially buried deposits. Careful examinations of one of them allowed finding diverse archaeological remains. It is worth to mention Middle Holocene triangular projectile points, lithic artifacts, mollusks, varied faunal remains and a hearth that was carefully excavated. Using conventional ^{14}C method at the LATYR laboratory, University of La Plata (Argentina) a charcoal sampled for the hearth was dated at 5300 ± 40 uncalibrated years BP. Mollusks remains were also dated at 5310 ± 70 and 5320 ± 60 years BP (Sanguinetti de Bórmida, 2005). After finished the hearth excavation, a horizontal paleomagnetic sampling (n = 15) was performed on a sand deposit at 5 cm below the hearth.

4) Cueva Montecarlo (CM) (51˚54.86'S, 69˚38.79'W) is a small cave formed in

an ancient crater called Montecarlo hill at ~1 km west of Markatch Aike ranch, in the Gallegos-Chico River basin, south of Santa Cruz province, southern Patagonia (Nami, 1995b, 1999b). Underlying the bedrock, the deposit of ~0.4 m has three layers: layer 1 is sheep dung, 2 is silt (Bayarski, pers.com), and 3 is mostly formed by ash charcoal product of human hearths. This layer contains a notably archaeological level with stone tools used by hunter-gatherers living in the area during the late Holocene (Bird, 1988; Nami, 1995b). A conventional ^{14}C date obtained at 50 cm from the ash layer yielded a date of 1040 ± 50 uncalibrated years BP (Beta-124706). Twelve paleomagnetic samples in two section named CM1 (n = 6) and CM2 (n = 6) were made in layers 2 (samples 1 to 3) and 3 (samples 4 to 6).

5) Laguna Montecarlo (LMo) (51˚55'S, 69˚39'W) is a small temporary lagoon located at 2.5 km west from CM. To check the records obtained from archaeological sites from the region, a 1 m^2 trial pit by 0.9 m depth was made in center of the lagoon. Only one stratum of a uniform grayish green clay was sampled (n = 23) up to 52 cm depth. The Holocene age of the deposit may be suggested because these sort of small lagoons have been regionally formed after the post glacial times (Grondona, 1975).

6) Cueva Saenz (CS) (51˚44.46'S, 70˚09.92'W) located 60 km to the west of the Río Gallegos city. This cave is located 400 m east of Las Buitreras cave, which was previously sampled (Nami, 1999a). Two palaeomagnetic samplings were performed in two parts of the site with different sedimentary deposits; one in the front part and the other in the inner portion. In this paper, is reported only the preliminary results obtained in the cores (n = 5) taken from a ~30 cm sand level deposit located in the frontal part.

3. Paleomagnetic Study

Sampling, Methods, and Results

With exception of LS1 that the sampling was horizontally performed, all samplings were done in vertical form from the top to the base of the sedimentary deposits (**Figure 2(e)**). Samples were collected using 2.5 cm long and 2 cm diameter plastic containers carefully pushed into the sediments and overlying the next one about 50% each. Their orientation was measured using a Brunton compass; they were consolidated with sodium silicate once removed and finally, numerated from the top to the bottom. In some cases samples were not taken near the surface because the sediments were unconsolidated and they may have been disturbed by recent events, such as animal and/or human trampling (PR2, CM), the upper part might be disturbed by roots (SB2) or, because the presence of pebbles and rocks (CS).

All samples were subjected to progressive AF demagnetization in steps of 3, 6, 9, 12, 15, 20, 25, 30, 40 and 60 mT in a 3-axis static degausser, attached to a 2G cryogenic magnetometer and subsequently measured with the magnetometer. Additional steps of 80, 100 and 120 mT were used in some samples. Characteristic

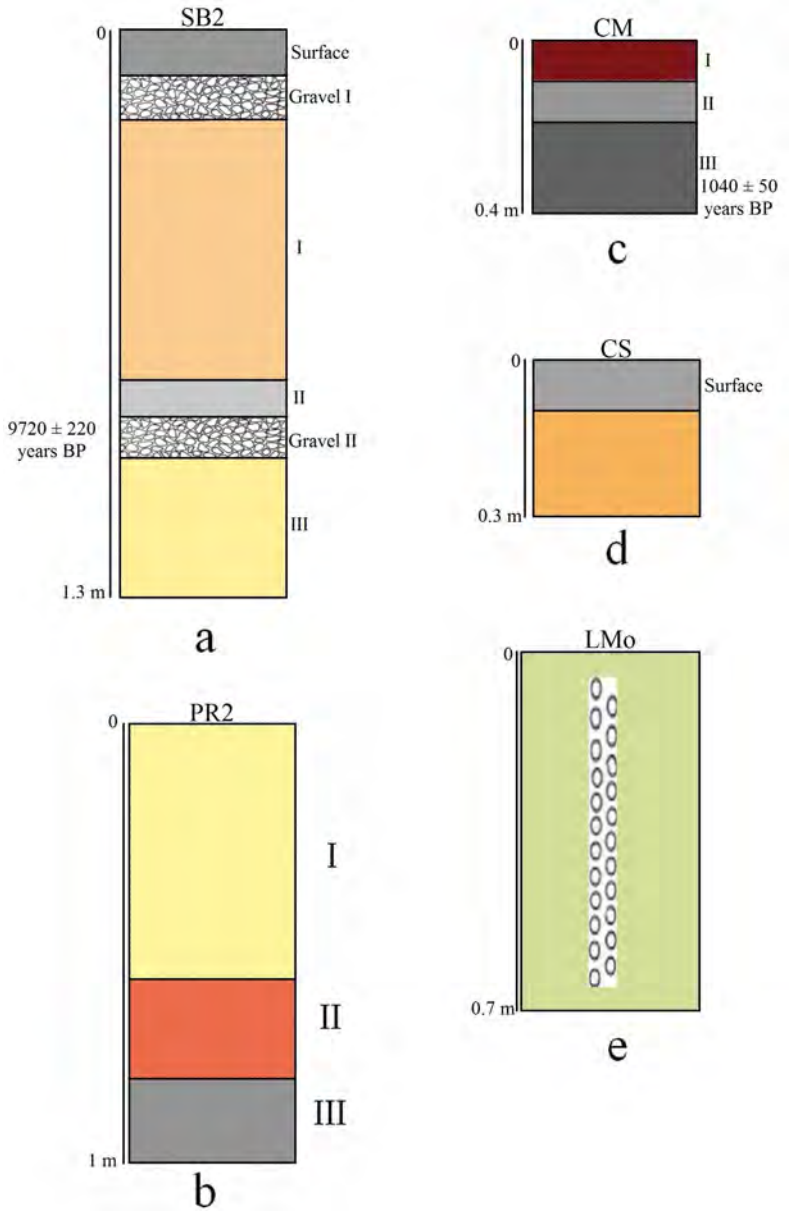

Figure 2. Schematic profiles showing the stratigraphic sections sampled related with ^{14}C dates. (a) San Blas 2; (b) Punta Rubia 2; (c) Cueva Montecarlo; (d) Cueva Saenz; (e) Laguna Montecarlo showing the paleomagnetic sampling. Numbers to the right of the sections show numbers of layers, its sediments description and samples locations are given in the text.

remanent magnetization (ChRM) was calculated using Principal Components Analysis (PCA). The inherent scatter in directions was measure using the Maximum Angular Deviation (MAD) (Kirschvink, 1980).

According to the number of magnetic components and stability, remanence directions in most palaeomagnetic samples were highly reliable (HRe), with practically univectorial behavior with decay towards the origin (i.e. SB2 16, Figure 3(c); CM 12, Figure 6(a); LMo 10, Figure 7(d)) and moderately reliable (MRe), with noisy behavior during demagnetization and/or, well defined prin-

cipal component but with erratic behavior during final steps (i.e. SB2 3, SB2 8, Figure 3(a), Figure 3(b)) unreliable, with unstable behavior (e.g. Figure 16); in this case, they were rejected (SB2 11, LS1 4, LS1 10). In general samples from each site showed a common pattern with similar reliability. They are as follows:

SB2: Vector diagrams projection (VDP) depicted in Figure 3 illustrates samples that showed a viscous remanence which was removed at 3 - 12 mT (e.g. SB2 3, SB2 16, Figure 3(a), Figure 3(c)). The ChRM show cores with normal directions with either steep (SB2 16, Figure 3(c)) or shallow negative inclinations (SB2 8, Figure 3(b)). A few samples showed southward directions (SB2 23, Figure 3(d)).

PR2: Most of the samples were HRe with linear decay towards the origin (PR2 14, PR2 18, Figure 4(a), Figure 4(b)). VDP diagrams illustrated in Figure 4 show specimens with either single component (PR2 14, PR2 18, Figure 4(a) & Figure 4(b)) and with the anchored line of some of them decaying to the origin (PR2 24, Figure 4(d)); others ones had two components, one with an anomalous southward direction (PR2 24, Figure 4(b), Figure 4(d)). Zijderveld diagrams show reverse samples (PR2 18, PR2 24, Figure 4(b), Figure 4(d)) and normal with either shallow (PR2 19, Figure 4(c)) or steep inclinations with north-easterly (PR2 36, Figure 4(e)).

LS1: Samples from this site showed a common pattern with similar magnetic behavior. Many of them presented linear demagnetization plots with one of two magnetic components (Figure 5). In the majority, a ChRM could be defined trending in the Zijderveld diagrams towards the origin. More secondary components were a soft viscous magnetism that was easily eliminated between 3 and 9 mT (LS1 9, LS1 13, Figure 5(b) & Figure 5(c)). In most LS1 cores the NRM

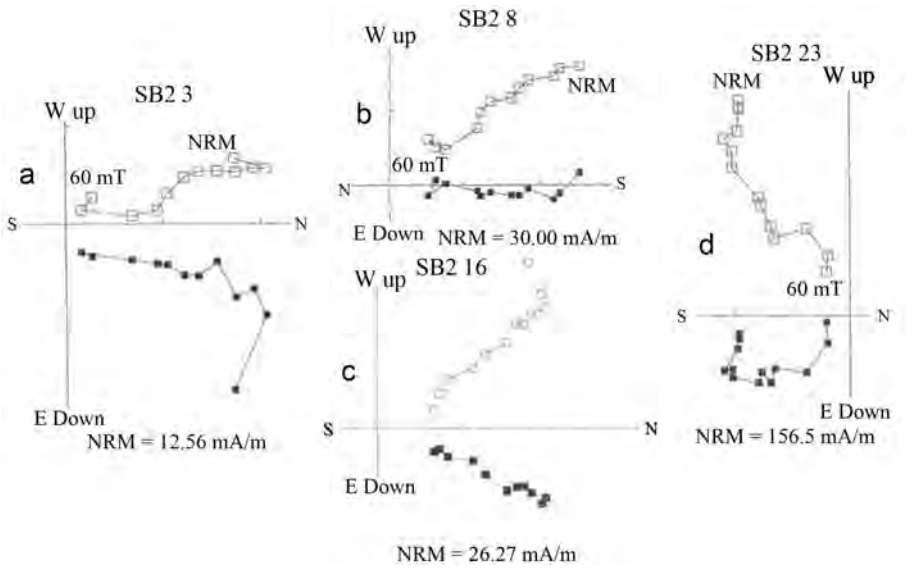

Figure 3. Typical Zijderveld diagrams from the SB2 section. The totality of the vector projection diagrams illustrated in the figures is directional data with corrected field. Solid symbols correspond to the projection onto the horizontal plane, while open symbols are projection onto the vertical plane.

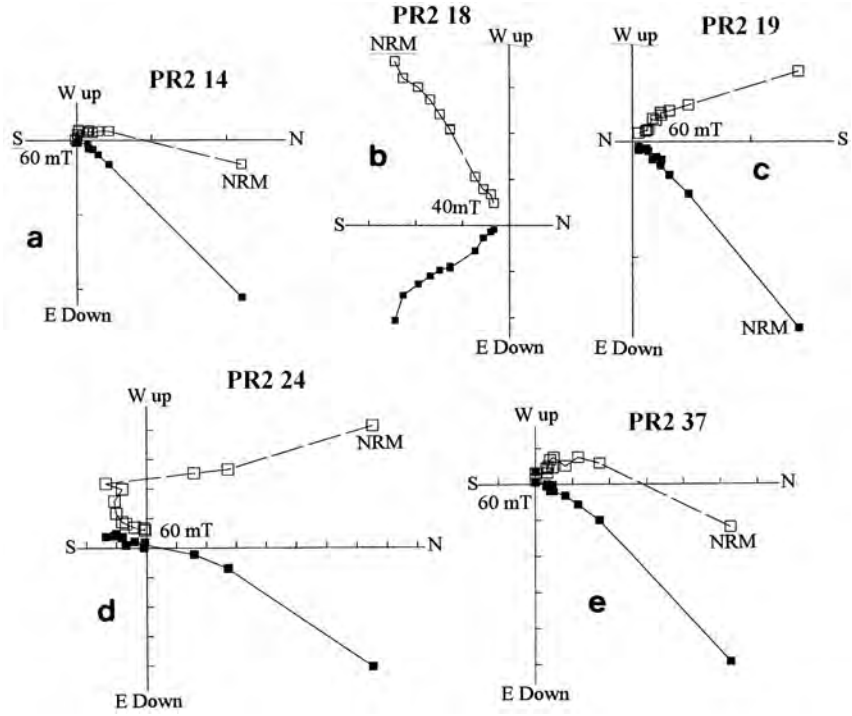

Figure 4. Vector components diagrams showing the behavior of typical samples from PR2 profile.

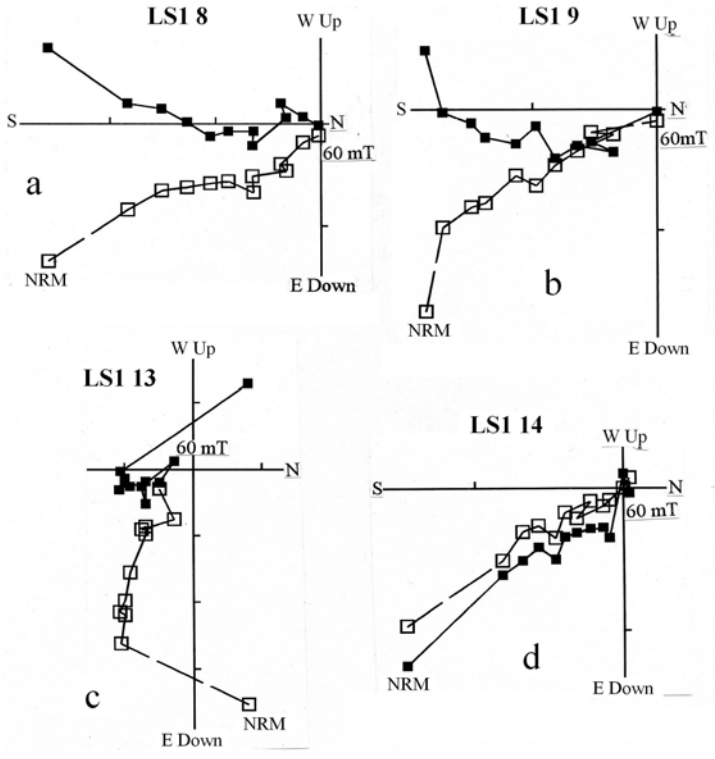

Figure 5. Zijderveld diagrams of some samples from LS1.

removed at fields of 60 mT (Figure 5). LS1 14 (Figure 5(d)) are examples of specimens with univectorial behavior with decay towards the coordinates origin.

CM: Specimens from this site showed similar magnetic behavior with linear demagnetization plots with one of two magnetic components. In the majority, a ChRM could be defined trending in the Zijderveld diagrams towards the origin (CM1 2, CM1 4, CM2 1, Figure 6(a), Figure 6(b), Figure 6(d)). More secondary components were a soft viscous magnetism that was easily removed between 3 and 12 mT (CM1 3, CM2 4, Figure 6(b), Figure 6(f)). Normal and intermediate directions (CM1 2, Figure 6(a)), were found in several samples. In most CM cores less than 10% of the NRM eliminated at fields of 60 - 80 mT (CM1 2, CM2 2, Figure 6(a), Figure 6(e)). CM1 2, CM1 4 CM2 1 (Figure 6(a), Figure 6(c), Figure 6(d)) exemplify cores with univectorial behavior decaying towards the coordinate's origin with normal directions (CM1 2, CM1 4, CM2 1, Figure 6(a), Figure 6(c), Figure 6(d)), and low inclination values (CM2 1, CM2 4, Figure 6(d), Figure 6(f)). A few samples had two components with the second one decaying to the origin in the VDP (CM2 2, CM2 4, Figure 6(e), Figure 6(f)). Some isolated cores showed three components, one of them going to the origin with southwesterly direction (CM1 3, Figure 6(b)).

LMo: The majority of the samples were highly reliable single components, displaying similar pattern going to the origin in the Zijderveld diagrams (LMo 12, LMo 16, LMo 29, Figure 7(b), Figure 7(d), Figure 7(e)). Some samples had univectorial behavior with south- and north-westerly (LMo 8, LMo 21, Figure 9(b), Figure 9(e)) and westerly directions (LMo 1, LMo 9, LMo 10, Figure 7(a), Figure 7(c), Figure 7(d)).

CS: The samples showed either single component remanence (CS 5, Figure 8(b)) and other ones had two magnetic components with anchored fitting line to the origin in the VDP diagrams; some cores showed a viscous remanence removed at 3 mT (CS 1, Figure 8(a)). They recorded univectorial reverse (CS 16, Figure 8(b)) and intermediate (CS 5, Figure 8(a)) directions.

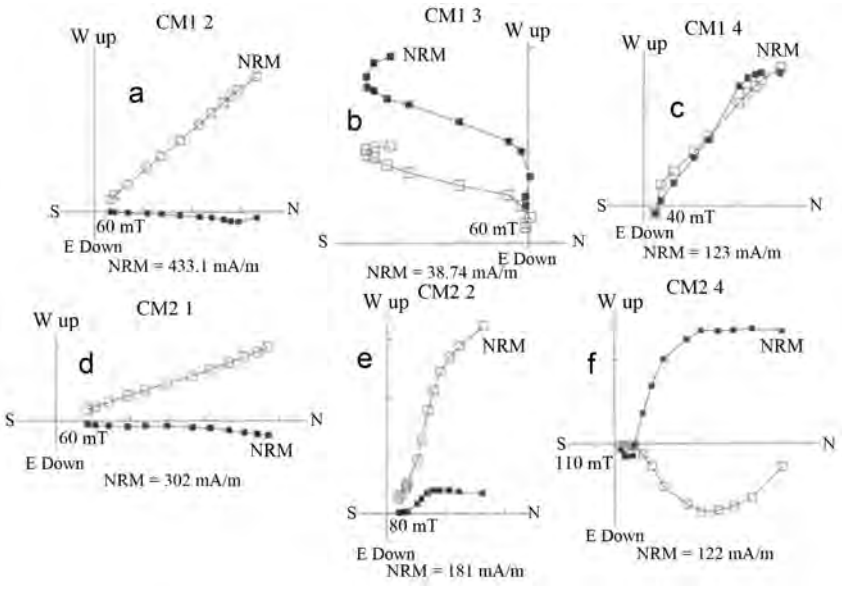

Figure 6. Examples of vector projection diagrams for CM site.

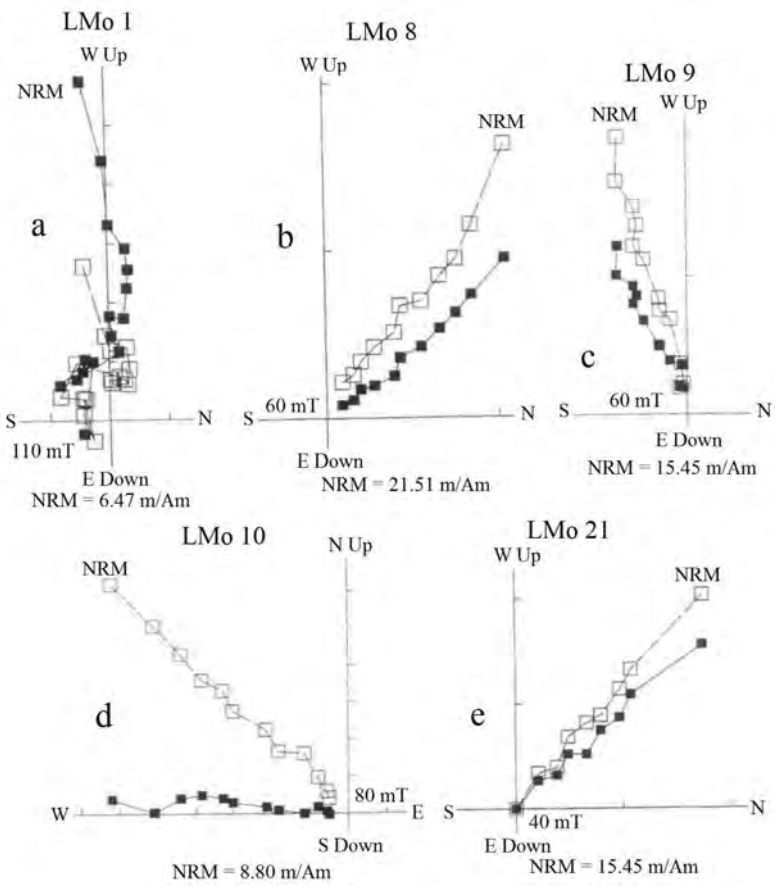

Figure 7. Vector components diagrams showing the behavior of typical samples from LMo site.

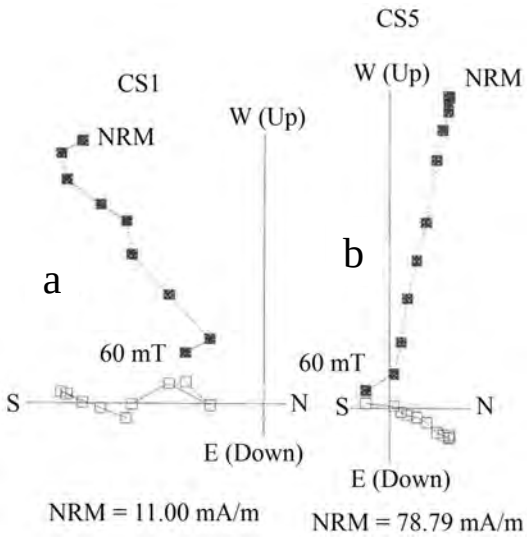

Figure 8. Examples of Zijderveld diagrams for CS site.

As depicted in Table 1, in general MAD values were very low. The number and intervals of demagnetization steps to isolate the ChRM and VGPs positions are described in Table 2. Except LS1, the sections shows normal and intermediate

Table 1. Range and percentage of MAD values discriminate by sites.

Site	0˚ - 5˚ (%)	5.1˚ - 10˚ (%)	10.1˚ - 15˚ (%)
SB2	-	50.0	50.0
PR2	69.23	30.77	-
LS1	30.77	46.15	23.08
CM	66.7	33.3	-
LMo	21.74	65.22	13.04
CS	25.0	75.0	-

Table 2. Values of characteristic remanent magnetization, virtual geomagnetic pole positions, and intervals of selected ChRM for each sample. Negatives values show negative inclination or VGP located in the Southern Hemisphere. Intervals of selected ChRM are given in mT. References: D: Declination, I: Inclination, Long.: Longitude, Lat.: Latitude, IChRM: Intervals of selected ChRM, Or.: Origin in the Zijderveld diagram.

Sample	D˚	I˚	Long. E	Lat.	Int. ChRM	Sample	D˚	I˚	Long. E	Lat.	Int. ChRM
			SB2			33	45	−13	360	37	0 - Or.
1	5	−36	311	69	12 - 60	34	38	−5	350	39	9 - Or.
2	15	−44	343	71	6 - 25	35	31	−35	358	56	9 - Or.
3	8	−2	310	50	25 - 60	36	45	16	348	26	0 - 15
4	12	−49	345	76	0 - 90	37	62	47	349	0	0 - 20
5	25	1	333	43	30 - 60	38	41	−7	353	38	0 - 20
6	20	−35	343	63	6 - Or.	39	41	−12	356	40	0 - Or.
7	350	−28	276	63	9 - 40				**LS1**		
8	1	−33	300	68	0 - Or.	1	147	31	58	−53	0 - Or.
9	53	−24	13	36	3 - 25	2	175	30	106	−65	12 - 30
10	40	−7	353	39	12 - Or.	3	62	70	331	−18	0 - 25
12	22	−50	7	70	3 - 25	5	160	51	50	−72	0 - 50
13	359	−29	296	65	12 - 40	6	177	9	112	−54	6 - 25
14	8	−23	314	61	15 - 50	7	229	70	247	−55	3 - 20
15	333	−58	204	69	15 - 60	8	183	19	123	−59	3 - 60
16	25	−37	352	60	6 - 50	9	192	30	144	−63	3 - 40
17	15	−37	335	67	12 - 50	11	281	80	274	−34	3 - 15
18	2	−30	303	66	12 - 40	12	184	28	126	−64	3 - Or.
19	22	−41	352	65	9 - 40	13	199	75	275	−66	3 - 30
20	334	−54	216	69	0 - 80	14	142	27	55	−48	0 - Or.
21	1	−46	302	67	6 - Or.	15	149	18	68	−48	0 - 30
22	69	−70	69	43	3 - 20				**LMo**		
23	173	−58	110	−10	20 - 50	1	261	−25	185	5	0 - 25
24	69	−25	25	24	40 - Or.	2	284	2	212	8	6 - 20
25	351	33	288	31	3 - 12	3	305	−36	216	37	0 - 6

Continued

26	287	76	268	−29	15 - 60	4	278	−35	194	20	0 - 40
27	7	−33	315	67	3 - Or.	5	298	−59	191	47	0 - 25
30	69	−76	82	45	9 - 30	6	304	−36	215	36	0 - Or.
31	73	−58	52	35	3 - 25	7	308	−33	220	37	0 - 25
34	142	−77	326	−57	3 - Or.	8	318	−46	222	50	0 - Or.
36	91	−50	53	19	3 - 30	9	244	−57	158	15	0 - Or.
			PR2			10	274	−44	187	22	0 - Or.
1	40	−2	351	36	0 - Or.	11	298	−48	202	39	0 - 60
2	33	9	340	36	0 - Or.	12	304	−56	199	48	0 - 50
3	31	4	339	39	0 - Or.	13	289	−40	200	29	0 - Or.
4	49	3	357	29	0 - Or.	14	295	−54	194	41	0 - 40
5	41	−14	356	41	0 - Or.	15	316	−59	204	58	0 - 25
6	40	8	347	32	0 - Or.	16	344	−36	263	56	3 - 25
7	38	8	345	33	0 - 25	17	222	−15	156	−21	25 - 80
8	45	11	351	28	0 - Or.	18	347	−33	267	65	6 - 25
9	52	−3	181	29	0 - Or.	19	19	−74	67	76	0 - 40
10	10	−35	323	67	0 - Or.	20	355	−44	280	64	9 - Or.
11	41	15	346	29	0 - Or.	21	318	−41	227	48	0 - Or.
12	37	19	340	29	0 - Or.	22	317	−67	187	63	0 - Or.
13	37	0	347	37	0 - Or.	23	322	−69	183	67	12 - Or.
14	44	8	351	30	0 - Or.				**CM1**		
15	49	11	354	26	0 - Or.	1	37	−15	339	37	12 - Or.
16	32	14	337	34	0 - 15	2	4	−40	298	61	0 - Or.
17	12	−51	348	77	12 - Or.	3	313	−66	188	60	30 - Or.
18	145	−53	8	59	6 - Or.	4	307	−31	220	36	3 - 40
19	50	−14	5	34	0 - 40	5	334	−6	257	37	4 - Or.
20	32	−44	60	8	15 - Or.	6	8	1	301	37	3 - 100
21	354	−36	282	69	12 - 30				**CM2**		
22	49	−6	320	32	0 - Or.	1	3	−20	295	49	0 - Or.
23	29	−6	340	44	0 - Or.	2	331	−70	181	72	3 - Or.
24	201	−25	142	−33	18 - 60	3	44	−24	349	37	9 - Or.
25	48	−8	180	33	0 - 30	4	47	7	343	22	60 - Or.
26	59	−73	74	50	9 - 25	5	15	−6	310	40	40 - Or.
27	2	−77	116	66	10 - 40	6	324	−45	229	53	40 - Or.
28	345	−72	144	71	12 - Or.				**CS**		
29	38	−8	351	40	0 - 60	1	230	1	167	−24	3 - 25
30	56	−3	5	26	0 - Or.	3	21	18	313	27	6 - 50
31	35	−40	7	56	12 - Or.	5	283	6	212	6	3 - Or.
32	47	−16	3	37	0 - Or.	6	354	71	286	−17	3 - 30

polarity directions far from the present GF, while reversed polarities were recorded at SB2, PR2 and LS1. Figure 9 illustrates the stereographic projection of ChRM isolated from the sites under study. Figures 10-12 summarize the changes in the declinations and inclinations of the ChRM for the sections reported here.

The declination and inclination profiles from SB2 shows an important correlative shift toward higher negative values in inclination of ~40˚ - 50˚ between samples 1 and 16 in the upper portion of the section; also shows wide pulses with reverse directions and transitional positions between samples SB2 20 and SB2 30 (Figure 10). The more conspicuous long declination and inclination departures from SB2 are depicted between dashed lines and indicated with arrows. SB2 records suggest a shift from to intermediate and reversed positions during the early and middle Holocene (9 - 5 ky BP). As illustrated in Figure 11, a similar fact is also observed in the PR2 log that shows positive inclination values in the upper portion until sample PR2 16 with a shift to higher negative values between samples PR2 17 and PR2 35. The more notably fluctuations in declination occurs between samples PR2 18 and PR2 28. The stereoplots depicted in Figure 9 shows that the totality of the samples horizontally taken at LS1 recorded reverse magnetization directions dated at ~5.3 ky BP during the middle Holocene.

In LMo a significant but gently westward shift in declination (over 90˚) and less conspicuous shallowing of the inclination can be observed (Figure 12(a)).

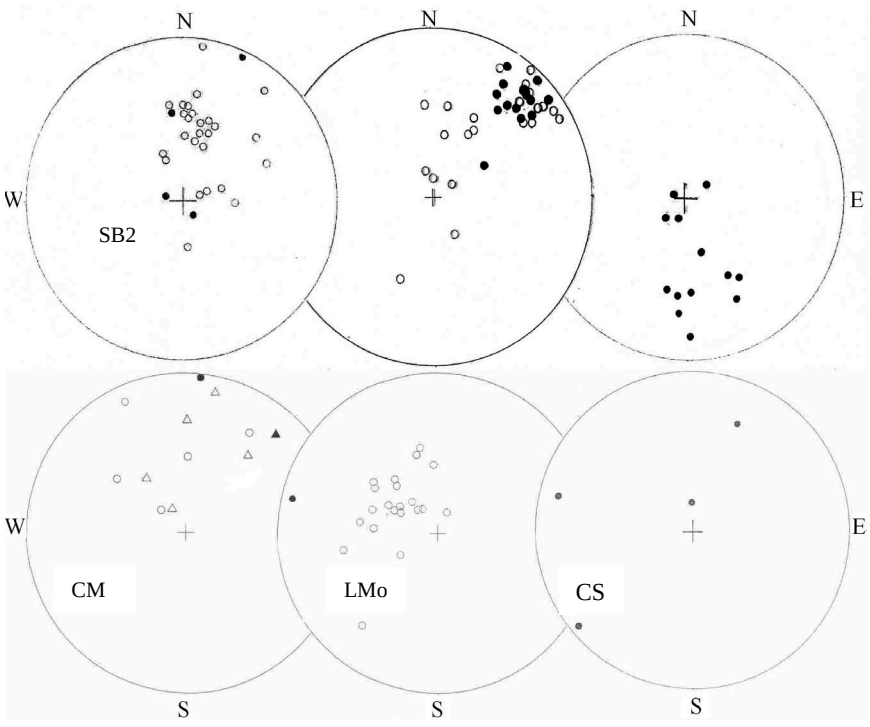

Figure 9. Directional data with field correction of characteristic remanent magnetizations (ChRM) of each sample for the section reported in this paper. Negative inclination (open circle), and positive inclination (solid circle). The triangles in Figure 9, Figure 13 and Figure 14 represent CM2.

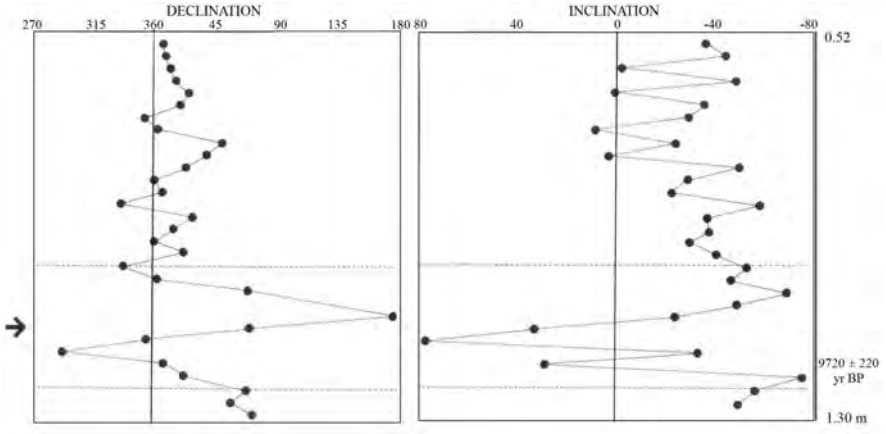

Figure 10. Magnetograms showing the stratigraphic presentation of declination and inclination profile from SB2. The more conspicuous long directions departures are depicted between dashed lines and pointed with an arrow.

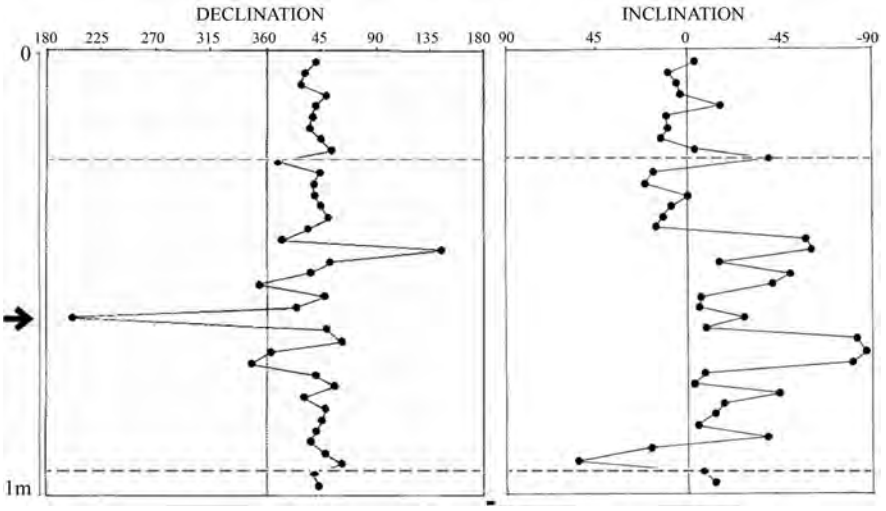

Figure 11. Declination and inclination logs from PR2 site.

Both samplings in CM recorded negative to positive changes in inclination with similar directions during the first millennium bp (Figure 12(b)). Despite that scarce number of cores from CS, they exhibit intermediate and reverse directions, a fact also observed in other sites from southern Patagonia in Argentina and Chile (see below).

Figure 13 depicts the virtual geomagnetic pole positions (VGP) calculated from the directions of Table 2. When plotted on a present world map, they show intermediate VGPs from the rotation axis of the Earth in the northern Hemisphere between 60˚ and 30˚ (mainly in North Africa) and reverse VGPs located in the southern Hemisphere (Figure 14). Particularly, the PR2 VGPs coincides with the ones calculated for PA11 and Las Buitreras sites, respectively located in NW and SE Patagonia (Nami, 1999b). The geographical distribution defined from spherical statistical analysis suggests that not only the transitional VGPs have peculiar distributions, but VGPs corresponding to stable polarity fields

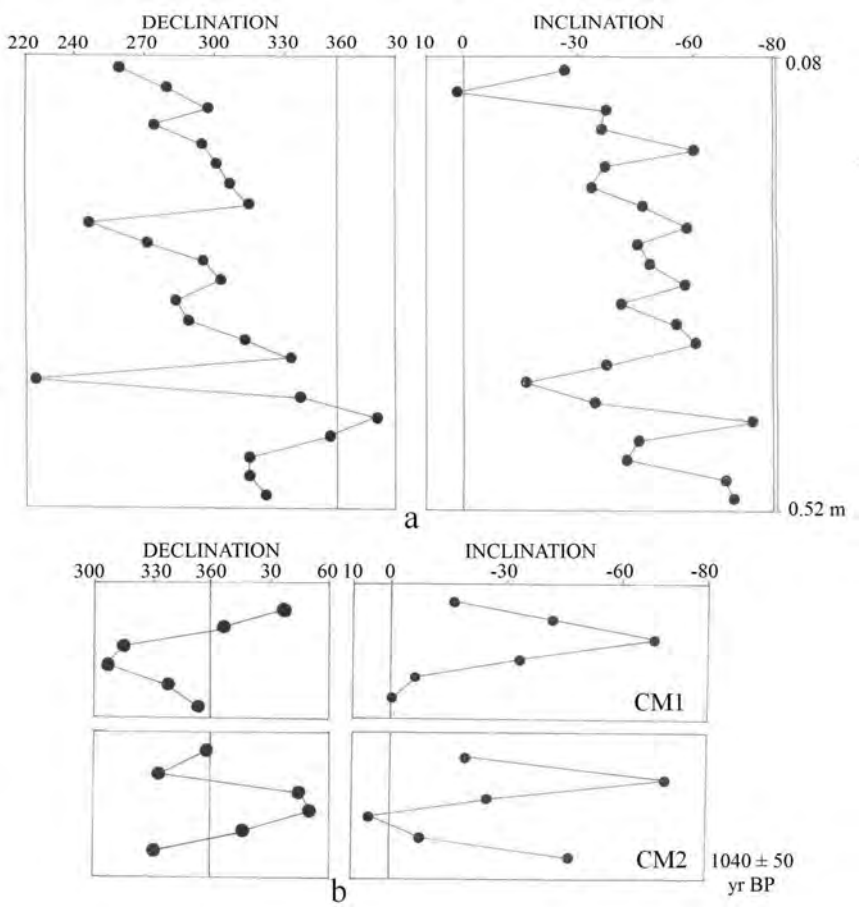

Figure 12. Declination and inclination logs according to their stratigraphic presentation from LM (a) and CMo (b).

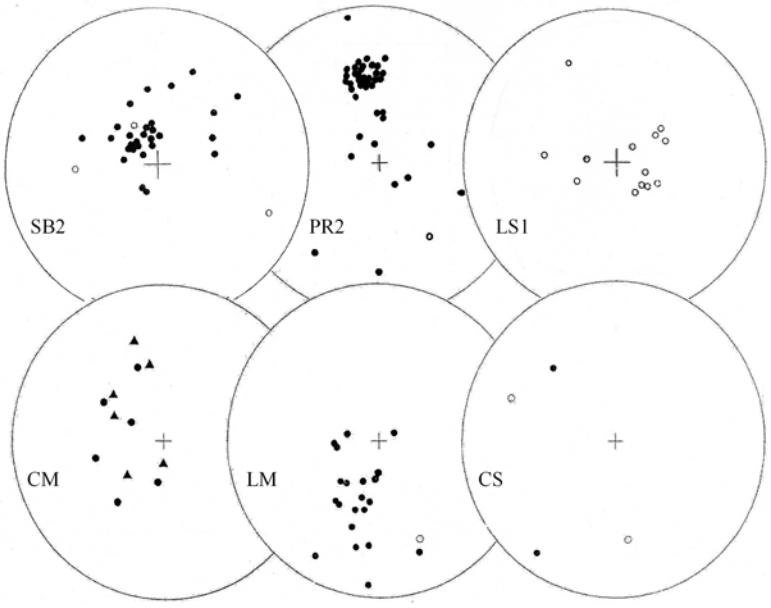

Figure 13. Stereographic projection of VGP calculated from directions of ChRM isolated in the sites mentioned in the text. Solid circles show those ones located in the Northern Hemisphere. The center of the projection is the Geographic Southern Pole.

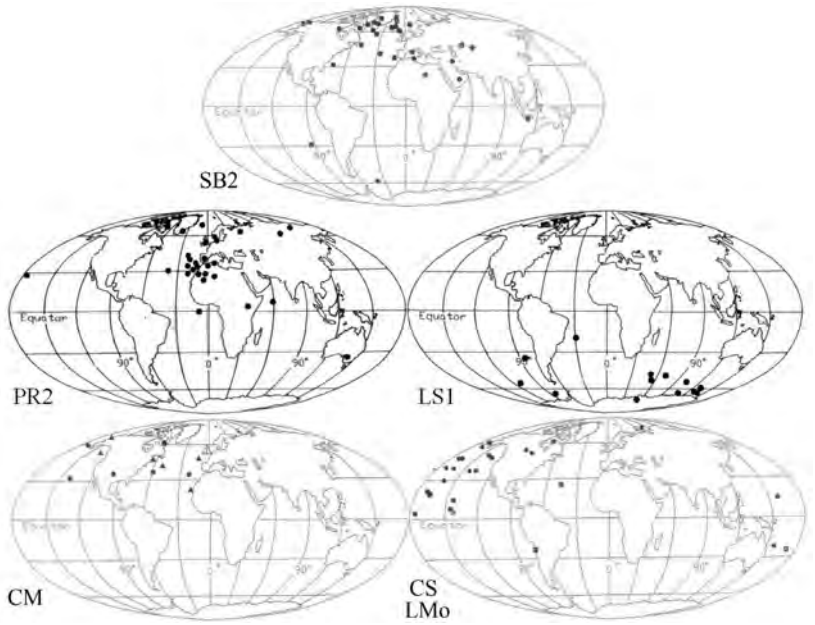

Figure 14. World map showing the location of the VGP obtained from the sites described in Table 2.

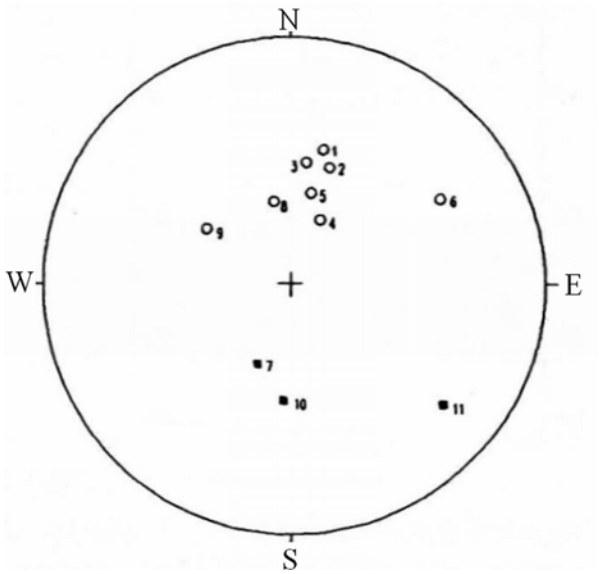

Figure 15. Stereographic projection of the Angostura Blanca directions. Open and solid circles respectively show negative and positive inclination (After Sinito et al., 1997; Figure 4(b)).

or to excursional fields seem to follow a geographical pattern that shows a non uniform distribution in longitude (Mena & Nami, 2002; Nami & Mena, 2010), those ones in the southern hemisphere are located in South America, South Africa, Australasia and Antarctica. These positions agree remarkably well with VGPs observed in previous paleomagnetic studies performed on Latest Pleistocene and Holocene sections from the southern cone of South America (Nami, 1999a, 2006, 2008, 2011, 2012; Nami et al., 2017). Remarkably is that this dis-

tribution shows strong similarities with the VGPs calculated for the Laschamp and Iceland basin excursions respectively dated at ~40 ky and ~180 - 220 ky BP interval (Laj & Channell, 2007). Is also remarkably, the agreement of VGPs located in southern Africa with the VGPs calculated for the Late Pleistocene excursion identified in several parts of Argentina and dated at ~26 - 30 ky BP (Orgeira et al., 1990, 1996; Vizán & Azcuy, 2010). Besides, the location of transitional VGPs in Africa and Australasia were observed in several records from different periods of the Earth history (e.g., Coe & Glen, 2004; Creer & Ispir, 1970; Gurarii, 2005; Herrero-Bervera & Coe, 1999; Hoffman & Singer, 2004; Ohno et al., 2008).

4. Discussion

In conclusions of the investigations described above, new data obtained at sediments from various environments and lithologies cored in northern and southern Patagonia have been found to contain records of anomalous GF behavior during the Holocene. Actually, besides normal and intermediate polarity directions far from the present GF, most of the sections reported here shows reversed polarities. They were recorded at SB2, LS1 and PR2 sites in San Blas Bay as well Saenz cave in the Pali Aike area, showing similar directions observed in nearby sites from southern Patagonia in Argentina and Chile. In fact, previous results obtained at several sections produced diverse samplings, stable and instable records with normal, intermediate and reverse directions happening at different times during the last ~11 - 10 ky. A brief summary follows. Early in 1990, the Angostura Blanca rockshelter, Chubut province in central Patagonia, yielded reverse directions at ~2 ky BP (**Figure 15**). At Piedra del Aguila 11 rockshelter (Neuquén province) in Northwestern Patagonia, a multicomponent sample showed that despite unreliable to isolated directions, the vector changes from negative to positive inclinations (intermediate or reverse) moving in a great circle at ~2 ky BP (**Figure 16**). In southern Chilean Patagonia, Mylodon cave (Nami, 1995a), yielded a stable record with reverse directions between 10 and ≤5 ky BP (**Figure 17(b)**, **Figure17(c)**). There, clear reverse samples were dated during the middle Holocene at ~5.5 ky BP (**Figure 17(d)**, **Figure 17(e)**); nearby, Cueva del Medio yielded a record from a section dated at ~10.0 ky BP with samples that recorded two magnetic components with normal and intermediate directions (**Figure 18**) indicating the presence of an anomalous GF behaviour after deposition (Nami & Sinito, 1995). At about 135 km east in southern Argentina, Las Buitreras cave yielded an unstable record with normal, intermediate and reverse directions dated at ~4.3 ≥ 10 ky BP (**Figure 19**; Nami, 1999a). Highly reliable samples taken at Don Ariel cave (Nami, 1994) also yielded remanence directions corresponding to intermediate and reversed magnetization directions during the early and middle Holocene (**Figure 20**). These records along with the ones presented in this paper strengthen the hypothesis of the existence of the Mylodon excursion in southern Patagonia. On the other hand, the presence of intermediate

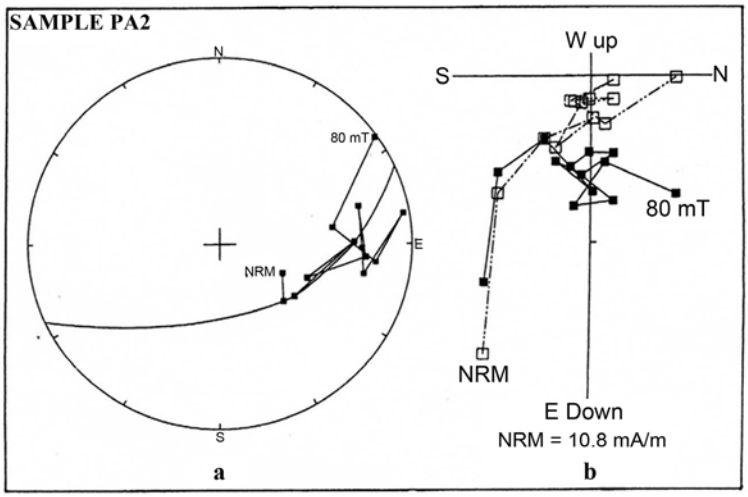

Figure 16. Multicomponent sample from Piedra del Aguila 11 site (#2) from NW Patagonia that despite unreliable to isolate directions shows that the vector changes from negative to positive inclinations (intermediate or reverse) moving in a great circle. (a) Stereographic projection; (b) Zijderveld diagram (After Nami, 1999a; **Figure 7**).

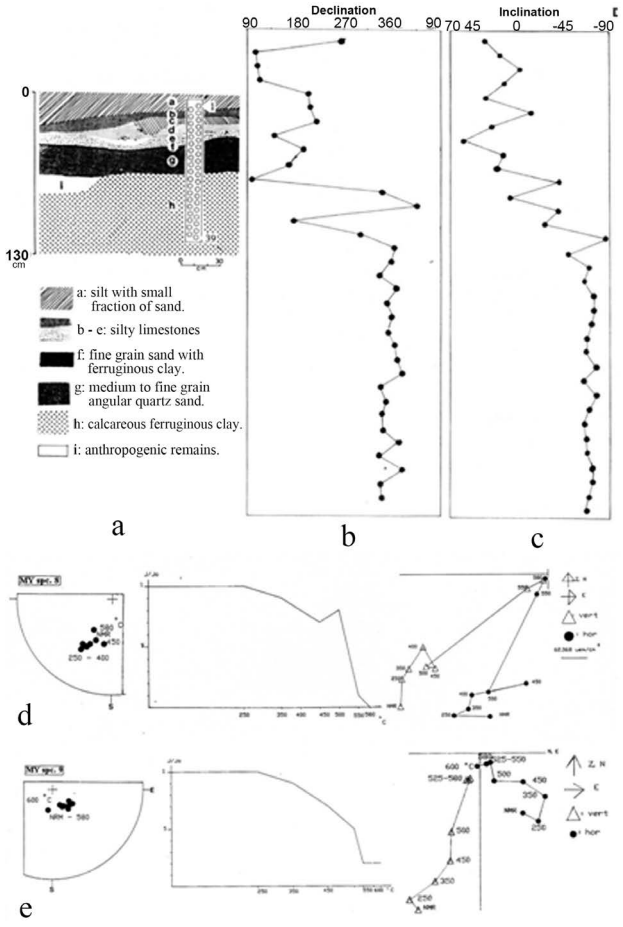

Figure 17. Different details of the Mylodon cave paleomagnetic sampling. (a) Stratigraphic section and sampling location; (b, c) Declination and Inclination logs; (d, e) Examples of reverse samples showing its stereoplot, demagnetization curves using thermal cleaning and Zijderveld diagrams (modified after Nami, 1995a).

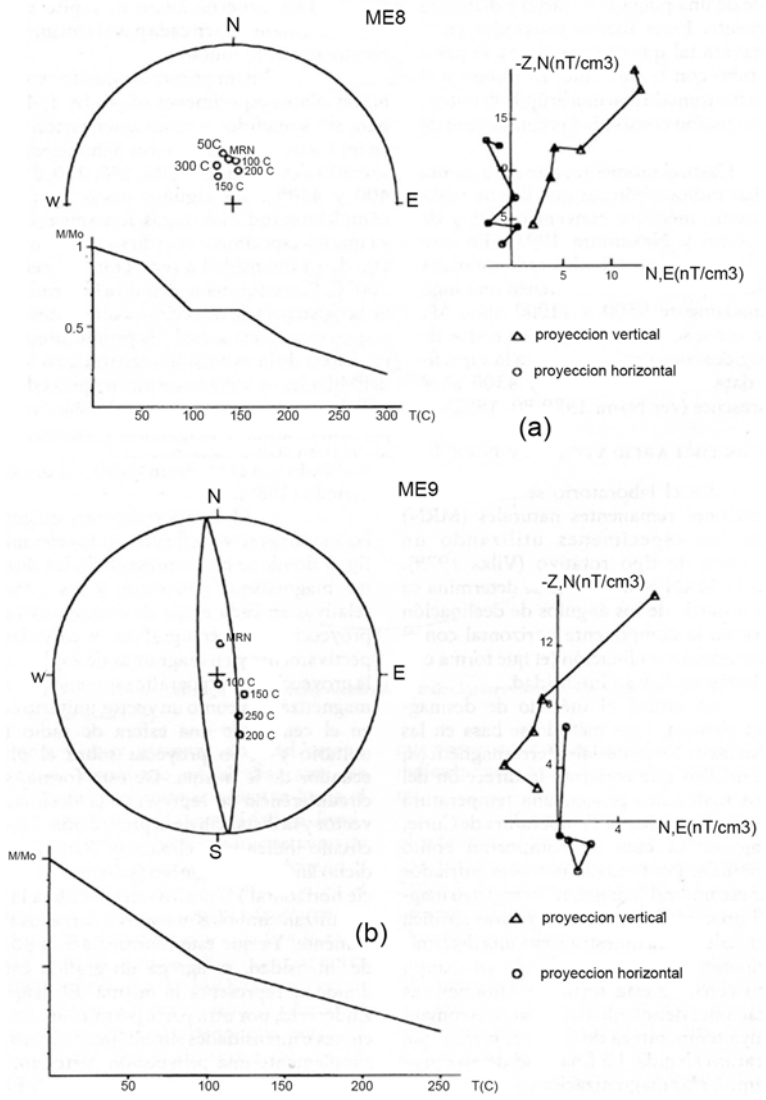

Figure18. Examples of samples from Cueva del Medio with normal and oblique directions. The maximum circle indicates at least two at least two overlapped directions (After Nami & Sinito, 1995: **Figure 3**).

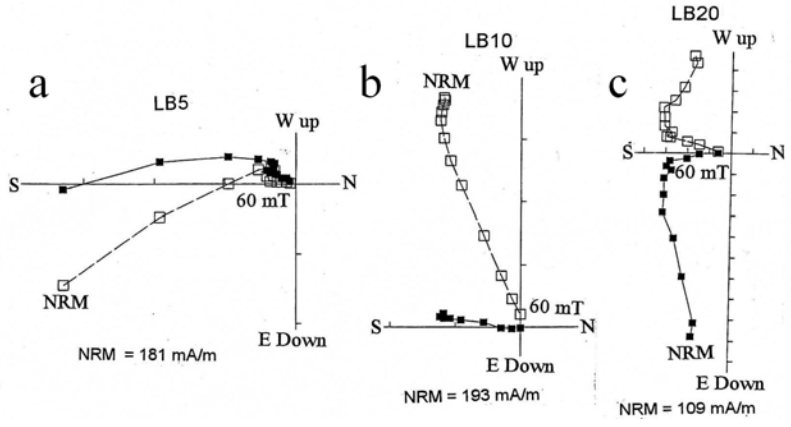

Figure 19. Examples of Zijderveld diagrams with southward directions from Las Buitreras cave (modified after Nami, 1999a, **Figure 6**).

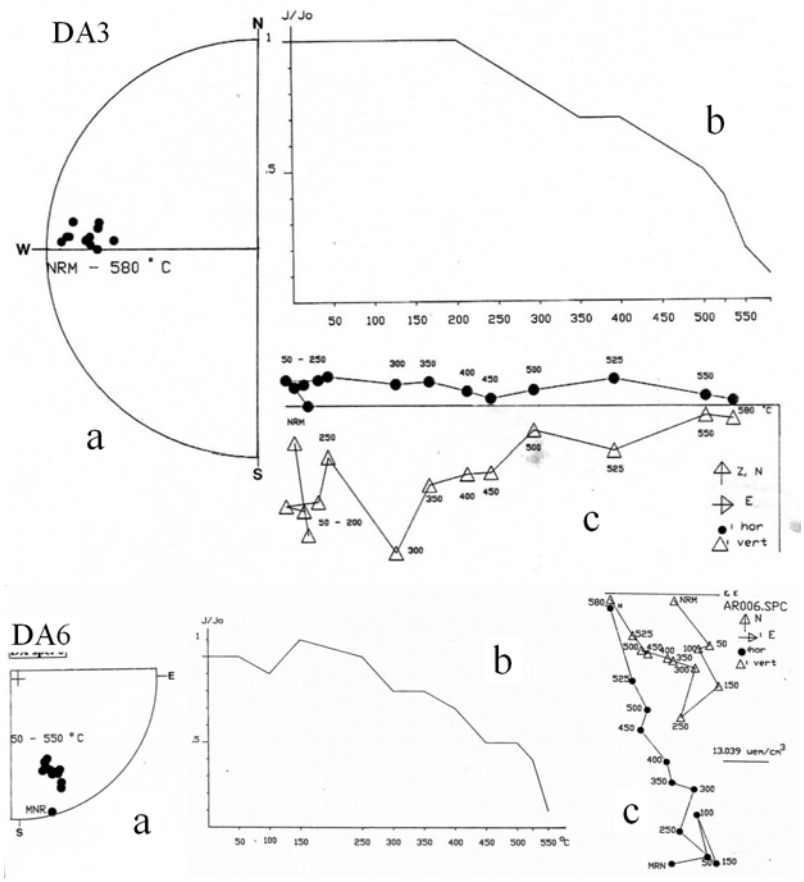

Figure 20. Examples of reverse samples (DA3 and DA6) dated at 2590 ± 50 (Beta-54775) and 2760 ± 80 (Beta-54774) years BP from Don Ariel cave. (a) Stereographic projection; (b) Demagnetization curves using thermal cleaning; (c) Zijderveld diagram (modified after Nami, 1994).

and reverse VGPs in San Blas records and other sites also supports its regional extent in the southern cone of South America with evidence records in Northeastern Patagonia. In the particular case presented in the previous sections, SB2, PR2, and mainly LS1 yielded new light to date with precision one of the largest amplitude GF fluctuations with reverse directions that happened during the Middle Holocene showing that one of the peaks of these oscillations occurred at ~5.3 ky BP. This situation strengthens the hypothesis of the real existence of anomalous GF behavior during the Holocene in southern Patagonia (Nami, 1994, 1995a, 1999a, 2012; Nami & Sinito, 1995).

As previously was noted by Nami (2012), in some areas of the southern cone of South America, during at least the last ~11 - 10 ky BP, the GF might have been undergoing an anomalous behavior with large amplitude fluctuations, occasionally reaching reverse polarity positions, more than once. If correctly represent the GF record, they are revealing that these kinds of directions might haen in a very short time span, probably decades or centuries; mainly during the terminal Pleistocene and early Holocene (~11 - 9/7 ky BP), middle (~5 - 4 ky BP) and late (~2.5 - 2.0 ky BP) Holocene. Also, very low negative and positive

inclination values occurred in the last millennia and centuries (i.e. LM and CS; Nami, 2006, 2012). These kind of anomalous records were also observed in several parts of the Earth (Burakow & Nachasova, 1990; Clark & Kennett, 1973; Dergachev et al., 2004; Guskova et al., 2008; Kochegura & Pisarevsky, 1994; Lund et al., 2007, 2008; Nami, 1999c, 2012, 2015; Nami et al. 2016, 2019; Noël, 1975, 1977; Noël & Tarling, 1975; Pospelova, 1981, 1990; Ransom, 1973; Raspopov et al., 2003; Urrutia Fucugauchi et al., 1995; Ortega-Guerrero & Urrutia Fucugauchi, 1997; Vitorello & Van der Voo, 1977; Woolin et al., 1971; Zhu et al., 1998; Wiegank et al., 1990). Hence, the hypothesis of the global excursional state of the Holocene GF with not coetaneous intermediate and reverse directions was proposed (Nami, 1999c). The records informed in this paper, suort this idea. Besides, LS1 shed new light about the chronological position of one of the largest amplitude fluctuations that occurred in SE Buenos Aires province in eastern part of Northern Patagonia which agrees with other records with reverse directions across the world.

During the last 780 ky BP, the Brunhes Chron showed that the GF polarity has been "normal" as it is now. However, there have been a number of occasions when the GF either briefly reverse or behaves anomalously. In other words, this normal polarity has been interrupted by significant departures from the dipole field configuration (Lund et al., 2001; Petrova & Pospelova, 1990; Tarling, 1983; Thouveny & Creer, 1992). These kinds of departures are considerably larger than those seen in secular variations observed during historical times, and sometimes even attain oosite polarity, originating GF excursions. They are short intervals of anomalous field directions that occur within a broader interval of "stable" normal or reversed magnetic polarity. While certain excursions may have regional or continental scale; other ones show a global existence (Bogue & Merril, 1992; Merrill & McFadden, 1994; Laj & Channell, 2007; Roberts, 2008). During the Middle Holocene several anomalous records with intermediate and reverse VGPs were registered at different materials, times and places across de world. In the Northern Hemisphere, reliable records obtained in lava flows from central Mexico dated by 14C at 4070 ± 150 and 4700 ± 200 uncalibrated years bp show a strong eastward swing in declination (González et al., 1997). Similar swings with wide amplitude variations in declination and inclination were observed in lake sediments of the Valley of Mexico during the same time span (Ortega-Guerrero & Urrutia-Fucugauchi, 1997; Urrutia-Fucugauchi et al., 1995). Chalco lake lacustrine declination record shows a pronounced swing at ~5 ky BP. Also, the Red Rock site in California (USA) yielded intermediate and reverse polarity positions also at ~5 ky BP (Nami, 1999c). In Asia, Chinese fresh-water sediments from Beijing yielded an excursion occurring between 5060 and 4860 ± 90 years BP (Zhu et al., 1998) and besides, several cores from the Barents sea sediments yielded records of the Solovki excursion dated at 4.5 - 7.5 ky BP (Guskova et al., 2008). As previously described, the Southern Cone of South America 22 sections (12 located in Patagonia), showed anomalous intermediate

Table 3. Summary of number of sites, location, number and range of ^{14}C dates of sampled deposits, number, quality and polarity of the samples. References: ND: number of ^{14}C dates in the sites, *: indicate indirect dates, N: number of samples used in the analysis, P: polarity of the core, N: normal, I: Intermediate, R: reverse. HRe: highly reliable, MRe: moderately reliable, PRe: poorly reliable (Nami, 1999a, 2012).

Site	Coordinates	Age (ky BP)	ND	P	N	SQ
Alero de las Circunferencias	22˚56'S 65˚21'W	~10.7 - 7.9	5	N-I	36	HRe-MRe
Puerto Segundo	25˚59.03'S 54˚39.74'W	~7 - 0.6	*	I-R	50	HRe
Aserradero	26˚S 54˚36.44'W	~7 - 1	*	N-I-R	20	HRe-MRe
Arroyo Yarará	26˚S 55˚W	~7 - 1	*	N-I	14	HRe-MRe
Barranca Pelada	30˚15'S 57˚37'W	~3.2 - 0.3	*	N-I	34	HRe-MRe
San Juan	30˚S 57˚44'W	≥3.0	*	N-I	21	HRe-MRe
Santa Lucía	30˚15.7'S 57˚37.30'W	~11 - 0.2	1	N-I	74	HRe-MRe
Barranca de Maipú	33˚7'36S 68˚41'29W	~9.7	1	I	47	HRe
Lomas del Mirador	34˚39.29'S 58˚32.17W	~10 - 0.05	14	N-I	149	HRe-MRe
Urupez	34˚49'15S 55˚19'02W	~10 - 11	2	N-I	13	HRe-MRe
Piedra del Aguila 11	40˚02_S, 70˚W	~4.9 - 1.9	9	N-I	90	HRe-MRe
San Blas 2	40˚33.39'S. 62˚14.35W	~9.6 - ≤5	1	N-I-R	30	HRe-MRe
Punta Rubia 2	40˚46.0'S, 62˚16.02W	~10 - ≤5.	-	N-I-R	39	HRe-MRe
La Serranita 1	40˚33.02'S 62˚38.16'W	~5.3	3	R	15	HRe-MRe
Angostura Blanca	42˚30'S 70˚W	~2.9 - 2.1	2	R-N	11	HRe-MRe-Pre
Cueva del Medio	51˚35'S 72˚38'W	~11 - 2.1	51	N-I	12	MRe-Pre
Mylodon Cave	51˚35'S 72˚38'W	~11 - 5.5	31	N-R	34	HRe
Cueva Saenz	51˚44.46'S 70˚09.92'W	≤ 10	-	I-R	5	HRe-MRe
Las Buitreras	51˚45'S 70˚10'W	≥10 - 4.3	2	N-I-R	40	HRe-MRe
Laguna Montecarlo	51˚55'S, 69˚39'W	≤ 10	-	N-I	23	HRe-MRe
Cueva Montecarlo	51˚54.86'S 69˚38.79'W	~1	1	N-I	12	HRe-MRe
Don Ariel	52˚S 70˚09'W	~7 - 2.6	6	N-R	15	HRe-MRe

and reverse directions that remarkably agree with the above mentioned chronologies (**Table 3**).

5. Conclusion

In conclusion, paleomagnetic studies carried out at different sites belonging from diverse sedimentary environments in northern and southern Patagonia yielded normal, intermediate and reversed directions. This suggests that the Earth's magnetic field probably underwent an excursion in southern South America during the Middle Holocene. Similar events were found in different sections and materials from Eurasia, North and South America. These facts may suggest that some anomalous geomagnetic phenomena might have occurred

globally during the more recent geological epoch; probably a global reverse excursion (Laj & Channell, 2007; Roberts, 2008) that might have occurred in the Middle Holocene. According to Nami (2012), during about the last 11/10 ka BP, the normal polarity of the Earth's magnetic field has been interrupted by several short-lived reversed polarity events. In this scenario, the observed Middle Holocene excursion might be another short-term manifestation of this process. Finally, if the presented paleomagnetic features are true GMF behavior, the remarkably PSV record can serve to correlate regional stratigraphies, and to determine relative and absolute chronologies (e.g., Tarling, 1983; Barendrest, 1984). Besides, if the anomalous directions represent excursions (cf. Nami et al. 2016), they may be also used as dating devices (Tarling, 1983; Barendrest, 1984; Parkes, 1986; Herz & Garrison, 1998; Merrill & McFadden, 2005), becoming excellent magnetostratigraphic markers for the time-span covered by the paleomagnetic record of the sites presented in this paper.

Acknowledgements

I am indebted to M. Cuadrado Woroszylo, D. Curzio and M. Silveira. They were very helpful during the fieldwork and palaeomagnetic sampling. Also I thank the University of Buenos Aires and CONICET for their support; J. L. Sáenz, A. Manero and G. Clifton for his friendship, continuous support and help in Río Gallegos, A. C. Sanguinetti de Bórmida was very supportive during the sampling in the northern Patagonian project (PMT-PICT0458). Several aspects of this research was supported by Agencia de Promoción Científica y Tecnológica, CONICET; National Geographic Society (Grant 5691-96); Logistic suort during the fieldwork was provided by Secretaría de Cultura de la provincia de Misiones, Museo Regional Juan P. Molina, Secretaría de Deportes de Santa Cruz, INTA and FOMICRUZ S.A. from Santa Cruz, Ariztizábal family for allowing to work in his Estancia at the Chico river. Paleomagnetic data were processed with IAPD and MAG88 programs developed by Torsvik (Norwegian Geological Survey) and E. Oviedo (University of Buenos Aires) respectively; Especially to H. Vizán for his useful comments and stimulating feedback. Additional thanks to all the fellows at the Institute for their fruitful discussion and invaluable help during this research.

Conflicts of Interest

The author declares no conflicts of interest regarding the publication of this paper.

References

Barendrest, R. W. (1984). Using Paleomagnetic Remanence and Magnetic Susceptibility Data for the Differentiation, Relative Correlation and Absolute Dating of Quaternary Sediments. In W. C. Mahaney (Ed.), *Quaternary Dating Methods* (pp. 101-140). Amsterdam: Elsevier. https://doi.org/10.1016/S0920-5446(08)70067-0

Bird, J. (1988). *Travels and Archaeology in South Chile* (246 p). Iowa City, IA: Iowa Uni-

versity Press. https://doi.org/10.2307/j.ctt20h6v8q

Bogue, S. W., & Merrill, R. T. (1992). The Character of the Field during Geomagnetic Reversals. *Annual Review of Earth Science, 20,* 181-219. https://doi.org/10.1146/annurev.ea.20.050192.001145

Burakow, K. S., & Nachasova, I. E. (1990). Anomalous Behaviour of the Geomagnetic Field in the 1st Thousand Years B.P. *Geomagnetic Field in Quaternary*. Zipe 62, Postdam, DDR: Akademie der Wissenschaften der DDR, 135-138.

Clark, H. C., & Kennet, J. P. (1973). Paleomagnetic Excursion Recorded in Latest Pleistocene Deep-Sea Sediments, Gulf of Mexico. *Earth and Planetary Science Letters, 19,* 267-274. https://doi.org/10.1016/0012-821X(73)90127-1

Coe, R. S., & Glen, J. M. G. (2004). The Complexity of Reversals. In J. E. E. Channell, D. V. Kent, W. Lowrie, & J. G. Meert (Eds.), *Timescales of the Paleomagnetic Field* (pp. 221-232). Washington DC: AGU. https://doi.org/10.1029/145GM16

Creer, K. M., & Ispir, Y. (1970). An Interpretation of the Behaviour of the Geomagnetic Field during Polarity Transitions. *Physics of the Earth and Planetary Interiors, 2,* 283-293. https://doi.org/10.1016/0031-9201(70)90015-4

Creer, K. M., Tucholka, P., Valencio, D. A., Sinito, A. M., & Vilas, J. F. (1983). Results from Argentina. In K. M. Creer, P. Tucholka, & C. E. Barton (Eds.), *Geomagnetism and Baked Clays and Recent Sediments* (pp. 231-236). Amsterdam, Holland: Elsevier Publishers.

Dergachev, V. A., Raspopov, O. M., van Geel, B., & Zaitseva, G. I. (2004). The "Sterno-Etrussia" Geoamagnetic Excursion around 2700 BP and Changes of Solar Activity, Cosmic Ray Intensity, and Climate. *Radiocarbon, 46,* 661-681. https://doi.org/10.1017/S0033822200035724

Gogorza, C. S. G., Di Tommaso, I., Sinito, A. M., Jackson, B., Nuñez, H., Creer, K., & Vilas, J. F. (1998). Preliminary Results from Paleomagnetic Records on Lake Sediments from South America. *Studia Geophysica and Geodaetica, 42,* 12-29. https://doi.org/10.1023/A:1023312104722

Gogorza, C. S. G., Sinito, A. M., Vilas, J. F., Creer, K., & Nuñez, H. (2000). Geomagnetic Secular Variations over the Last 6500 Years as Recorded by Sediments from the Lakes of South Argentina. *Geophysical Journal International, 143,* 787-798. https://doi.org/10.1046/j.1365-246X.2000.00277.x

González, S., Sherwood, G., Bohnel, H., & Schne, E. (1997). Palaeosecular Variation in Central Mexico over the Last 30000 Years: The Record from Lavas. *Geophysical Journal International, 130,* 201-219. https://doi.org/10.1111/j.1365-246X.1997.tb00999.x

Grondona, M. F. (1975). Pendiente del Océano Atlántico. In *Geografía de la República Argentina. Hidrografía* (VII, 2˚parte pp. 203-394). Buenos Aires, Argentina: Sociedad Argentina de Estudios Geográficos.

Gurarii, G. Z. (2005). Geomagnetic Field Reversals: Main Results and Basic Problems. *Russian Journal of Earth Sciences, 7,* ES3003. https://doi.org/10.2205/2005ES000175

Guskova, E. G., Raspopov, O. M., Piskarev, A. L., & Dergachev, V. A. (2008). Magnetism and Paleomagnetism of the Russian Arctic Marine Sediments. In *Proceedings of the 7th International Conference Problems of Geocosmos* (pp. 380-385). St. Petersburg, Russia.

Herrero-Bervera, E., & Coe, R. S. (1999). Transitional Field Behaviour during the Gilbert-Gauss and Lower Mammoth Reversals Recorded in Lavas from the Waianae cano, O'ahu, Hawaii, *Journal of Geophysical Research, 104,* 29157-29173. https://doi.org/10.1029/1999JB900208

Herz, N., & Garrison, E. G. (1998). *Geological Methods for Archaeology*. New York: Oxford University Press.

Hoffman, K. A., & Singer, B. S. (2004). Regionally Recurrent Paleomagnetic Transitional Fields and Mantle Processes. In J. E. E. Channell, D. V. Kent, W. Lowrie, & J. G. Meert (Eds.), *Timescales of the Paleomagnetic Field* (pp. 233-243). Washington DC: AGU. https://doi.org/10.1029/145GM17

Kirschvink, J. L. (1980). The Least-Squares Line and Plane and the Analysis of Palaeomagnetic Data. *Geophysical Journal International, 62,* 699-718. https://doi.org/10.1111/j.1365-246X.1980.tb02601.x

Kochegura, V. V., & Pisarevsky, S. A. (1994). Paleomagnetic Study of the Holocene and Late-Glacial Sediments of the North-Western Russia. In *XXI International Union of Geodesy and Geophysics General Assembly* (p. A173). Boulder, CO: Abstracts.

Laj, C., & Channell, J. E. T. (2007). Geomagnetic Excursions. In *Treatise of Geophysics* (pp. 373-416). Amsterdam, Holland: Elsevier. https://doi.org/10.1016/B978-044452748-6.00095-X

Lund, S. P., Platzman, E., Thouveny, N., & Camoin, G. (2007). Evidence for Two New Paleomagnetic Field Excursions ~2,500 and ~12,500 Years Ago from the South Pacific Ocean Region (Tahiti). *American Geophysical Union, Fall Meeting 2007,* Abstract ID: GP42A-05.

Lund, S. P., Platzman, E., Thouveny, N., Camoin, G., Yokoyama, Y., Matsuzaki, H. et al. (2008). Evidence for Two New Magnetic Field Excursions (11,000 and 13,000 Cal Yrs BP) from Sediments of the Tahiti Coral Reef (Maraa tract). *American Geophysical Union, Fall Meeting 2008,* Abstract ID: GP21B-0786.

Lund, S. P., Williams, T., Acton, G. D., Clement, B., & Okada, M. (2001). Brunhes Chron Magnetic Field Excursions Recovered from Leg 172 Sediments. In L. D. Keigwin, D. Rio, G. D. Acton, & E. Arnold (Eds.), *Proceedings of the Ocean Drilling Program, Scientific Results* (pp. 1-18). https://doi.org/10.2973/odp.proc.sr.172.216.2001

Mena, M., & Nami, H. G. (2002). Distribución Geográfica de PGVs Pleistoceno Tardío-Holoceno obtenidos en sedimentos de América del norte y América del Sur. In *XXI Reunión Científica de la Asociación Argentina de Geofísicos y Geodestas* (pp. 213-218). Buenos Aires: Asociación Argentina de Geofísicos y Geodestas.

Merrill, R. T., & McFadden, P. L. (1994). Geomagnetic Field Stability: Reversal Events and Excursions. *Earth and Planetary Science Letters, 121,* 57-69. https://doi.org/10.1016/0012-821X(94)90031-0

Merrill, R. T., & McFadden, P. L. (2005). The Use of Magnetic Field Excursions in Stratigraphy. *Quaternary Research, 63,* 232-237. https://doi.org/10.1016/j.yqres.2005.02.007

Nami, H. G. (1994). Excursiones Geomagnéticas y Arqueología: Nuevos Datos y Perspectivas en la Patagonia Actas y Memorias del XI Congreso Nacional de Arqueología Argentina (Resúmenes). *Revista del Museo de Historia Natural de San Rafael*, XIII, 362-367.

Nami, H. G. (1995a). Holocene Geomagnetic Excursion at Mylodon Cave, Ultima Esperanza, Chile. *Journal of Geomagnetism and Geoelectricity, 47,* 1325-1332.

Nami, H. G. (1995b). Archaeological Research in the Argentinean Río Chico Basin. *Current Anthropology, 36,* 661-664. https://doi.org/10.1086/204413

Nami, H. G. (1999a). Possible Holocene Excursion of the Earth's Magnetic Field in Southern South America: New Records from Archaeological Sites in Argentina *Earth Planets and Space, 51,* 175-191. https://doi.org/10.1186/BF03352222

Nami, H. G. (1999b). Arqueología de la localidad arqueológica de Pali Aike, Cuenca del

río Chico (provincia de Santa Cruz, Argentina). I. Las investigaciones arqueológicas. *Praehistoria, 3,* 189-201.

Nami, H. G. (1999c). Probable Middle Holocene Geomagnetic Excursion at the Red Rock Archaeological Site, California. *Geofísica Internacional, 38,* 239-250.

Nami, H. G. (2006). Preliminary Paleomagnetic Results of a Terminal Pleistocene/Holocene Record from Northeastern Buenos Aires Province (Argentina). *Geofizika, 23,* 119-141.

Nami, H. G. (2008). Paleomagnetic Results from the Urupez Paleoindian Site, Maldonado Department, Uruguay. *Current Research in the Pleistocene, 25,* 40-43.

Nami, H. G. (2011). New Detailed Paleosecular Variation Record at Santa Lucía Archaeological Site (Corrientes Province, Northeastern Argentina). *Geofísica Internacional, 50,* 9-21.

Nami, H. G. (2012). New Detailed Holocene Paleomagnetic Records with Anomalous Geomagnetic Field Bahavior in Argentina. *Geoacta, 37,* 83-116.

Nami, H. G. (2015). New Paleomagnetic Results and Evidence for a Geomagnetic Field Excursion during the Pleistocene-Holocene Transition at Pichincha Province, Ecuador. *Geofísica Internacional, 54,* 127-148. https://doi.org/10.1016/j.gi.2015.04.009

Nami, H. G., & Mena, M. (2010). Geographical Distribution Analysis of Pleistocene/Holocene VGPs from North and South America. *Eos Transactions AGU, 91,* Abstract GP11C-03.

Nami, H. G., & Sinito, A. M. (1991). Preliminary Paleomagnetic Results, the Campo Cerda Rockshelter, Province of Chubut, Argentina. *Quaternary of South America and Antarctic Peninsula, 9,* 141-151.

Nami, H. G., & Sinito, A. M. (1993). Evidence of a Possible Excursion of the Geomagnetic Field Registered during the Late Holocene in the Province of Chubut, Argentina. *Geoacta, 20,* 9-26.

Nami, H. G., & Sinito, A. M. (1995). Primeros resultados de los estudios paleomagnéticos en sedimentos de Cueva del Medio (Ultima Esperanza, Chile). *Anales del Instituto de la Patagonia Serie Ciencias Humanas, 23,* 135-142.

Nami, H. G., de la Peña, P., Vásquez, C., Feathers, J., & Wurz, S. (2016). Paleomagnetic Results and New Dates from Late Pleistocene and Holocene Deposits from Klasies River Cave 1, South Africa. *South African Journal of Science, 112*, Article No. 2016-0051. https://doi.org/10.17159/sajs.2016/20160051

Nami, H. G., Vásquez, C. A., & Durán, V. A. (2017). Detailed Early Holocene (10.3 cal kybp) Paleomagnetic Record with Anomalous Directions from Mendoza Province, Western Argentina. *Latinmag Letters, 7,* LL17-0702Rs.

Nami, H. G., Vásquez, C. A., Wadley, L., & de la Peña, P. (2019). Detailed Paleomagnetic Record at Rose Cottage Cave, South Africa: Implications for the Holocene Geomagnetic Field Behavior and Chronostratigraphy. Submitted for publication.

Noël, M. (1975). The Palaeomagnetism of Varved Clays from Blekinge, Southern Sweden. *Geologiska Föreningen i Stockholm Förhandlingar, 97,* 357-367. https://doi.org/10.1080/11035897509454326

Nöel, M. (1977). The Late Weichselian Geomagnetic Event. *Nature, 267,* 181. https://doi.org/10.1038/267181a0

Noël, M., & Tarling, D. (1975). The Laschamp Geomagnetic "Event". *Nature, 253,* 705-707. https://doi.org/10.1038/253705a0

Ohno, M., Murakami, F., Komatsu, F., Guyodo, Y., Acton, G., Kanamatsu, T. et al. (2008). Paleomagnetic Directions of the Gauss-Matuyama Polarity Transition Record-

ed in Drift Sediments (IODP Site U1314) in the North Atlantic. *Earth, Planets and Space, 60,* e13-e16. https://doi.org/10.1186/BF03352845

Orgeira, M. J., Beraza, L. A., Vizán, H., & Vilas, J. F. A. (1990). Evidence for a Geomagnetic Field Excursion in the Late Pleistocene (Entre Ríos, Argentina). *Quaternary of South America and Antarctic Peninsula, 6,* 173-188.

Orgeira, M. J., Walter, A. M., Sinito, A. M., Vilas, J. F. A., & Conti, C. (1996). New Evidence of an Excursion of the Geomagnetic Field Recorded in Late Pleistocene Sediments in Argentina. *Journal of South American Earth Sciences, 9,* 237-242. https://doi.org/10.1016/0895-9811(96)00009-0

Ortega-Guerrero, B., & Urrutia-Fucugauchi, J. (1997). A Paleomagnetic Secular Variation Record from Late Pleistocene-Holocene Lacustrine Sediments from Chalco Lake, Basin of Mexico. *Quaternary International, 43-44,* 87-96. https://doi.org/10.1016/S1040-6182(97)00024-4

Parkes, P. A. (1986). *Current Scientific Techniques in Archaeology*. New York: St. Martin's Press, 190 p.

Petrova, G. N., & Pospelova, G. A. (1990). Excursions of the Magnetic Field during the Brunhes Chron. *Physics of the Earth and Planetary Interiors, 63,* 135-143. https://doi.org/10.1016/0031-9201(90)90067-8

Pirazzolli, P. (1996). *Sea-Level Changes in the Last 20000 Years.* Chichester: John Wiley & Sons.

Pospelova, G. A. (1981). Excursions of the Geomagnetic Field during Brunhes Epoch. *Internationales Symposium, Aktuelle Probleme der Geomagnetischen Forschungm Veröffentlichungen des Zentralinstituts für Physik der Erde, 70,* 245-261.

Pospelova, G. A. (1990). Excursions of the Brunhes Chron as the Base of Magnetochronostratigraphical Scale for the Quaternary. In *Geomagnetic Field in Quaternary* (No. 62, pp. 49-80). Postdam, DDR: Veröffentlichung.

Ransom, C. J. (1973). Magnetism and Archaeology. *Nature, 242,* 518-519. https://doi.org/10.1038/242518b0

Raspopov, O. M., Dergachev, V. A., Goos'kova, E. G., & Morner, N. A. (2003). Visual Evidence of the Sterno-Etrussia Geomagnetic Excursion (~2700 BP)? *Geophysical Research Abstracts, 5,* Article ID: 3208.

Ré, G. H., Mena, M., & Vilas, J. F. (2008). Late Cenozoic Paleomagnetic Studies in Patagonia. In J. Rabassa (Ed.), *The Late Cenozoic of Patagonia and Tierra Del Fuego* (pp. 121-150). Rotterdam, Holland: Elsevier.

Roberts, A. P. (2008). Geomagnetic Excursions: Knows and Unknowns. *Geophysical Research Letters, 35,* L17307. https://doi.org/10.1029/2008GL034719

Sanguinetti de Bórmida, A. C. (2005). El Norpatagoniense. Expansión y límites: Evidencias arqueológicas, In A. Guiance (Ed.), *La Frontera: Realidades y representaciones* (pp. 111-126). Buenos Aires: Editorial Dunken.

Sinito, A. M., & Nuñez, H. J. (1997). Paleosecular Variations Recorded on Lake Sediments from South America *Journal of Geomagnetism and Geoelectricity, 49,* 473-483. https://doi.org/10.5636/jgg.49.473

Sinito, A. M., Gogorza, C., Nami, H. G., & Irurzun, M. A. (2001). Observaciones Paleomagnéticas en el Sitio Arqueológico Puesto Segundo (Misiones, Argentina). *Anales de la Asociación Física Argentina, 13,* 237-241.

Sinito, A. M., Nami, H. G., & Gogorza, C. (1997). Analysis of Palaeomagnetic Results from Holocene Sediments Sampled at Archaeological Excavations in South America. *Quaternary of South America and Antarctic Peninsula, 10,* 31-44.

Sylwan, C. A. (1989). *Paleomagnetism, Paleoclimate and Chronology of Late Cenozoic Deposits in Southern Argentina* (110 p). Stockholm, Sweden: Department of Geology, Stockholm University.

Tarling, D. (1983). *Palaeomagnetism: Principles and Applications in Geology, Geophysics and Archaeology*. New York: Chapman and Hall. https://doi.org/10.1007/978-94-009-5955-2

Thouveny, N., & Creer, K. M. (1992). Geomagnetic Excursions in the Past 60 ka: Ephemeral Secular Variation Features. *Geology, 20,* 399-402. https://doi.org/10.1130/0091-7613(1992)020<0399:GEITPK>2.3.CO;2

Thouveny, N., Creer, K. M., Smith, G., & Tucholka, P. (1985). Geomagnetic Oscillations and Excursions and Upper Pleistocene Chronology. *Episodes, 8,* 180-182.

Trebino, L. G. (1987). Geomorfología y eución de la costa en los alrededores del pueblo de San Blas, provincia de Buenos Aires. *Revista de la Asociación Geológica Argentina, XLII,* 9-22.

Urrutia-Fucugauchi, J., Lozano-García, S., Ortega-Guerrero, B., & Caballero-Miranda, M. (1995). Paleomagnetic and Paleoenvironmental Studies in the Southern Basin of Mexico-II Last Pleistocene-Holocene Chalco Lacustrine Record. *Geofísica Internacional, 34,* 33-53.

Valencio, D. A., Sinito, A. M., Creer, K. M., Mazzoni, M. M., Alonso, M. S., & Markgraf, V. (1985). Paleomagnetism, Sedimentology, Radiocarbon Age Determinations and Palynology of the Llao-Llao Area, Southwestern Argentina (lat. 41˚S, long. 71˚30'W): Paleolimnological Aspects. *Quaternary of South America and Antarctic Peninsula, 3,* 109-147.

Verosub, K., & Banerjee, S. K. (1977). Geomagnetic Excursions and Their Paleomagnetic Record. *Review of Geophysics, 15,* 145-155. https://doi.org/10.1029/RG015i002p00145

Violante, R. A., Parker, G., & Cavallotto, J. L. (2001). Evolución de las llanuras costeras del este bonaerense entre la bahía de Samborombón y la laguna Mar Chiquita durante el Holoceno. *Revista de la Asociación Geológica Argentina, 56,* 51-66.

Vitorello, I., & Van Der Voo, R. (1977). Magnetic Stratigraphy of Lake Michigan Sediments Obtained from Cores of Lacustrine Clay. *Quaternary Research, 7,* 398-412. https://doi.org/10.1016/0033-5894(77)90030-8

Vizán, H., & Azcuy, C. (2010). Is a Geomagnetic Field Excursion Stratigraphically Correlated to the Record of a Human Foot Print? *Eos Trans AGU, 91,* Abstract GP12A-03.

Watkins, N. D. (1972). Review of the Development of the Geomagnetic Polarity Time Scale and Discussion of Prospects for Its Finer Definition. *Geological Society of America Bulletin, 83,* 551-574. https://doi.org/10.1130/0016-7606(1972)83[551:ROTDOT]2.0.CO;2

Wiegank, F., Petrova, G. N., & Pospelova, G. A. (1990). Magneto-Chronostratigraphic Scale Model, Brunhes Chron, *Geomagnetic Field in Quaternary*, Zipe 62, Postdam., DDR: Akademie der Wissnschafter der DDR, 169-177.

Woolin, G., Erickson, D. B., Ryan, B. F., & Foster, J. H. (1971). Magnetism of the Earth and Climatic Changes. *Earth and Planetary Science Letters, 12,* 175-183. https://doi.org/10.1016/0012-821X(71)90075-6

Zhu, R. X., Coe, R. S., & Zhao, X. X. (1998). Sedimentary Record of Two Geomagnetic Excursions within the Last 15,000 Years in Beijing, China. *Journal of Geophysical Research, 103,* 30323-30334. https://doi.org/10.1029/98JB02836

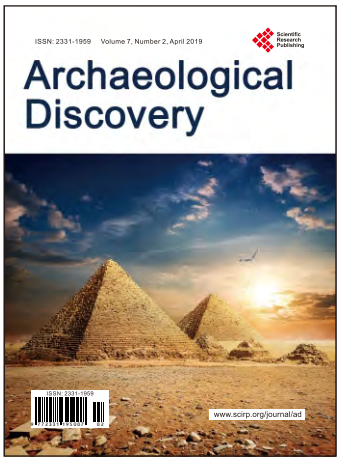

Call for Papers

Archaeological Discovery

ISSN Print: 2331-1959 **ISSN Online: 2331-1967**

http://www.scirp.org/journal/ad

Archaeological Discovery (AD) is an international journal dedicated to the latest advancement in the study of Archaeology. The goal of this journal is to provide a platform for scientists and academicians all over the world to promote, share, and discuss various new issues and developments in different areas of Archaeological studies.

Subject Coverage

All manuscripts must be prepared in English, and are subject to a rigorous and fair peer-review process. Accepted papers will immediately appear online followed by printed hard copy. The journal publishes original papers covering a wide range of fields but not limited to the following:

- Aerial Archaeology
- Archaeological Method and Theory
- Archaeological Science
- Archaeometry
- Art Archaeology
- Environmental Archaeology
- Ethnoarchaeology
- Experimental Archaeology
- Field Archaeology
- Geoarchaeology
- Historical Archaeology
- Island and Coastal Archaeology
- Lithic Studies
- Maritime Archaeology
- Prehistoric Archaeology
- Religious Archaeology
- Social Archaeology
- Underwater Archaeology
- World Archaeology
- Zooarchaeology

We are also interested in: 1) Short reports — 2-5 page papers in which an author can either present an idea with a theoretical background but has not yet completed the research needed for a complete paper, or preliminary data; 2) Book reviews — Comments and critiques, special peer-reviewed issue for colloquia, symposia, workshops.

Website and E-Mail

http://www.scirp.org/journal/ad **E-mail: ad@scirp.org**

What is SCIRP?

Scientific Research Publishing (SCIRP) is one of the largest Open Access journal publishers. It is currently publishing more than 200 open access, online, peer-reviewed journals covering a wide range of academic disciplines. SCIRP serves the worldwide academic communities and contributes to the progress and application of science with its publication.

What is Open Access?

All original research papers published by SCIRP are made freely and permanently accessible online immediately upon publication. To be able to provide open access journals, SCIRP defrays operation costs from authors and subscription charges only for its printed version. Open access publishing allows an immediate, worldwide, barrier-free, open access to the full text of research papers, which is in the best interests of the scientific community.

- High visibility for maximum global exposure with open access publishing model
- Rigorous peer review of research papers
- Prompt faster publication with less cost
- Guaranteed targeted, multidisciplinary audience

Scientific Research Publishing

Website: http://www.scirp.org

Subscription: sub@scirp.org

Advertisement: service@scirp.org